SAINT-PETERSBURG UNIVERSITY

Ruslan Andreevich SEVOSTYANOV

MULTIPURPOSE CONTROL OF THE MOVING PLANTS CONSIDERING DELAY

Scientific specialization

2.3.1. System analysis, control and information processing, statistics

Dissertation is submitted for the degree of

candidate of physical and mathematical sciences

Translation from Russian

Scientific supervisor:

Doctor of Physical and Mathematical Sciences,

Associate Professor Margarita V. Sotnikova

Saint-Petersburg

2023

TABLE OF CONTENTS

Introduction

1. Relevance, Goals and Main Results of the Dissertation

Modern technology level causes automation, to one degree or another, to affect almost all areas of human activity. At the same time, the pace of automation is increasing every year, and more and more professions are being replaced by machine labor. In turn, such progress is impossible without the use of automatic control systems based on the application of the feedback principle. The problems of motion control of various objects – mobile robots, unmanned aerial vehicles, sea vessels, robotic manipulators, etc. – are of particular interest here. It is important to note that the development of industry and economics determines the constant tightening of requirements for the quality of controlled motion dynamics in various modes and under various conditions. There are several important current areas of research in this area that are discussed in the dissertation.

First of all, these include the basic task of the moving plants motion stabilization. For example, it is important for a container ship to maintain a given heading angle when moving at sea, taking into account the specified requirements for the quality of control processes. In this case, the task is further complicated due to the possible presence of external disturbances. In this case, it is extremely important to have an on-board system for automatical stabilization of the vessel along the course, which would allow the cargo to be delivered without damage within a given time frame, with minimal fuel consumption. Let us note that the quality of control processes in various operating modes can be significantly improved by taking into account the dynamics of a moving plant.

The second important task is the use of visual information in the feedback loop. Generally, such tasks are relevant for automobile autopilots, mobile robots in warehouses and factories, as well as for aerial drones. These types of moving plants are equipped with a video camera rigidly mounted on the body. The control task may consist, for example, of positioning the robot relative to a given object. In this case, it is necessary to ensure the required quality of control processes taking into account

the influence of external disturbances. Here it is also important to take into account the equations of the dynamics of a moving plant in conjunction with equations representing changes in visual information in order to develop effective control algorithms.

Finally, let us explicitly note the problem of motion control of robotic manipulators. Here it is especially important to ensure the specified accuracy and speed of positioning, since, for example, the quality of car assembly on an automated conveyor may depend on it. In this case, vibrations of the body and the unaccounted mass of the load also act on the plant as external disturbances that must be compensated.

The implementation of modern control systems is usually carried out using digital devices. This inevitably leads to a delay in the feedback loop. The value of the delay can be small enough to not have a noticeable effect on the dynamics of the system. However, in some cases, delay can significantly deteriorate the quality of control processes, up to loss of stability. Therefore it is often necessary to take into account the presence of the delay during the design of the control systems.

Thus, we can highlight the main features of the problems considered in the dissertation: synthesis of multipurpose feedback taking into account the dynamics of a moving object, the use of visual information, the presence of a delay in the control signal, optimization of control processes in various operating modes, as well as the possibility of the practical implementation of the control algorithms on board of a moving plant in real time.

The problems of analysis and synthesis of stabilizing feedbacks in general have been studied quite thoroughly. For example, the works of V. I. Zubov [17–19], A. A. Krasovsky [24, 25], A. M. Letov [28–30], R. Kalman [20, 70], B. Francis [66], D. Doyle [63] and other outstanding scientists [1–3, 14, 21, 22, 26, 27, 33, 39, 50, 52, 57, 69, 71, 93] laid the fundamental foundations for control processes optimization. Problems of the moving plants control, including sea vessels, are widely studied in the works of Y.A. Lukomsky and V.M. Korchanov [32], Pelevin A.E. [15, 35], Y. P.

Petrov [36–38], T. Fossen [64, 65, 75], T. Perez [83] and other researchers [4, 13, 37, 91, 96].

However, published works usually tend to focus on individual operating modes. To take into account the entire complex of requirements for the dynamics of a closed-loop system in various operating modes, we can note the methodology of multipurpose control structure synthesis, first mentioned in [5]. In works [5–10], this idea was developed, and the application of multipurpose regulators to the problems of stabilizing marine moving plants is described, for example, in [99, 100].

The main advantage of a multipurpose structure usage is the fact that the initially complex task of the regulator synthesis of taking into account the entire set of requirements in all possible modes can be divided into separate simpler tasks corresponding to the synthesis of individual elements of the multipurpose structure. These problems can be solved relatively independently of each other, which simplifies the process of the full regulator synthesis. This leads to another advantage of the multipurpose structure: individual elements can be turned on or off depending on the current operating mode, for example, for more economical use of computing resources.

The issues of using visual information in the feedback loop are also quite widely covered in the literature. Here we can highlight, for example, the Visual Servoing approach [61, 62, 78]. The essence of this approach is to calculate the required motion velocity vector to minimize the error between the current and desired projection of some object in the image plane. The problems of achieving the required velocity usually are not considered in the literature devoted to Visual Servoing, thus the dynamics of the plant is not taken into account.

Motion stabilization taking into account the delay is one of the key topics in control theory. One of the first theoretical works in this area is the monograph [24], and practical issues are discussed in the book [54]. In [16], algebraic methods for studying the dynamics of systems with delay are considered. Questions of Lyapunov stability of motion of dynamic systems from the perspective of the

methods developing the ideology of Lyapunov-Krasovsky functionals usage are given in the monograph [72].

Currently we can mark out the two main practical approaches for solution of the problem of ensuring the stability of systems with delay. The first approach, described in [80], is based on the use of static feedback for linear systems with delay with an infinite-dimensional spectrum, providing a shift of a finite number of rightmost eigenvalues into the left open half-plane. Despite the simplicity of the feedback structure, the synthesis procedure in this case has a number of disadvantages that limit its practical application.

The idea of the second approach is to use the system state prediction in the feedback for the delay compensation. Closed-loop system with such feedback has a finite set of eigenvalues. This idea was first mentioned in the paper [94]. Further development is described in the monograph [79], and a generalization to the case of nonlinear systems is given in [73]. The details of the implementation of this approach are of a particular interest, as well as its generalization to the case of the dynamic regulators usage. Similar issues are discussed in article [10], and the main problem here is to preserve the transfer matrix of the original system without delay, closed by a multipurpose controller.

The possibility of the described methods combination: a multipurpose approach to the control laws synthesis, the visual information usage in the feedback loop, as well as the delay compensation through the prediction usage is a promising area of research and determines the **relevance** of this work.

The goal of the dissertation is to conduct a research aimed at the development of new methods for synthesis of multipurpose algorithms for moving plants control, allowing to increase the efficiency and quality of their functioning in various modes.

To achieve this goal, the following specific areas of research are considered in the work:

- development of the methods for multipurpose control laws synthesis for moving plants with delay compensation;

- research of the issues and development of the methods for multipurpose regulators synthesis using visual information for dynamic positioning of the moving plants taking delay into account;
- development of the methods for multipurpose regulators synthesis for moving plants with nonlinear mathematical models that allow the possibility of the application of the feedback linearization;
- building software systems for modeling the dynamics of the plants closed by the specified regulators, as well as conducting the numerical experiments.

Specific examples of the plants to demonstrate the performance of the proposed methods include a hovercraft, a mobile robot with a video camera, and a two-link robot manipulator.

The main results submitted to the defense:

1. New methods have been developed for equivalent transformation of the multipurpose controllers for the feedback delay compensation.

2. New algorithms are proposed for the synthesis of the multipurpose regulators with visual information in the feedback loop in the problem of dynamic positioning of moving plants in various modes.

3. New effective methods for the multipurpose regulators synthesis for moving plants based on the feedback linearization method have been constructed.

4. Multipurpose control algorithms with the delay compensation have been developed for the air cushion vehicle.

Theoretical and practical value of the dissertation results.

The theoretical value of the results obtained in the dissertation is based on the creation of new methods and algorithms for the multipurpose regulators synthesis for the moving plants in various operating modes, taking into account external disturbances, delay of the control signal and using the visual information in the feedback loop.

The practical significance of the obtained results is determined by the possibility of the onboard implementation of the described multipurpose regulators

on the real plants, which, in turn, is supported by the results of numerical experiments demonstrating the effectiveness of the proposed approach.

Dissertation results are successfully used in the research of the moving plants control systems design, in particular – air cushion vehicle and mobile robots (RFBR Grants № 18-37-00463 мол_а, № 20-07-00531, SPBU Contracts № 9.21.1415.2017, № 11456826).

Approbation of work. Results of this dissertation were reported at the following conferences: XLV International Scientific Conference of Post-Graduate Students and Students «Control Processes and Stability» (Saint-Petersburg, 2014), XI International Scientific-Practical Conference «Modern Information Technologies and IT-Education» (Moscow, 2016), XI International Conference «Modern Methods of Applied Mathematics, Control Theory and Computer Technologies», (PMTCT-2018, Voronezh, 2018), III International Scientific Conference «Convergent Cognitive Information Technologies» (Moscow, 2018), IV International Scientific Conference «Convergent Cognitive Information Technologies» (Moscow, 2019), IV International Conference «Stability and Control Processes» (SCP2020, Saint-Petersburg, 2020), Conference «Mathematical Control Theory and its Applications» Saint-Petersburg, 2020), VI International Scientific Conference «Convergent Cognitive Information Technologies» (Moscow, 2021), VII International Scientific Conference «Convergent Cognitive Information Technologies» (Moscow, 2022), 22nd International Conference on Mathematical Optimization Theory and Operations Research (MOTOR, Yekaterinburg, 2023), and at the seminars at the Department of computer technology and systems of Saint-Petersburg State University.

2. Brief Summary of the Work

The thesis consists of the introduction, four chapters, a conclusion, and a list of references that includes 103 titles. The volume of the thesis is 132 pages.

The introduction is devoted to a brief presentation of the considered problems, and also contains a review of the literature on the research topic.

The first chapter describes the main operating modes of the moving plants

and the requirements for the plants dynamics in these modes, introduces a formal definition of a multipurpose regulator, discusses the search of the multipurpose feedback tunable element, and also presents a methodology for the control channel delay compensation and the corresponding transformation of the multipurpose regulator.

The second chapter is devoted to the issues of the dynamic positioning of moving plants using visual information in a feedback loop, taking into account delay and external disturbances. An approach to the synthesis of the control law has been developed based on a combination of a multipurpose approach, the ideology of the visual servoing, and the delay compensation. The performance of the proposed methods is demonstrated based on the numerical experiments with a computer model of the fully-actuated omni-wheeled mobile robot with a video camera and the underactuated differential-drive robot with a video camera.

The third chapter is related to the problem of delay-compensating control synthesis for moving plants based on a multipurpose approach and the feedback linearization method. The issues of the constant and polyharmonic external disturbances compensation are investigated. The results of numerical experiments with a computer model of a two-link robot manipulator are presented.

In the fourth chapter, as a practical application to demonstrate the effectiveness of the developed approach, the solution to the problem of the multipurpose feedback synthesis with delay compensation for the air cushion vehicle is considered, and the results of numerical experiments are also presented.

Publications. The main content of the thesis is reflected in **17** publications, **3** of which are published in the journals included in the List of peer-reviewed journals recommended for publication of papers that represent the main results of dissertations, **5** works are published in journals indexed in the Web of Science CC and Scopus and **9** papers – in the journals indexed in the Russian Science Citation Index.

Chapter 1. Issues of the Multipurpose Control With Delay Compensation

This chapter discusses the main issues of multipurpose regulator synthesis for the moving plants motion stabilization, taking into account the delay of the control signal. Delays are inevitably presented in real physical control systems and, generally, lead to worse dynamics quality, up to loss of stability. Multipurpose regulators turn out to be useful in the case when the problem formulation implies the presence of a number of requirements for the controlled motion dynamics in various operating modes. A special transformation of the multipurpose regulator, synthesized for a system without delay, makes it possible to compensate the delay while maintaining the original transfer matrix.

The first paragraph is devoted to the basic operating modes of moving plants that are of interest within the framework of this work, and the requirements for the dynamics of the plants in these modes. The second paragraph introduces a description of the multipurpose control structure and the general approach to tunable elements search. Finally, the last paragraph presents the delay compensation approach by using the prediction of the plant state.

1.1. Plant Operating Modes

Let us consider an arbitrary moving plant with nonlinear dynamics that can be described by a system of differential equations

$$\begin{aligned} \dot{\mathbf{x}} &= \mathbf{F}(\bar{\mathbf{x}}, \bar{\boldsymbol{\delta}}, \bar{\mathbf{d}}_e), \\ \bar{\mathbf{y}} &= \mathbf{S}(\bar{\mathbf{x}}, \bar{\boldsymbol{\delta}}), \end{aligned} \tag{1.1}$$

where $\bar{\mathbf{x}} \in E^n$ – plant state vector, including linear and angular velocity components, $\bar{\boldsymbol{\delta}} \in E^m$ – control action vector (actuator deflections from the neutral position), $\bar{\mathbf{d}}_e \in E^{n_d}$ – external disturbances vector, $\mathbf{F}$ – vector function with elements that are continuously differentiable by a set of arguments, $\bar{\mathbf{y}} \in E^k$ – measurement vector, $\mathbf{S}$ – vector function.

Assume that feedback is defined for system (1.1) by specifying some operator $\mathbf{U}$ on the measurement vector in the form

$$\overline{\boldsymbol{\delta}} = \mathbf{U}(\overline{\mathbf{y}}). \tag{1.2}$$

Let us list the main operating modes and requirements for the dynamics of the plant in these modes. Necessary prerequisite for all modes is to ensure asymptotic stability of motion. To formalize the requirements for dynamics, we define a generalized quality functional on the movements of system (1.1), (1.2)

$$J = J(\overline{\mathbf{y}}, \overline{\boldsymbol{\delta}}) = J(\mathbf{U}), \tag{1.3}$$

particular form of which depends on the current operating mode.

1) *Proper motion* is characterized by zero initial conditions with the absence of the external disturbance. The control goal is to ensure the transition of the system from the initial position to the equilibrium position, determined by a constant reference signal $\mathbf{r}$ which is fed to the feedback loop. The dynamics requirements in this mode are the most important.

Let us introduce an auxiliary scalar function with the Euclidean space norm

$$\rho(t) = \left\| \overline{\mathbf{y}}(t) \right\|,$$

defined at $t \in [0, \infty)$. One option for representation of the functional (1.3) might be overshoot magnitude for variable ρ in the form

$$J_1 = \frac{\rho_m - \rho_r}{\rho_r}, \tag{1.4}$$

where $\rho_r = \|\mathbf{r}\|$, $\rho_m = \sup\limits_{t \in [0,\infty)} \rho(t)$.

Besides (1.4) let us introduce another functional

$$T_p = \inf \left\{ t_m : \rho(t) \in M(\rho_r, \Delta), \forall t \geq t_m \right\}, \tag{1.5}$$

where $M(\rho_r, \Delta) = \left\{ \rho : \|\rho - \rho_r\| / \|\rho_r\| \leq \Delta \right\}$, Δ – fixed real number. Functional (1.5), in fact, defines closed-loop settling time. Fig. 1.1 shows schematic representation of the essence of the given functionals (1.4) and (1.5).

The selected values of the tunable feedback elements must provide a simultaneous minimum of the functionals (1.4) and (1.5) on such a set that ensures

the asymptotic stability of the equilibrium position of the closed-loop system. In particular, it is possible to introduce a more rigid requirement for the location of the roots of the characteristic polynomial of the linear approximation of a closed-loop system in a certain given region of the open left complex half-plane.

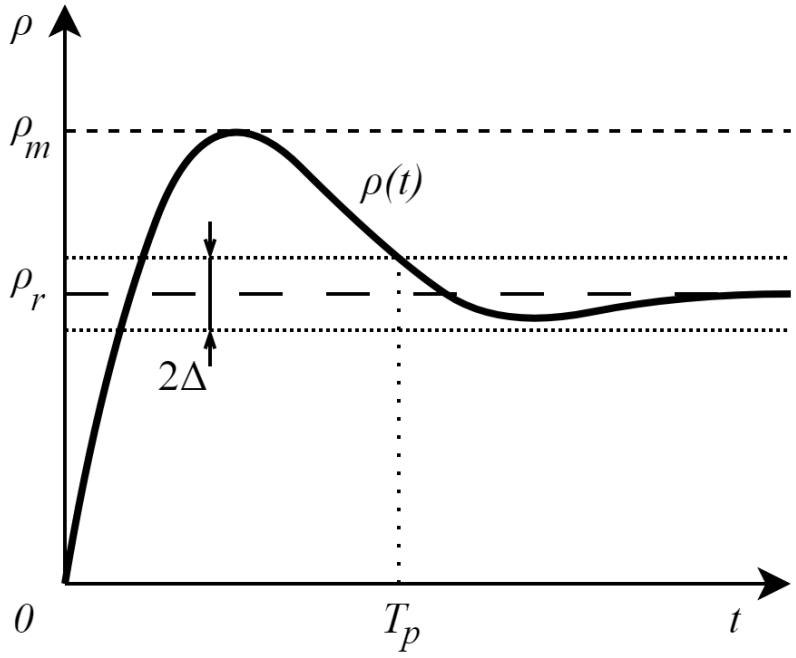

Fig. 1.1. Visualization of the overshoot and settling time.

Let us note that simultaneous achievement of the minimum of functionals (1.4) and (1.5) is often impossible in practice, and therefore tunable elements of the control law must be selected taking into account the desired restrictions of the specified functionals

$$J_1 \le J_{10},\ T_p \le T_{p0},$$

where constant values J_{10} and T_{p0} are taken from the practical perspective.

2) *Forced motion under the influence of a constant external disturbance* $\overline{\mathbf{d}}_e(t) = \overline{\mathbf{d}}_{e0}$ (for example, side wind or sea current) with zero initial conditions. There is no reference signal in this mode, and the control goal is to provide astatism of the closed system, i.e. ensure the condition

$$\lim_{t \to +\infty} \rho(t) = 0$$

for any vector $\overline{\mathbf{d}}_{e0}$.

Let us define a functional on the movements of the closed-loop system that determines the maximum deviation of the controlled variables

$$\rho_p = \max_{t\in[0,\infty)} \rho(t).$$

In fact, it is necessary to ensure the minimum value of the «dip» of the controlled coordinates when exposed to a step disturbance, without deteriorating the quality of operation of the control system in the previous mode.

3) *Forced motion under the influence of a periodic external disturbance* (for example, sea waves or rough roads). The initial conditions in this mode are zero, and there is no reference signal. The control goal is to minimize the influence of disturbance on the control signal response to save the actuators resource. The quality functional here can be the norm of the transfer matrix from the disturbance to the control signal.

1.2. Multipurpose Control Structure

Let us define some controlled motion of the plant by specifying vector functions $\overline{\mathbf{x}} = \overline{\mathbf{x}}_c(t)$, $\overline{\boldsymbol{\delta}} = \overline{\boldsymbol{\delta}}_c(t)$ and $\overline{\mathbf{d}}_e = \overline{\mathbf{d}}_c(t)$, satisfying the system (1.1):

$$\dot{\overline{\mathbf{x}}}_c = \mathbf{F}(\overline{\mathbf{x}}_c, \overline{\boldsymbol{\delta}}_c, \overline{\mathbf{d}}_c). \tag{1.6}$$

Let us introduce the notations

$$\mathbf{x}(t) = \overline{\mathbf{x}}(t) - \overline{\mathbf{x}}_c(t),\ \boldsymbol{\delta}(t) = \overline{\boldsymbol{\delta}}(t) - \overline{\boldsymbol{\delta}}_c(t),\ \mathbf{d}(t) = \overline{\mathbf{d}}_e(t) - \overline{\mathbf{d}}_c(t)$$

for the deviations of the variable values of the system (1.1) from the defined motion. Taking into account (1.1) and (1.6), the dynamics of these deviations can be described by a system of equations

$$\dot{\mathbf{x}} = \mathbf{P}(\mathbf{x}, \boldsymbol{\delta}, \mathbf{d}), \tag{1.7}$$

where

$$\mathbf{P}(\mathbf{x}, \boldsymbol{\delta}, \mathbf{d}) = \mathbf{F}(\overline{\mathbf{x}}_c + \mathbf{x}, \overline{\boldsymbol{\delta}}_c + \boldsymbol{\delta}, \overline{\mathbf{d}}_c + \mathbf{d}) - \mathbf{F}(\overline{\mathbf{x}}_c, \overline{\boldsymbol{\delta}}_c, \overline{\mathbf{d}}_c),$$

from which it is clear that system (1.7) has an equilibrium position with zero values of the variables $\mathbf{x}$, $\boldsymbol{\delta}$ and $\mathbf{d}$.

Let us linearize system (1.7) in the vicinity of the zero equilibrium position. As a result we get

$$\dot{\mathbf{x}} = \mathbf{A}\mathbf{x} + \mathbf{B}\boldsymbol{\delta} + \mathbf{H}\mathbf{d}, \tag{1.8}$$

assuming that the initial plant model is such that the matrices $\mathbf{A}$, $\mathbf{B}$ and $\mathbf{H}$ of the linearized system (1.8) are constant.

Let us assume that in general case the complete state vector is not available for measurement. In this regard, we add to system (1.8) the output equations

$$\mathbf{y} = \mathbf{C}\mathbf{x}, \tag{1.9}$$

where $\mathbf{y} \in E^k$ – measurement vector, $\mathbf{C}$ – matrix with constant components.

Let us also assume that the actuator drives has their own linear dynamics in the form

$$\dot{\boldsymbol{\delta}} = \mathbf{u}, \tag{1.10}$$

where $\mathbf{u} \in E^m$ – control signal, which is directly fed to the input of the plant.

Let us consider the linear equations of dynamics of a moving object (1.8) – (1.10) without the delay, taking into account the measurement vector and the linear equation of the actuator drives dynamics:

$$\begin{aligned} \dot{\mathbf{x}} &= \mathbf{A}\mathbf{x} + \mathbf{B}\boldsymbol{\delta} + \mathbf{H}\mathbf{d}, \\ \mathbf{y} &= \mathbf{C}\mathbf{x}, \\ \dot{\boldsymbol{\delta}} &= \mathbf{u}. \end{aligned} \tag{1.11}$$

In general, the multipurpose structure of the control law for system (1.11) includes the following elements [7]:

$\dot{\mathbf{z}} = \mathbf{A}\mathbf{z} + \mathbf{B}\boldsymbol{\delta} + \mathbf{G}(\mathbf{y} - \mathbf{C}\mathbf{z})$ – asymptotic observer equation;

$\boldsymbol{\xi} = \mathbf{F}(\frac{d}{dt})(\mathbf{y} - \mathbf{C}\mathbf{z})$ – dynamic corrector equation; (1.12)

$\mathbf{u} = \boldsymbol{\mu}\dot{\mathbf{z}} + \boldsymbol{\nu}\mathbf{y} + \boldsymbol{\xi}$ – speed control signal equation. (1.13)

The asymptotic observer is used mainly to solve two problems. First of all, in the case when the dimension of the measurement vector is less than the dimension of the state vector, but the system is completely observable, the observer provides an estimate of the complete state vector of the system. In addition, the choice of matrix

$\mathbf{G}$ affects the dynamics of the closed-loop system, including the response to the constant external disturbances.

The dynamic corrector (1.12) can also be used for several purposes depending on the selection of tunable elements. Basically, two modes of operation of the corrector can be distinguished, subject to the presence of external periodic disturbances (for example, sea waves). In the first mode, the corrector ensures that the influence of disturbances on the measured parameters of the system is minimized, acting as an optimal dynamic compensator. In the second mode, the corrector is an optimal dynamic filter, minimizing the reaction of the actuator drives to the disturbance. This makes it possible, for example, to ensure an increased wear resistance of rudders and fuel economy for sea vessels in the case of motion in conditions of strong waves.

The most important part of the multipurpose regulator is the speed control law equation (1.13). This element ensures the asymptotic stability of the closed-loop system, as well as providing the desired characteristics of the dynamics quality of controlled motion either in the absence or the presence of external disturbances. Equation (1.13) can be transformed to an equivalent positional control law for the output of an asymptotic observer in the form [7]

$$\mathbf{u} = \mathbf{k}\mathbf{z} + \mathbf{k}_0\boldsymbol{\delta} + \boldsymbol{\nu}_0\mathbf{y} + \boldsymbol{\xi}, \tag{1.14}$$

где $\mathbf{k} = \boldsymbol{\mu}(\mathbf{A} - \mathbf{G}\mathbf{C})$, $\mathbf{k}_0 = \boldsymbol{\mu}\mathbf{B}$, $\boldsymbol{\nu}_0 = \boldsymbol{\mu}\mathbf{G} + \boldsymbol{\nu}$.

We will further use the control law in the form (1.14), since this form is the most preferable for taking into account the delay of the control signal, which is described in the following paragraphs.

Let us note that in the optimal control synthesis process, constant matrices $\mathbf{G}$, $\boldsymbol{\mu}$, $\boldsymbol{\nu}$ and the corrector transfer matrix $\mathbf{F}$ are subject to search. The search is carried out depending on the specified requirements for the plant dynamics in various operating modes, including in the presence of external disturbances.

Let us pay attention to the fact that the dynamic corrector equation (1.12) can be transformed to the linear system

$$\begin{aligned}\dot{\mathbf{p}} &= \boldsymbol{\alpha}\mathbf{p} + \boldsymbol{\beta}(\mathbf{y} - \mathbf{cz}),\\ \boldsymbol{\xi} &= \boldsymbol{\gamma}\mathbf{p} + \mathbf{m}_f(\mathbf{y} - \mathbf{cz}),\end{aligned} \tag{1.15}$$

where $\mathbf{p} \in E^{n_1}$ – corrector state vector, $\boldsymbol{\xi} \in E^m$ – its output vector (dimension of this vector must be same as the dimension of the actuators deflection vector $\boldsymbol{\delta}$), $\boldsymbol{\alpha}$, $\boldsymbol{\beta}$, $\boldsymbol{\gamma}$, $\mathbf{m}_f$ – are the constant matrices satisfying the condition

$$\boldsymbol{\gamma}(\mathbf{E}_{n_1} s - \boldsymbol{\alpha})^{-1}\boldsymbol{\beta} + \mathbf{m}_f \equiv \mathbf{F}(s).$$

Taking into account (1.14) and (1.15), multipurpose regulator equations can be represented as

$$\begin{aligned}\dot{\mathbf{z}} &= \mathbf{Az} + \mathbf{B}\boldsymbol{\delta} + \mathbf{G}(\mathbf{y} - \mathbf{Cz}),\\ \dot{\mathbf{p}} &= \boldsymbol{\alpha}\mathbf{p} + \boldsymbol{\beta}(\mathbf{y} - \mathbf{Cz}),\\ \mathbf{u} &= \mathbf{kz} + \mathbf{k}_0\boldsymbol{\delta} + \boldsymbol{\nu}_0\mathbf{y} + \boldsymbol{\xi}.\end{aligned} \tag{1.16}$$

Since modern control systems are implemented on the digital onboard devices, direct application of the continuous system (1.16) to the plant is impossible. Therefore let us specify some discretization period T_d and transform regulator (1.16) to the linear difference equations system

$$\begin{aligned}\mathbf{z}[n+1] &= \mathbf{A}_d\mathbf{z}[n] + \mathbf{B}_d\delta[n] + \mathbf{G}_d(\mathbf{y}[n] - \mathbf{Cz}[n]),\\ \mathbf{p}[n+1] &= \boldsymbol{\alpha}_d\mathbf{p}[n] + \boldsymbol{\beta}_d(\mathbf{y}[n] - \mathbf{Cz}[n]),\\ \mathbf{u}[n] &= \mathbf{kz}[n] + \mathbf{k}_0\boldsymbol{\delta}[n] + \boldsymbol{\nu}_0\mathbf{y}[n] + \boldsymbol{\xi}[n],\end{aligned}$$

subject to the direct plant onboard implementation.

Let us discuss the issues of the multipurpose regulator tunable elements synthesis. The first task is searching the coefficients of the feedback (1.14) which are uniquely determined by the parameters of the basic control law

$$\mathbf{u} = \mathbf{K}_x(\mathbf{x} - \mathbf{r}) + \mathbf{K}_\delta\boldsymbol{\delta}, \tag{1.17}$$

where $\mathbf{r} \in \mathbf{E}^n$ – given fixed reference signal vector, $\mathbf{K}_x$ and $\mathbf{K}_\delta$ – constant matrices subject to search. Feedback (1.17) must not be directly implemented, but it is a basis for solving the further problems.

The coefficients of the law (1.17) must be chosen based on the requirements for the dynamics quality of the plant's proper motion. These are the highest

priority requirements, the fulfillment of which is mandatory for any mode of operation of the control system.

The next step is the transition to a speed control law to ensure astatism of the closed-loop system. In the general case, this transition is quite complicated, but in particular cases the approach to deriving speed control law formulas can be significantly simplified [11, 12]. The procedure for searching the tunable elements will be demonstrated in the fourth chapter for the problem of stabilizing a hovercraft.

The next element to find is the matrix $\mathbf{G}$ of the asymptotic observer coefficients, based on the requirements for the dynamics of controlled motion under the influence of external step disturbances. In this mode, we will assume that the reference signal is zero.

Finally, the last required element of the multipurpose structure is the corrector transfer matrix $\mathbf{F}(s)$. In this work, the main requirement that determines the value of this matrix is to minimize the intensity of the control signal in the presence of external periodic disturbances.

Let us formalize the problem of searching a transfer matrix $\mathbf{F}(s)$. Note that the actuators channel in the closed-loop system (1.11), (1.16) is an LTI system, the input of which receives measurements $\mathbf{y}$, and the output is the vector $\boldsymbol{\delta}$ of the actuator drives state. In this case, we can assume that this system itself is closed by a dynamic corrector as feedback. The plant here is the main part of the control channel in the form

$$\begin{aligned} \dot{\mathbf{z}} &= \mathbf{A}\mathbf{z} + \mathbf{B}\boldsymbol{\delta} + \mathbf{G}(\mathbf{y} - \mathbf{C}\mathbf{z}), \\ \dot{\boldsymbol{\delta}} &= \mathbf{k}\mathbf{z} + \mathbf{k}_0\boldsymbol{\delta} + \boldsymbol{\nu}_0\mathbf{y} + \boldsymbol{\xi}. \end{aligned} \tag{1.18}$$

Assuming that the input of the main part is the vector $\begin{pmatrix} \mathbf{y} \\ \hline \boldsymbol{\xi} \end{pmatrix}$, let us add to the system (1.18) the output equation for the vector $\begin{pmatrix} \boldsymbol{\delta} \\ \hline \boldsymbol{\zeta} \end{pmatrix}$, where $\boldsymbol{\zeta} = \mathbf{y} - \mathbf{C}\mathbf{z}$, thus in the state space the model of the main part of the actuator drives channel can be represented as

$$\begin{pmatrix}\dot{\mathbf{z}}\\ \dot{\boldsymbol{\delta}}\end{pmatrix}=\left(\begin{array}{c|c}\mathbf{A}-\mathbf{GC} & \mathbf{B}\\ \hline \mathbf{k} & \mathbf{k}_0\end{array}\right)\begin{pmatrix}\mathbf{z}\\ \boldsymbol{\delta}\end{pmatrix}+\left(\begin{array}{c|c}\mathbf{G} & \mathbf{0}_{n\times m}\\ \hline \boldsymbol{\nu}_0 & \mathbf{E}_m\end{array}\right)\begin{pmatrix}\mathbf{y}\\ \boldsymbol{\xi}\end{pmatrix},$$
$$\begin{pmatrix}\boldsymbol{\delta}\\ \boldsymbol{\zeta}\end{pmatrix}=\left(\begin{array}{c|c}\mathbf{0}_{m\times n} & \mathbf{E}_m\\ \hline -\mathbf{C} & \mathbf{0}_{k\times m}\end{array}\right)\begin{pmatrix}\mathbf{z}\\ \boldsymbol{\delta}\end{pmatrix}+\left(\begin{array}{c|c}\mathbf{0}_{m\times k} & \mathbf{0}_{m\times m}\\ \hline \mathbf{E}_k & \mathbf{0}_{k\times m}\end{array}\right)\begin{pmatrix}\mathbf{y}\\ \boldsymbol{\xi}\end{pmatrix}. \qquad (1.19)$$

In the frequency domain (1.19) is of the form

$$\begin{pmatrix}\boldsymbol{\delta}\\ \boldsymbol{\zeta}\end{pmatrix}=\mathbf{T}(s)\begin{pmatrix}\mathbf{y}\\ \boldsymbol{\xi}\end{pmatrix}=\left(\begin{array}{c|c}\mathbf{T}_{11}(s) & \mathbf{T}_{12}(s)\\ \hline \mathbf{T}_{21}(s) & \mathbf{T}_{22}(s)\end{array}\right)\begin{pmatrix}\mathbf{y}\\ \boldsymbol{\xi}\end{pmatrix}, \qquad (1.20)$$

where $\mathbf{T}(s)$ – transfer matrix of the main part of the actuator drives channel. In the explicit form this matrix can be expressed through the constant matrices of the system (1.19) as

$$\mathbf{T}(s)=\left(\begin{array}{c|c}\mathbf{0}_{m\times n} & \mathbf{E}_m\\ \hline -\mathbf{C} & \mathbf{0}_{k\times m}\end{array}\right)\left(\mathbf{E}_{n+m}s-\left(\begin{array}{c|c}\mathbf{A}-\mathbf{GC} & \mathbf{B}\\ \hline \mathbf{k} & \mathbf{k}_0\end{array}\right)\right)^{-1}\left(\begin{array}{c|c}\mathbf{G} & \mathbf{0}_{n\times m}\\ \hline \boldsymbol{\nu}_0 & \mathbf{E}_m\end{array}\right)+$$
$$+\left(\begin{array}{c|c}\mathbf{0}_{m\times k} & \mathbf{0}_{m\times m}\\ \hline \mathbf{E}_k & \mathbf{0}_{k\times m}\end{array}\right).$$

Closing the system (1.20) by the dynamic corrector we get

$$\begin{pmatrix}\boldsymbol{\delta}\\ \boldsymbol{\zeta}\end{pmatrix}=\left(\begin{array}{c|c}\mathbf{T}_{11}(s) & \mathbf{T}_{12}(s)\\ \hline \mathbf{T}_{21}(s) & \mathbf{T}_{22}(s)\end{array}\right)\begin{pmatrix}\mathbf{y}\\ \boldsymbol{\xi}\end{pmatrix},$$
$$\boldsymbol{\xi}=\mathbf{F}(s)\boldsymbol{\zeta}. \qquad (1.21)$$

Excluding the variables $\boldsymbol{\zeta}$ and $\boldsymbol{\xi}$ from (1.21) we are getting the transfer matrix from the input $\mathbf{y}$ to the output $\boldsymbol{\delta}$

$$\mathbf{F}_{y\delta}(s)=\mathbf{T}_{11}(s)+\mathbf{T}_{12}(s)\mathbf{F}(s)\left[\mathbf{E}_k-\mathbf{T}_{22}(s)\mathbf{F}(s)\right]^{-1}\mathbf{T}_{21}(s).$$

Next let us introduce the functional

$$J_2=J_2(\mathbf{F})=\left\|\mathbf{F}_{y\delta}(s,\mathbf{F})\right\|,$$

which is defined in the set Ω of the matrices $\mathbf{F}(s)$ with regular rational components whose denominators have roots in the left open half-plane. Then minimization of the control intensity comes down to the optimization problem

$$J_2(\mathbf{F})\to\min_{\mathbf{F}\in\Omega},\ J_{20}=\min_{\mathbf{F}\in\Omega}J_2(\mathbf{F}),\ \mathbf{F}(s)=\arg\min_{\mathbf{F}\in\Omega}J_2(\mathbf{F}).$$

Let us also note here that in particular cases the problem of optimal search for the corrector transfer matrix is significantly simplified due to a number of assumptions, which will be shown in the fourth chapter using the example of the problem of a hovercraft control.

1.3. Usage of the Prediction for the Delay Compensation

Now let us face the problem of plant stabilization in case of the presence of a constant delay in the control channel. To demonstrate the general idea of the proposed approach, let us first consider the simplest solution to the problem. Let us introduce the linearized system (1.8), (1.9) without taking into account the dynamics of the drives and adding a constant delay h to the control channel and external disturbance:

$$\begin{aligned} \dot{\mathbf{x}} &= \mathbf{A}\mathbf{x} + \mathbf{B}\boldsymbol{\delta}(t-h) + \mathbf{H}\mathbf{d}(t-h), \\ \mathbf{y} &= \mathbf{C}\mathbf{x}. \end{aligned} \tag{1.22}$$

Consider together with system (1.22) an auxiliary LTI object without the delay in control channel

$$\begin{aligned} \dot{\mathbf{x}} &= \mathbf{A}\mathbf{x} + \mathbf{B}\boldsymbol{\delta} + \mathbf{H}\mathbf{d}(t-h), \\ \mathbf{y} &= \mathbf{C}\mathbf{x}. \end{aligned} \tag{1.23}$$

For system (1.23) let us synthesize stabilizing control

$$\boldsymbol{\delta} = \mathbf{K}\mathbf{x}, \tag{1.24}$$

ensuring the matrix $\mathbf{A} + \mathbf{B}\mathbf{K}$ is Hurwitz. Equations of the closed-loop system (1.23), (1.24) are converted to the form

$$\begin{aligned} \dot{\mathbf{x}} &= (\mathbf{A} + \mathbf{B}\mathbf{K})\mathbf{x} + \mathbf{H}\mathbf{d}(t-h), \\ \mathbf{y} &= \mathbf{C}\mathbf{x}. \end{aligned} \tag{1.25}$$

Now let us return to the original system with delay (1.22) and formulate the delay compensation problem, i.e. synthesis of such a control

$$\boldsymbol{\delta} = \mathfrak{R}(\mathbf{x}, \mathbf{d}), \tag{1.26}$$

that closed-loop system (1.22), (1.26) takes form (1.25). This problem for delay systems is also called the finite spectrum assignment problem in the literature [81].

It is known (for example, [73]) that the solution to this problem is ensured by choosing control (1.26) in the form

$$\boldsymbol{\delta}(t-h)=\mathbf{K}\mathbf{x}(t),$$

or equivalently

$$\boldsymbol{\delta}(t)=\mathbf{K}\mathbf{x}(t+h). \tag{1.27}$$

It is obvious that direct implementation of control (1.27) is generally impossible from the physical perspective, since that requires knowledge of the future state of the plant at the moment of time $t+h$. However, since the plant is the LTI system, it is possible to use the Cauchy formula to calculate the prediction of the future system state.

Theorem 1.1. *If the matrix* $\mathbf{A}$ *is Hurwitz, then the dynamic regulator*

$$\begin{aligned}&\dot{\mathbf{z}}_p=\mathbf{A}\mathbf{z}_p+\mathbf{B}\boldsymbol{\delta}+\mathbf{H}\mathbf{d},\\&\boldsymbol{\delta}=\mathbf{K}e^{\mathbf{A}h}\mathbf{x}+\mathbf{K}\mathbf{z}_p-\mathbf{K}e^{\mathbf{A}h}\mathbf{z}_p(t-h)\end{aligned} \tag{1.28}$$

is equivalent to the regulator (1.27).

Proof. Knowing the current vector $\mathbf{x}(t)$ and vectors $\boldsymbol{\delta}(t)$ and $\mathbf{d}(t)$, defined on the segment $t\in[t-h,t]$, from Cauchy formula we get

$$\mathbf{x}(t+h)=e^{\mathbf{A}h}\,\mathbf{x}(t)+e^{\mathbf{A}h}\int_t^{t+h}e^{-\mathbf{A}(\tau-t)}\left[\mathbf{B}\boldsymbol{\delta}(\tau-h)+\mathbf{H}\mathbf{d}(\tau-h)\right]d\tau. \tag{1.29}$$

Next let us transform the prediction representation (1.29). Let us introduce auxiliary vector variable $\mathbf{z}_p\in E^n$:

$$\mathbf{z}_p(t)=e^{\mathbf{A}t}\int_0^t e^{-\mathbf{A}\theta}\left[\mathbf{B}\boldsymbol{\delta}(\theta)+\mathbf{H}\mathbf{d}(\theta)\right]d\theta.$$

Consider the identity

$$\begin{aligned}&\int_0^t e^{-\mathbf{A}\theta}\left[\mathbf{B}\boldsymbol{\delta}(\theta)+\mathbf{H}\mathbf{d}(\theta)\right]d\theta\equiv\int_0^{t-h}e^{-\mathbf{A}\theta}\left[\mathbf{B}\boldsymbol{\delta}(\theta)+\mathbf{H}\mathbf{d}(\theta)\right]d\theta+\\&+\int_{t-h}^{t}e^{-\mathbf{A}\theta}\left[\mathbf{B}\boldsymbol{\delta}(\theta)+\mathbf{H}\mathbf{d}(\theta)\right]d\theta,\end{aligned}$$

from which it follows that

$$\mathbf{x}(t+h) = e^{\mathbf{A}h}\mathbf{x}(t) + e^{\mathbf{A}h}\int_{t}^{t+h} e^{-\mathbf{A}(\tau-t)}\left[\mathbf{B}\boldsymbol{\delta}(\tau-h) + \mathbf{H}\mathbf{d}(\tau-h)\right]d\tau =$$

$$= e^{\mathbf{A}h}\mathbf{x}(t) + e^{\mathbf{A}t}\int_{t-h}^{t} e^{-\mathbf{A}\theta}\left[\mathbf{B}\boldsymbol{\delta}(\theta) + \mathbf{H}\mathbf{d}(\theta)\right]d\theta =$$

$$= e^{\mathbf{A}h}\mathbf{x}(t) + e^{\mathbf{A}t}\left[\int_{0}^{t} e^{-\mathbf{A}\theta}[\ldots]d\theta - \int_{0}^{t-h} e^{-\mathbf{A}\theta}[\ldots]d\theta\right] = e^{\mathbf{A}h}\mathbf{x}(t) +$$

$$+ e^{\mathbf{A}t}\int_{0}^{t} e^{-\mathbf{A}\theta}[\ldots]d\theta - e^{-\mathbf{A}h}e^{\mathbf{A}h}e^{\mathbf{A}t}\int_{0}^{t-h} e^{-\mathbf{A}\theta}[\ldots]d\theta = e^{\mathbf{A}h}\mathbf{x}(t) +$$

$$+ e^{\mathbf{A}t}\int_{0}^{t} e^{-\mathbf{A}\theta}\left[\mathbf{B}\boldsymbol{\delta}(\theta) + \mathbf{H}\mathbf{d}(\theta)\right]d\theta - e^{\mathbf{A}h}e^{\mathbf{A}(t-h)}\int_{0}^{t-h} e^{-\mathbf{A}\theta}\left[\mathbf{B}\boldsymbol{\delta}(\theta) + \mathbf{H}\mathbf{d}(\theta)\right]d\theta =$$

$$= e^{\mathbf{A}h}\mathbf{x}(t) + \mathbf{z}_p(t) - e^{\mathbf{A}h}\mathbf{z}_p(t-h).$$

Thus the prediction (1.28) can be transformed to the

$$\mathbf{x}(t+h) \equiv \mathbf{z}_p(t) + e^{\mathbf{A}h}\left[\mathbf{x}(t) - \mathbf{z}_p(t-h)\right]. \tag{1.30}$$

Taking into account (1.30), let us rewrite the prediction feedback formula (1.27) in the form

$$\boldsymbol{\delta} = \mathbf{K}e^{\mathbf{A}h}\mathbf{x} + \mathbf{K}\mathbf{z}_p - \mathbf{K}e^{\mathbf{A}h}\mathbf{z}_p(t-h). \tag{1.31}$$

Since, as noted in a number of works (for example, [73]), the direct implementation of feedback (1.31) causes a number of significant problems associated with numerical integration, let us transform the resulting representation of the prediction (1.30). Differentiating the auxiliary variable $\mathbf{z}_p$ we get

$$\begin{aligned}\dot{\mathbf{z}}_p(t) &= \mathbf{A}e^{\mathbf{A}t}\int_{0}^{t} e^{-\mathbf{A}\theta}\left[\mathbf{B}\boldsymbol{\delta}(\theta) + \mathbf{H}\mathbf{d}(\theta)\right]d\theta + e^{\mathbf{A}t}e^{-\mathbf{A}t}\left[\mathbf{B}\boldsymbol{\delta}(t) + \mathbf{H}\mathbf{d}(t)\right] \equiv \\ &\equiv \mathbf{A}\mathbf{z}_p(t) + \mathbf{B}\boldsymbol{\delta}(t) + \mathbf{H}\mathbf{d}(t).\end{aligned} \tag{1.32}$$

Usage of the expression (1.32) allows instead of the feedback (1.31) to get the dynamic regulator (1.28), onboard implementation of which is quite easy. However we should note that such replacement is possible only if matrix $\mathbf{A}$ is Hurwitz. To prove this fact let us consider the characteristic polynomial of the closed-loop system

$$\begin{aligned}
&\dot{\mathbf{x}} = \mathbf{A}\mathbf{x} + \mathbf{B}\boldsymbol{\delta}(t-h) + \mathbf{H}\mathbf{d}(t-h),\\
&\dot{\mathbf{z}}_p = \mathbf{A}\mathbf{z}_p + \mathbf{B}\boldsymbol{\delta} + \mathbf{H}\mathbf{d},\\
&\boldsymbol{\delta} = \mathbf{K}e^{\mathbf{A}h}\mathbf{x} + \mathbf{K}\mathbf{z}_p - \mathbf{K}e^{\mathbf{A}h}\mathbf{z}_p(t-h).
\end{aligned} \tag{1.33}$$

Assume that $\mathbf{x}(0) = \mathbf{z}(0) = \mathbf{0}$, $\boldsymbol{\delta}(t) = \mathbf{d}(t) = \mathbf{0}$ $\forall t < 0$. Excluding $\boldsymbol{\delta}$ and applying Laplace transform we get

$$\begin{aligned}
&\left(\mathbf{E}s - \mathbf{A} - \mathbf{B}\mathbf{K}e^{\mathbf{A}h}e^{-sh}\right)\mathbf{x} + \left(\mathbf{B}\mathbf{K}e^{\mathbf{A}h}e^{-2sh} - \mathbf{B}\mathbf{K}e^{-sh}\right)\mathbf{z}_p = \mathbf{H}\mathbf{d}e^{-sh},\\
&-\mathbf{B}\mathbf{K}e^{\mathbf{A}h}\mathbf{x} + \left(\mathbf{E}s - \mathbf{A} - \mathbf{B}\mathbf{K} + \mathbf{B}\mathbf{K}e^{\mathbf{A}h}e^{-sh}\right)\mathbf{z}_p = \mathbf{H}\mathbf{d}.
\end{aligned} \tag{1.34}$$

Thus, characteristic polynomial of the system (1.33) can be written as

$$\Delta(s) = \det\left(\begin{array}{c|c} \mathbf{E}s - \mathbf{A} - \mathbf{B}\mathbf{K}e^{\mathbf{A}h}e^{-sh} & \mathbf{B}\mathbf{K}e^{\mathbf{A}h}e^{-2sh} - \mathbf{B}\mathbf{K}e^{-sh} \\ \hline -\mathbf{B}\mathbf{K}e^{\mathbf{A}h} & \mathbf{E}s - \mathbf{A} - \mathbf{B}\mathbf{K} + \mathbf{B}\mathbf{K}e^{\mathbf{A}h}e^{-sh} \end{array}\right).$$

Multiplying second row by e^{-sh} and subtracting it from the first one we get

$$\Delta(s) = \det\left(\begin{array}{c|c} \mathbf{E}s - \mathbf{A} & -\mathbf{E}se^{-sh} + \mathbf{A}e^{-sh} \\ \hline -\mathbf{B}\mathbf{K}e^{\mathbf{A}h} & \mathbf{E}s - \mathbf{A} - \mathbf{B}\mathbf{K} + \mathbf{B}\mathbf{K}e^{\mathbf{A}h}e^{-sh} \end{array}\right).$$

Now let us multiply the first column by e^{-sh} and add it to the second one:

$$\Delta(s) = \det\left(\begin{array}{c|c} \mathbf{E}s - \mathbf{A} & \mathbf{0} \\ \hline -\mathbf{B}\mathbf{K}e^{\mathbf{A}h} & \mathbf{E}s - \mathbf{A} - \mathbf{B}\mathbf{K} \end{array}\right) = \det\left(\mathbf{E}s - \mathbf{A}\right)\det\left(\mathbf{E}s - \mathbf{A} - \mathbf{B}\mathbf{K}\right),$$

which shows that the system (1.33) will be stable if and only if the matrix $\mathbf{A}$ is Hurwitz.

Finally, let us consider the question of the equivalence of regulators (1.27) and (1.28). Transfer matrix $\mathbf{F}_{dy}(s)$ of the closed-loop system (1.22), (1.27) from the input $\mathbf{d}$ to the output $\mathbf{y}$ can be described by the expression

$$\mathbf{F}_{dy}(s) = \mathbf{C}\left(\mathbf{E}s - \mathbf{A} - \mathbf{B}\mathbf{K}\right)^{-1}\mathbf{H}e^{-sh}.$$

Not let us multiply the second equation of the system (1.34) by e^{-sh} and subtract it from the first one, thus getting

$$\left(\mathbf{E}s - \mathbf{A}\right)\mathbf{x} - \left(\mathbf{E}s - \mathbf{A}\right)e^{-sh}\mathbf{z}_p = 0,$$

whence it follows that $\mathbf{z}_p = \mathbf{x}e^{sh}$. Substituting the derived expression into the second equation of the system (1.34):

$$\left(\mathbf{E}s - \mathbf{A} - \mathbf{BK}\right)\mathbf{x}e^{sh} = \mathbf{Hd},$$

i.e.

$$\mathbf{x} = \left(\mathbf{E}s - \mathbf{A} - \mathbf{BK}\right)^{-1}\mathbf{Hd}e^{-sh},$$

from where

$$\mathbf{y} = \mathbf{C}\left(\mathbf{E}s - \mathbf{A} - \mathbf{BK}\right)^{-1}\mathbf{Hd}e^{-sh}.$$

Thus the transfer matrix $\mathbf{G}_{dy}(s)$ of the closed-loop system (1.22), (1.28) matches the transfer matrix $\mathbf{F}_{dy}(s)$. ■

Let us additionally note that transfer matrix $\mathbf{G}_{dy}(s)$ matches the transfer matrix of the closed-loop system (1.25) without the delay in control channel.

The above reasoning was about the delay compensation problem in case of the static feedback. However this chapter is focused on the multipurpose structure which is in fact dynamic regulator, i.e. it has its own dynamics. Taking this fact into account, let us consider the generalization of the above method to the case of the arbitrary dynamic regulator usage.

Such generalization is possible for the following reason. Usually, a system of linear equations describing the dynamics of a moving object in the considered operating modes (this is especially typical for marine plants) is stable, but not asymptotically, since the matrix $\mathbf{A}$ has a nonzero eigenvalue. However, this matrix can be considered as Hurwitz with a low degree of stability, since the use of the prediction to some extent compensates the dynamics of the plant.

We will assume that for an auxiliary system without delay in the control channel (1.23), a dynamic regulator on the output of the general form is synthesized as

$$\boldsymbol{\delta} = \mathbf{W}(p)\mathbf{y}, \tag{1.35}$$

where $p = d/dt$.

Regulator (1.35) can be represented in state space with equations

$$\begin{aligned} \dot{\boldsymbol{\xi}} &= \mathbf{A}_k\boldsymbol{\xi} + \mathbf{B}_k\mathbf{y}, \\ \boldsymbol{\delta} &= \mathbf{C}_k\boldsymbol{\xi} + \mathbf{D}_k\mathbf{y}, \end{aligned} \tag{1.36}$$

where $\xi \in E^q$ – regulator state vector. Constant matrices of the system (1.36) satisfy the identity

$$\mathbf{W}(s) \equiv \mathbf{C}_k \left(\mathbf{E}_q s - \mathbf{A}_k\right)^{-1} \mathbf{B}_k + \mathbf{D}_k,$$

where $\mathbf{E}_q$ – identity matrix with dimensions $q \times q$.

Let us transform closed-loop system (1.23), (1.36), excluding $\boldsymbol{\delta}$:

$$\begin{aligned} \dot{\mathbf{x}} &= \left(\mathbf{A} + \mathbf{B}\mathbf{D}_k\mathbf{C}\right)\mathbf{x} + \mathbf{B}\mathbf{C}_k\boldsymbol{\xi} + \mathbf{H}\mathbf{d}(t-h), \\ \dot{\boldsymbol{\xi}} &= \mathbf{B}_k\mathbf{C}\mathbf{x} + \mathbf{A}_k\boldsymbol{\xi}. \end{aligned} \tag{1.37}$$

Next let us close the delay system (1.22) by the stabilizing feedback

$$\boldsymbol{\delta}(t) = \mathbf{W}(p)\mathbf{C}\mathbf{x}(t+h), \tag{1.38}$$

reducing system (1.22) to the form (1.37). System state prediction, as it was mentioned in the previous paragraph, can be calculated using the formula (1.30):

$$\mathbf{x}(t+h) \equiv e^{\mathbf{A}h}\mathbf{x}(t) + \mathbf{z}_p(t) - e^{\mathbf{A}h}\mathbf{z}_p(t-h),$$

The dynamics of the vector function $\mathbf{z}_p(t)$ is defined by the equation

$$\dot{\mathbf{z}}_p = \mathbf{A}\mathbf{z}_p + \mathbf{B}\boldsymbol{\delta} + \mathbf{H}\mathbf{d}.$$

Substituting the prediction into the equation (1.38), we get the compensating regulator on the output

$$\boldsymbol{\delta}(t) = \mathbf{W}(p)\mathbf{C}\left[e^{\mathbf{A}h}\mathbf{x} + \mathbf{z}_p - e^{\mathbf{A}h}\mathbf{z}_p(t-h)\right].$$

Next, to represent the output prediction of the system (1.22), we introduce the auxiliary variable

$$\boldsymbol{\gamma} = \mathbf{C}\left(e^{\mathbf{A}h}\mathbf{x} + \mathbf{z}_p - e^{\mathbf{A}h}\mathbf{z}_p(t-h)\right),$$

which we will consider as the input of the regulator (1.35). By adding the dynamics of the vector function $\mathbf{z}_p(t)$ to the regulator equations, we get the feedback in the form

$$\begin{aligned} \dot{\mathbf{z}}_p &= \mathbf{A}\mathbf{z}_p + \mathbf{B}\boldsymbol{\delta} + \mathbf{H}\mathbf{d}, \\ \dot{\boldsymbol{\xi}} &= \mathbf{A}_k\boldsymbol{\xi} + \mathbf{B}_k\boldsymbol{\gamma}, \\ \boldsymbol{\delta} &= \mathbf{C}_k\boldsymbol{\xi} + \mathbf{D}_k\boldsymbol{\gamma}, \\ \boldsymbol{\gamma} &= \mathbf{C}\left(e^{\mathbf{A}h}\mathbf{x} + \mathbf{z}_p - e^{\mathbf{A}h}\mathbf{z}_p(t-h)\right). \end{aligned} \tag{1.39}$$

It is important to note that the generalized dynamic regulator (1.39) allows the control system delay compensation based on the feedback which stabilizes the system without the delay while keeping the transfer matrix of the original system.

Theorem 1.2. *If matrix* $\mathbf{A}$ *is Hurwitz, then the dynamic regulator (1.39) is equivalent to the regulator (1.38).*

Proof. Consider the closed-loop system equations (1.22), (1.39):

$$\begin{aligned}
&\dot{\mathbf{x}} = \mathbf{A}\mathbf{x} + \mathbf{B}\boldsymbol{\delta}(t-h) + \mathbf{H}\mathbf{d}(t-h),\\
&\dot{\mathbf{z}}_p = \mathbf{A}\mathbf{z}_p + \mathbf{B}\boldsymbol{\delta} + \mathbf{H}\mathbf{d},\\
&\dot{\boldsymbol{\xi}} = \mathbf{A}_k\boldsymbol{\xi} + \mathbf{B}_k\boldsymbol{\gamma},\\
&\boldsymbol{\delta} = \mathbf{C}_k\boldsymbol{\xi} + \mathbf{D}_k\boldsymbol{\gamma},\\
&\boldsymbol{\gamma} = \mathbf{C}\left(e^{\mathbf{A}h}\mathbf{x} + \mathbf{z}_p - e^{\mathbf{A}h}\mathbf{z}_p(t-h)\right).
\end{aligned} \tag{1.40}$$

Exclude the variable $\boldsymbol{\gamma}$:

$$\begin{aligned}
&\dot{\mathbf{x}} = \mathbf{A}\mathbf{x} + \mathbf{B}\boldsymbol{\delta}(t-h) + \mathbf{H}\mathbf{d}(t-h),\\
&\dot{\mathbf{z}}_p = \mathbf{A}\mathbf{z}_p + \mathbf{B}\boldsymbol{\delta} + \mathbf{H}\mathbf{d},\\
&\dot{\boldsymbol{\xi}} = \mathbf{A}_k\boldsymbol{\xi} + \mathbf{B}_k\mathbf{C}\left(e^{\mathbf{A}h}\mathbf{x} + \mathbf{z}_p - e^{\mathbf{A}h}\mathbf{z}_p(t-h)\right),\\
&\boldsymbol{\delta} = \mathbf{C}_k\boldsymbol{\xi} + \mathbf{D}_k\mathbf{C}\left(e^{\mathbf{A}h}\mathbf{x} + \mathbf{z}_p - e^{\mathbf{A}h}\mathbf{z}_p(t-h)\right).
\end{aligned}$$

Then we substitute the expression for $\boldsymbol{\delta}$ into the first two equations:

$$\begin{aligned}
&\dot{\mathbf{x}} = \mathbf{A}\mathbf{x} + \mathbf{B}\mathbf{C}_k\boldsymbol{\xi}(t-h) + \mathbf{B}\mathbf{D}_k\mathbf{C}\left(e^{\mathbf{A}h}\mathbf{x}(t-h) + \mathbf{z}_p(t-h) - e^{\mathbf{A}h}\mathbf{z}_p(t-2h)\right) + \mathbf{H}\mathbf{d}(t-h),\\
&\dot{\mathbf{z}}_p = \mathbf{A}\mathbf{z}_p + \mathbf{B}\mathbf{C}_k\boldsymbol{\xi} + \mathbf{B}\mathbf{D}_k\mathbf{C}\left(e^{\mathbf{A}h}\mathbf{x} + \mathbf{z}_p - e^{\mathbf{A}h}\mathbf{z}_p(t-h)\right) + \mathbf{H}\mathbf{d},\\
&\dot{\boldsymbol{\xi}} = \mathbf{A}_k\boldsymbol{\xi} + \mathbf{B}_k\mathbf{C}\left(e^{\mathbf{A}h}\mathbf{x} + \mathbf{z}_p - e^{\mathbf{A}h}\mathbf{z}_p(t-h)\right).
\end{aligned}$$

Applying the Laplace transform:

$$\begin{aligned}
&\left(\mathbf{E}s - \mathbf{A} - \mathbf{B}\mathbf{D}_k\mathbf{C}e^{\mathbf{A}h}e^{-hs}\right)\mathbf{x} - \left(\mathbf{B}\mathbf{D}_k\mathbf{C}e^{-hs} - \mathbf{B}\mathbf{D}_k\mathbf{C}e^{\mathbf{A}h}e^{-2hs}\right)\mathbf{z}_p -\\
&-\mathbf{B}\mathbf{C}_k\boldsymbol{\xi}e^{-hs} = \mathbf{H}\mathbf{d}e^{-hs},\\
&-\mathbf{B}\mathbf{D}_k\mathbf{C}e^{\mathbf{A}h}\mathbf{x} + \left(\mathbf{E}s - \mathbf{A} - \mathbf{B}\mathbf{D}_k\mathbf{C} + \mathbf{B}\mathbf{D}_k\mathbf{C}e^{\mathbf{A}h}e^{-hs}\right)\mathbf{z}_p - \mathbf{B}\mathbf{C}_k\boldsymbol{\xi} = \mathbf{H}\mathbf{d},\\
&\mathbf{B}_k\mathbf{C}e^{\mathbf{A}h}\mathbf{x} + \left(\mathbf{B}_k\mathbf{C} - \mathbf{B}_k\mathbf{C}e^{\mathbf{A}h}e^{-hs}\right)\mathbf{z}_p - (\mathbf{E}s - \mathbf{A}_k)\boldsymbol{\xi} = \mathbf{0}.
\end{aligned} \tag{1.41}$$

Thus, the characteristic polynomial of the closed-loop system (1.40) is defined by the expression

$$\Delta_d(s)=\det\left(\begin{array}{c|c|c}\mathbf{E}s-\mathbf{A}-\mathbf{B}\mathbf{D}_k\mathbf{C}e^{\mathbf{A}h}e^{-hs} & -\mathbf{B}\mathbf{D}_k\mathbf{C}e^{-hs}+\mathbf{B}\mathbf{D}_k\mathbf{C}e^{\mathbf{A}h}e^{-2hs} & -\mathbf{B}\mathbf{C}_k e^{-hs}\\ \hline -\mathbf{B}\mathbf{D}_k\mathbf{C}e^{\mathbf{A}h} & \mathbf{E}s-\mathbf{A}-\mathbf{B}\mathbf{D}_k\mathbf{C}+\mathbf{B}\mathbf{D}_k\mathbf{C}e^{\mathbf{A}h}e^{-hs} & -\mathbf{B}\mathbf{C}_k\\ \hline \mathbf{B}_k\mathbf{C}e^{\mathbf{A}h} & \mathbf{B}_k\mathbf{C}-\mathbf{B}_k\mathbf{C}e^{\mathbf{A}h}e^{-hs} & \mathbf{E}s-\mathbf{A}_k\end{array}\right).$$

Multiplying second row by e^{-hs} and substituting from the first one, we get

$$\Delta_d(s)=\det\left(\begin{array}{c|c|c}\mathbf{E}s-\mathbf{A} & -(\mathbf{E}s-\mathbf{A})e^{-hs} & \mathbf{0}\\ \hline -\mathbf{B}\mathbf{D}_k\mathbf{C}e^{\mathbf{A}h} & \mathbf{E}s-\mathbf{A}-\mathbf{B}\mathbf{D}_k\mathbf{C}+\mathbf{B}\mathbf{D}_k\mathbf{C}e^{\mathbf{A}h}e^{-hs} & -\mathbf{B}\mathbf{C}_k\\ \hline \mathbf{B}_k\mathbf{C}e^{\mathbf{A}h} & \mathbf{B}_k\mathbf{C}-\mathbf{B}_k\mathbf{C}e^{\mathbf{A}h}e^{-hs} & \mathbf{E}s-\mathbf{A}_k\end{array}\right).$$

Now let us multiply the first column by e^{-hs} and substitute from the second one, then

$$\Delta_d(s)=\det\left(\begin{array}{c|c|c}\mathbf{E}s-\mathbf{A} & \mathbf{0} & \mathbf{0}\\ \hline -\mathbf{B}\mathbf{D}_k\mathbf{C}e^{\mathbf{A}h} & \mathbf{E}s-\mathbf{A}-\mathbf{B}\mathbf{D}_k\mathbf{C} & -\mathbf{B}\mathbf{C}_k\\ \hline \mathbf{B}_k\mathbf{C}e^{\mathbf{A}h} & \mathbf{B}_k\mathbf{C} & \mathbf{E}s-\mathbf{A}_k\end{array}\right).$$

Thus we get that

$$\Delta_d(s)=\det(\mathbf{E}s-\mathbf{A})\det\left(\begin{array}{c|c}\mathbf{E}s-\mathbf{A}-\mathbf{B}\mathbf{D}_k\mathbf{C} & -\mathbf{B}\mathbf{C}_k\\ \hline \mathbf{B}_k\mathbf{C} & \mathbf{E}s-\mathbf{A}_k\end{array}\right)=\Delta_0(s)\Delta_1(s),$$

where $\Delta_1(s)$ – characteristic polynomial of the asymptotically stable closed-loop system

$$\begin{aligned}\dot{\mathbf{x}}&=\mathbf{A}\mathbf{x}+\mathbf{B}\boldsymbol{\delta},\\ \dot{\boldsymbol{\xi}}&=\mathbf{A}_k\boldsymbol{\xi}+\mathbf{B}_k\mathbf{y},\\ \boldsymbol{\delta}&=\mathbf{C}_k\boldsymbol{\xi}+\mathbf{D}_k\mathbf{y}.\end{aligned}$$

Therefore the polynomial $\Delta_d(s)$ is Hurwitz if and only if the matrix $\mathbf{A}$ is Hurwitz.

Now let us prove the equivalency of the regulators (1.38) and (1.39). First of all, notice that the transfer matrix $\mathbf{F}_{dy}(s)$ of the closed-loop system (1.37) from the input $\mathbf{d}$ to the output $\mathbf{y}$ can be described by the expression

$$\mathbf{F}_{dy}(s)=\mathbf{C}\left(\mathbf{E}s-\mathbf{A}-\mathbf{B}\mathbf{D}_k\mathbf{C}-\mathbf{B}\mathbf{C}_k(\mathbf{E}s-\mathbf{A}_k)^{-1}\mathbf{B}_k\mathbf{C}\right)^{-1}\mathbf{H}e^{-hs}. \qquad (1.42)$$

Now let us return to the system (1.41). Multiplying the second equation by e^{-hs} and substituting from the first one, we get

$$(\mathbf{E}s-\mathbf{A})\mathbf{x}-(\mathbf{E}s-\mathbf{A})e^{-hs}\mathbf{z}_p=0,$$
$$-\mathbf{B}\mathbf{D}_k\mathbf{C}e^{\mathbf{A}h}\mathbf{x}+\left(\mathbf{E}s-\mathbf{A}-\mathbf{B}\mathbf{D}_k\mathbf{C}+\mathbf{B}\mathbf{D}_k\mathbf{C}e^{\mathbf{A}h}e^{-hs}\right)\mathbf{z}_p-\mathbf{B}\mathbf{C}_k\boldsymbol{\xi}=\mathbf{H}\mathbf{d},$$
$$\mathbf{B}_k\mathbf{C}e^{\mathbf{A}h}\mathbf{x}+\left(\mathbf{B}_k\mathbf{C}-\mathbf{B}_k\mathbf{C}e^{\mathbf{A}h}e^{-hs}\right)\mathbf{z}_p-(\mathbf{E}s-\mathbf{A}_k)\boldsymbol{\xi}=\mathbf{0}.$$

From the first equation let us express $\mathbf{z}_p=e^{hs}\mathbf{x}$ and substitute to the rest:

$$-\mathbf{B}\mathbf{D}_k\mathbf{C}e^{\mathbf{A}h}\mathbf{x}+\left(\mathbf{E}s-\mathbf{A}-\mathbf{B}\mathbf{D}_k\mathbf{C}+\mathbf{B}\mathbf{D}_k\mathbf{C}e^{\mathbf{A}h}e^{-hs}\right)e^{hs}\mathbf{x}-\mathbf{B}\mathbf{C}_k\boldsymbol{\xi}=\mathbf{H}\mathbf{d},$$
$$\mathbf{B}_k\mathbf{C}e^{\mathbf{A}h}\mathbf{x}+\left(\mathbf{B}_k\mathbf{C}-\mathbf{B}_k\mathbf{C}e^{\mathbf{A}h}e^{-hs}\right)e^{hs}\mathbf{x}-(\mathbf{E}s-\mathbf{A}_k)\boldsymbol{\xi}=\mathbf{0}.$$

Transforming:

$$(\mathbf{E}s-\mathbf{A}-\mathbf{B}\mathbf{D}_k\mathbf{C})e^{hs}\mathbf{x}-\mathbf{B}\mathbf{C}_k\boldsymbol{\xi}=\mathbf{H}\mathbf{d},$$
$$\mathbf{B}_k\mathbf{C}e^{hs}\mathbf{x}-(\mathbf{E}s-\mathbf{A}_k)\boldsymbol{\xi}=\mathbf{0}.$$

From the last equation let us express $\boldsymbol{\xi}=(\mathbf{E}s-\mathbf{A}_k)^{-1}\mathbf{B}_k\mathbf{C}e^{hs}\mathbf{x}$ and substitute to the first one:

$$(\mathbf{E}s-\mathbf{A}-\mathbf{B}\mathbf{D}_k\mathbf{C})e^{hs}\mathbf{x}-\mathbf{B}\mathbf{C}_k(\mathbf{E}s-\mathbf{A}_k)^{-1}\mathbf{B}_k\mathbf{C}e^{hs}\mathbf{x}=\mathbf{H}\mathbf{d},$$

from where:

$$\mathbf{x}=\left(\mathbf{E}s-\mathbf{A}-\mathbf{B}\mathbf{D}_k\mathbf{C}-\mathbf{B}\mathbf{C}_k(\mathbf{E}s-\mathbf{A}_k)^{-1}\mathbf{B}_k\mathbf{C}\right)^{-1}\mathbf{H}\mathbf{d}e^{-hs},$$

therefore

$$\mathbf{y}=\mathbf{C}\left(\mathbf{E}s-\mathbf{A}-\mathbf{B}\mathbf{D}_k\mathbf{C}-\mathbf{B}\mathbf{C}_k(\mathbf{E}s-\mathbf{A}_k)^{-1}\mathbf{B}_k\mathbf{C}\right)^{-1}\mathbf{H}\mathbf{d}e^{-hs}.$$

Thus, transfer matrix of the closed-loop system (1.22), (1.39) matches the transfer matrix (1.42) of the closed-loop system (1.37). ■

It is worth noting the fact that feedback (1.39) requires knowledge of the full system state vector at the each time moment. In case of the compensation on the output it can be shown that it is possible to keep the dynamics not of the initial plant but the auxiliary in the form [10]

$$\dot{\mathbf{x}}=\mathbf{A}\mathbf{x}+\mathbf{B}\boldsymbol{\delta}+\mathbf{H}\mathbf{d}(t-h),$$
$$\boldsymbol{\eta}=\mathbf{C}_1\mathbf{x},\ \mathbf{C}_1=\mathbf{C}e^{-\mathbf{A}h},$$

closed by some dynamic regulator

$$\boldsymbol{\delta}=\widetilde{\mathbf{W}}(p)\boldsymbol{\eta}.$$

However we will further use feedback of the form (1.39), because the focus of this work is keeping the dynamics of the initial system (1.22) by the delay compensation based on the multipurpose regulator. Particular structure of the multipurpose delay compensating feedback for the moving plant (e.g. marine vessel) can be expressed as

$$\begin{aligned}
&\dot{\mathbf{z}}_p = \mathbf{A}\mathbf{z}_p + \mathbf{B}\boldsymbol{\delta} + \mathbf{H}\mathbf{d},\\
&\dot{\mathbf{z}} = \mathbf{A}\mathbf{z} + \mathbf{B}\boldsymbol{\delta}_m + \mathbf{G}(\boldsymbol{\gamma}_k - \mathbf{C}\mathbf{z}),\\
&\dot{\boldsymbol{\delta}}_m = \mathbf{k}\mathbf{z} + \mathbf{k}_0\boldsymbol{\delta}_m + \boldsymbol{\nu}_0\boldsymbol{\gamma}_k + \boldsymbol{\gamma}\mathbf{p} + \mathbf{m}_f(\boldsymbol{\gamma}_k - \mathbf{C}\mathbf{z}),\\
&\dot{\mathbf{p}} = \boldsymbol{\alpha}\mathbf{p} + \boldsymbol{\beta}(\boldsymbol{\gamma}_k - \mathbf{C}\mathbf{z}),\\
&\boldsymbol{\gamma}_k = \mathbf{C}\left(e^{\mathbf{A}h}\mathbf{x} + \mathbf{z}_p - e^{\mathbf{A}h}\mathbf{z}_p(t-h)\right),\\
&\boldsymbol{\delta}_z = \boldsymbol{\delta}_m,
\end{aligned}$$

where $\boldsymbol{\delta}_m$ – model actuator, $\boldsymbol{\delta}_z$ – current deflection, calculated for the stabilization taking the delay into account.

The following feature should be noted. Feedback equations (1.39) imply that the calculated control signal is supplied to the plant directly. However, in reality, for a moving object, it is not the deflection of the rudders itself that is controlled, but rather the change rate. Because of this fact to ensure convergence of the deflection $\boldsymbol{\delta}$ to the calculated position $\boldsymbol{\delta}_z$ the actuator drive can be fed with the control signal

$$\mathbf{u} = \mathbf{k}_u(\boldsymbol{\delta}_z - \boldsymbol{\delta}),$$

transforming the actuator equation to the form

$$\dot{\boldsymbol{\delta}} = \mathbf{k}_u(\boldsymbol{\delta}_z - \boldsymbol{\delta}),$$

where $\mathbf{k}_u > 0$ – diagonal matrix with sufficiently large elements for rapid convergence of the dynamic processes.

Next we introduce the notation

$$\mathbf{A}_c = \left(\begin{array}{c|c|c} \mathbf{A}-\mathbf{G}\mathbf{C} & \mathbf{B} & \mathbf{0}_{n\times n_1} \\ \hline \mathbf{k}-\mathbf{m}_f\mathbf{C} & \mathbf{k}_0 & \boldsymbol{\gamma}_k \\ \hline -\boldsymbol{\beta}\mathbf{C} & \mathbf{0}_{n_1\times m} & \boldsymbol{\alpha} \end{array}\right),\ \mathbf{B}_c = \left(\begin{array}{c} \mathbf{G} \\ \hline \boldsymbol{\nu}_0 + \mathbf{m}_f \\ \hline \boldsymbol{\beta} \end{array}\right),\ \boldsymbol{\xi}_c = \begin{pmatrix} \mathbf{z} \\ \boldsymbol{\delta}_m \\ \mathbf{p} \end{pmatrix},$$

$$\mathbf{C}_c = \left(\mathbf{0}_{m\times n} \mid \mathbf{1}_{m\times m} \mid \mathbf{0}_{m\times n_1}\right).$$

Taking into account the introduced notations, we express the equations of the multipurpose delay-compensating regulator for arbitrary moving plant stabilization in the form

$$\begin{aligned}
&\dot{\mathbf{z}}_p = \mathbf{A}\mathbf{z}_p + \mathbf{B}\boldsymbol{\delta} + \mathbf{H}\mathbf{d},\\
&\dot{\boldsymbol{\xi}}_c = \mathbf{A}_c\boldsymbol{\xi}_c + \mathbf{B}_c\boldsymbol{\gamma}_k,\\
&\boldsymbol{\gamma}_k = \mathbf{C}\left(e^{\mathbf{A}h}\mathbf{x} + \mathbf{z}_p - e^{\mathbf{A}h}\mathbf{z}_p(t-h)\right),\\
&\boldsymbol{\delta}_z = \mathbf{C}_c\boldsymbol{\xi}_c,\\
&\mathbf{u} = \mathbf{k}_u(\boldsymbol{\delta}_z - \boldsymbol{\delta}).
\end{aligned} \tag{1.43}$$

Closed-loop system (1.22), (1.43) scheme is shown in Fig. 1.2.

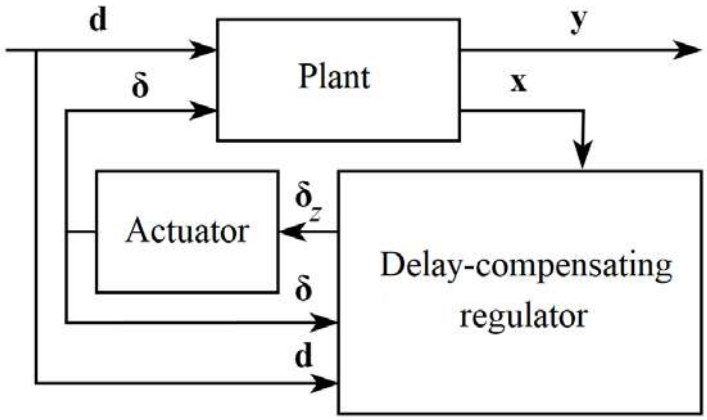

Fig. 1.2. Closed-loop control system with the delay-compensating regulator (1.43).

Taking into account the fact that multipurpose delay compensating regulator is subject to the implementation on the digital onboard device, let us discretize the feedback (1.43) with the given discretization period T_d. Let us pay attention to the fact that when calculating the auxiliary variable $\boldsymbol{\gamma}_k$ in the discrete time the exponents must be replaced with the powers of matrix $\mathbf{A}_d$, which is in fact the descretized version of the matrix $\mathbf{A}$. As a result, we obtain a system of difference equations

$$
\begin{aligned}
&\mathbf{z}_p[n+1] = \mathbf{A}_d \mathbf{z}_p[n] + \mathbf{B}_d \boldsymbol{\delta}[n] + \mathbf{H}_d \mathbf{d}[n], \\
&\boldsymbol{\xi}_c[n+1] = \mathbf{A}_{cd} \boldsymbol{\xi}_c[n] + \mathbf{B}_{cd} \boldsymbol{\gamma}_k[n], \\
&\boldsymbol{\gamma}_k[n] = \mathbf{C}\left(\mathbf{A}^{n_h} \mathbf{x}[n] + \mathbf{z}_p[n] - \mathbf{A}^{n_h} \mathbf{z}_p[n-n_h]\right), \\
&\boldsymbol{\delta}_z[n] = \mathbf{C}_c \boldsymbol{\xi}_c[n], \\
&\mathbf{u}[n] = \mathbf{k}_u(\boldsymbol{\delta}_z[n] - \boldsymbol{\delta}[n]),
\end{aligned}
\tag{1.44}
$$

where $n_h = [h/T_d]$.

Discrete regulator (1.44) is subject to the direct implementation on the plant onboard equipment, while the linear nature of the derived equations implies a relatively small amount of necessary calculations, which allows the use of fairly low-power and inexpensive computing devices.

1.4. Conclusions

The approach presented in this chapter makes it possible to synthesize stabilizing multipurpose regulators taking into account the set of requirements for the dynamics quality of the plant in various operating modes. Moreover, individual elements of such regulators can be turned off under appropriate conditions, and the initial rather complex synthesis problem is divided into a number of simpler problems that can be solved relatively independent of each other. It is also shown that with the help of a special transformation of the initial regulator, it is possible to compensate the delay in the channels of the control and external disturbances.

It is worth noting that the specific form of the equations of system (1.16) may differ depending on the problem being solved. For example, the next two chapters will examine control problems with visual feedback, as well as control of a nonlinear system using the feedback linearization method. In these cases, the multipurpose regulator takes appropriate specific forms different from (1.16). However, the general structure, consisting of an asymptotic observer, a dynamic corrector and a control signal equation remains unchanged, as well as the ideology of searching of the values of the tunable elements of this structure.

Chapter 2. Multipurpose Visual Positioning of the Moving Plants Considering Delay

This chapter discusses the use of a multipurpose approach to solve the problem of a moving plant positioning using visual information in a feedback loop, taking into account a set of requirements for the motion of an object in various operating modes, as well as taking into account the presence of delay in the control channel.

Paragraph 2.1 provides the problem formulation. Paragraph 2.2 is devoted to the multipurpose regulator synthesis procedure. Paragraph 2.3 describes the transformation of a multipurpose regulator for the delay compensation. Paragraphs 2.4 and 2.5 are devoted to performance demonstration of the above approach using the experiments with computer models of fully-actuated and underactuated mobile robots as examples.

2.1. Problem Formulation

Let us consider an arbitrary moving plant with mathematical model that can be described using the equations

$$\begin{aligned} \mathbf{M}\dot{\boldsymbol{\upsilon}} + \mathbf{D}\boldsymbol{\upsilon} &= \mathbf{u} + \tilde{\mathbf{d}}(t), \\ \dot{\boldsymbol{\eta}} &= \mathbf{R}(\boldsymbol{\eta})\boldsymbol{\upsilon}, \end{aligned} \tag{2.1}$$

where $\mathbf{M} = \mathbf{M}^{\mathrm{T}}$ – positive definite inertia matrix, $\mathbf{D}$ – positive definite damping matrix, $\boldsymbol{\upsilon} \in E^6$ – linear and angular velocities vector, $\mathbf{u} \in E^6$ – control signal, $\tilde{\mathbf{d}}(t) \in E^6$ – external disturbances vector, $\boldsymbol{\eta} \in E^6$ – vector describing the position of a rigid body in space relative to a fixed coordinate system, $\mathbf{R}(\boldsymbol{\eta})$ – rotation matrix with $\det \mathbf{R}(\boldsymbol{\eta}) \neq 0$, $\forall \boldsymbol{\eta}$. For convenience, let us solve the first equation of system (2.1) with respect to the derivative:

$$\begin{aligned} \dot{\boldsymbol{\upsilon}} &= \mathbf{A}\boldsymbol{\upsilon} + \mathbf{B}\mathbf{u} + \mathbf{d}(t), \\ \dot{\boldsymbol{\eta}} &= \mathbf{R}(\boldsymbol{\eta})\boldsymbol{\upsilon}, \end{aligned} \tag{2.2}$$

where $\mathbf{A} = -\mathbf{M}^{-1}\mathbf{D}$, $\mathbf{B} = \mathbf{M}^{-1}$, $\mathbf{d}(t) = \mathbf{B}\tilde{\mathbf{d}}(t)$.

Let us consider the coordinate systems used for plant mathematical models formulation and for positioning visual targets (Fig. 2.1). Let us denote the inertial coordinate system rigidly connected to the ground as $O_g x_g y_g z_g$. This system is stationary; the position of the plant and visual markers in space is specified relative to it. The system is right-handed, $O_g z_g$ axis is directed upwards, $O_g x_g y_g$ – horizontal plane.

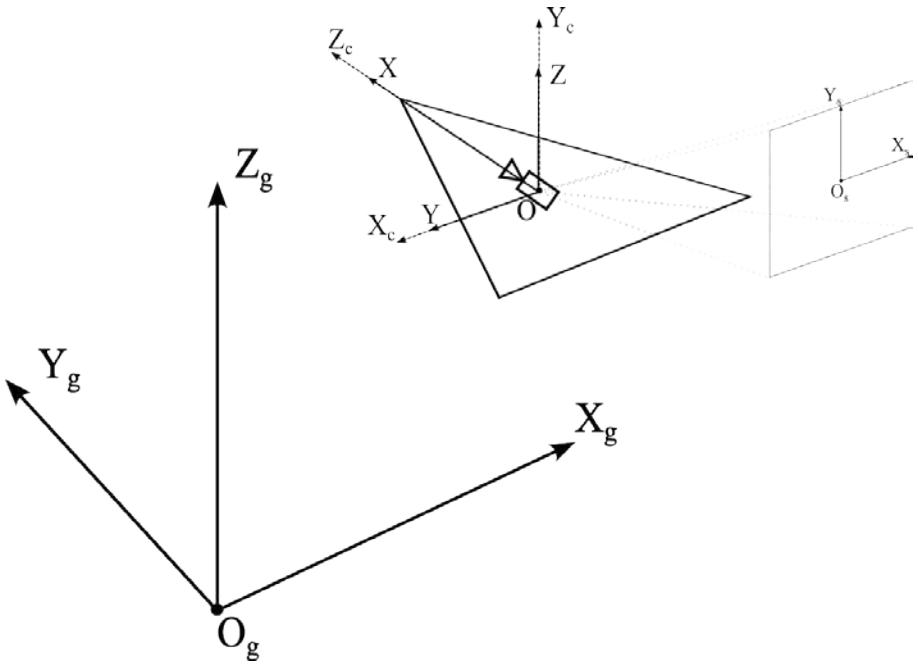

Fig. 2.1. Reference frames.

The body frame $Oxyz$ is located at the center of mass of the plant and is rigidly connected to it. The system is right-handed, Oz axis is directed upwards, Ox axis is longitudinal, Oy axis is directed to the left side of the plant. The velocity vectors of the plant are projected onto the axes of this system.

Let us assume that in the geometric center of a plant (pretend that it coincides with the center of mass) there is a rigidly fixed video camera, the optical axis of which is directed along the Ox axis, and the optical center is located at the point O. Let $Ox_c y_c z_c$ be the reference frame connected with the camera. Along with that Oz_c axis of the camera reference frame is aligned with Ox axis of the body

frame, Ox_c axis is aligned with the Oy axis, and Oy_c axis – with Oz. Let us also consider the normalized image plane [51], located at the focal length $f = 1$ from the optical center and perpendicular to the optical axis. Let us define reference frame $O_s x_s y_s$ in this plane, center of which is located on the optical axis, $O_s y_s$ axis is aligned with Oy_c axis, and $O_s x_s$ axis is opposite to Ox_c axis.

Let (X_c, Y_c, Z_c) be the coordinates of some point in the space, defined in the camera reference frame. Then projections of this point onto the image plane can be calculated using the formulas [51]

$$x_s = -\frac{X_c}{Z_c}, y_s = \frac{Y_c}{Z_c}.$$

We will assume that there is always a certain visual marker in the camera's field of view, represented in the image plane by a set of points $\mathbf{s} = (x_i, y_i)$, $i = \overline{1, N}$, which, in turn, are projections of the marker points (X_i, Y_i, Z_i), $i = \overline{1, N}$, defined in the camera reference frame. Let us formulate the problem of positioning the plant relative to a marker in such a way that the projections of the marker points $\mathbf{s}$ on the image must be in the desired position $\mathbf{s}_d$, i.e. it is necessary to ensure the fulfillment of the condition:

$$\lim_{t \to +\infty} \mathbf{s}(t) = \mathbf{s}_d . \tag{2.3}$$

Let us supplement the system (2.2) with an equation for the dynamics of changes in the marker points projections onto the image plane in accordance with the mathematical models described in [78]:

$$\dot{\mathbf{s}} = \mathbf{L}_s(\mathbf{s}, \mathbf{Z}_c)\boldsymbol{\upsilon} + \mathbf{d}_c(t). \tag{2.4}$$

Vector $\mathbf{Z}_c \in E^N$ consists of the values Z_i, $i = \overline{1, N}$ for each projected marker point, $\mathbf{d}_c(t)$ – external disturbances vector, $\mathbf{L}_s(\mathbf{s}, \mathbf{Z}_c)$ – interaction matrix, components of which for each pair (x_i, y_i) are defined as follows:

$$\mathbf{L}_s(x_i, y_i, Z_i) = \begin{pmatrix} \frac{x_i}{Z_i} & -\frac{1}{Z_i} & 0 & y_i & x_i y_i & -(1+x_i^2) \\ \frac{y_i}{Z_i} & 0 & -\frac{1}{Z_i} & -x_i & 1+y_i^2 & -x_i y_i \end{pmatrix}.$$

System (2.4) must be supplemented with the vector $\mathbf{Z}_c$ dynamics equation:

$$\dot{\mathbf{Z}}_c = \mathbf{L}_z(\mathbf{s}, \mathbf{Z}_c)\boldsymbol{\upsilon} + \mathbf{d}_z(t), \tag{2.5}$$

where $\mathbf{d}_z(t)$ – external disturbance, $\mathbf{L}_z(\mathbf{s}, \mathbf{Z}_c)$ – matrix with rows

$$\mathbf{L}_z(x_i, y_i, Z_i) = \begin{pmatrix} -1 & 0 & 0 & 0 & -y_i Z_i & x_i Z_i \end{pmatrix}.$$

Thus, the dynamics of a moving plant and marker projections in the image plane are completely defined by equations (2.2), (2.4), (2.5). We will assume that the vectors $\boldsymbol{\upsilon}$, $\mathbf{s}$ and $\mathbf{Z}_c$ are available for direct measurement.

Additionally, we introduce the error vector $\mathbf{e} = \mathbf{s} - \mathbf{s}_d$ between the actual and the desired positions of the points in the image plane. The error dynamics, accordingly, can be described by the equation

$$\dot{\mathbf{e}} = \mathbf{L}_s(\mathbf{e}, \mathbf{Z}_c)\boldsymbol{\upsilon} + \mathbf{d}_c(t). \tag{2.6}$$

Taking into account the introduced notation, condition (2.3) can be rewritten in the form

$$\lim_{t \to +\infty} \mathbf{e}(t) = \mathbf{0}. \tag{2.7}$$

To achieve the control goal (2.7), within the framework of a multipurpose approach, we consider three basic operating modes of the plant motion.

1) *The proper motion* is characterized by the absence of external disturbances, while the control goal is described by equation (2.7). In this mode, the main requirements for the controlled motion dynamics are to ensure the stability of the equilibrium position and to satisfy the specified restrictions on overshoot and the settling time.

2) *Forced motion under the influence of a constant external disturbance* is characterized by the absence of a reference signal, zero initial conditions, as well as the presence of constant external disturbances

$$\mathbf{d}(t) \equiv \mathbf{d}_0, \ \mathbf{d}_c(t) \equiv \mathbf{d}_{c0}, \ \mathbf{d}_z(t) \equiv \mathbf{d}_{z0}.$$

The control goal is to compensate for disturbances and ensure astatism of the controlled output $\mathbf{s}(t)$ of the closed-loop system. The main requirement for dynamics in this mode is satisfying the specified limit on the maximum permissible deviation of the controlled variables $\mathbf{s}(t)$.

3) *Forced motion under the influence of a periodic external disturbance* is determined by the presence of a disturbance in the form of a polyharmonic signal also under zero initial conditions and the absence of a reference signal. In this mode, the quality of dynamics is determined by minimizing the control intensity while maintaining the accuracy of system stabilization.

2.2. Multipurpose Control Law Synthesis

Let us set the task of the multipurpose control law synthesis that ensures the achievement of the control goal (2.7) and the fulfillment of all requirements in the operating modes given above. Let us introduce the multipurpose structure of the control law, which includes the following elements:

1) asymptotic observer

$$\begin{aligned} \dot{\mathbf{z}}_\upsilon &= \mathbf{A}\mathbf{z}_\upsilon + \mathbf{B}\mathbf{u} + \mathbf{H}_\upsilon(\boldsymbol{\upsilon} - \mathbf{z}_\upsilon), \\ \dot{\mathbf{z}}_e &= \mathbf{L}_s(\mathbf{e}, \mathbf{Z}_c)\mathbf{z}_\upsilon + \mathbf{H}_e(\mathbf{e} - \mathbf{z}_e), \end{aligned} \tag{2.8}$$

2) dynamic corrector

$$\begin{aligned} \dot{\mathbf{p}} &= \boldsymbol{\alpha}\mathbf{p} + \boldsymbol{\beta}_\upsilon(\boldsymbol{\upsilon} - \mathbf{z}_\upsilon) + \boldsymbol{\beta}_e(\mathbf{e} - \mathbf{z}_e), \\ \boldsymbol{\zeta} &= \boldsymbol{\gamma}\mathbf{p} + \boldsymbol{\mu}_\upsilon(\boldsymbol{\upsilon} - \mathbf{z}_\upsilon) + \boldsymbol{\mu}_e(\mathbf{e} - \mathbf{z}_e), \end{aligned} \tag{2.9}$$

3) control signal equation

$$\mathbf{u} = -\mathbf{K}_\upsilon\mathbf{z}_\upsilon - \mathbf{K}_e\mathbf{z}_e + \boldsymbol{\zeta}. \tag{2.10}$$

Here $\mathbf{z}_\upsilon \in E^6$ and $\mathbf{z}_e \in E^{2N}$ – asymptotic observer state vectors; $\mathbf{p} \in E^{n_p}$ – dynamic corrector state vector; $\boldsymbol{\zeta} \in E^6$ – dynamic corrector output. Tunable elements of the multipurpose structure (2.8) – (2.10) are matrices:

a) $\mathbf{K}_\upsilon$ and $\mathbf{K}_e$ of the basic control law;

b) $\mathbf{H}_\upsilon$ and $\mathbf{H}_e$ of the asymptotic observer;

c) $\boldsymbol{\alpha}$, $\boldsymbol{\beta}_{\upsilon}$, $\boldsymbol{\beta}_{e}$, $\boldsymbol{\gamma}$, $\boldsymbol{\mu}_{\upsilon}$, $\boldsymbol{\mu}_{e}$ of the dynamic corrector.

The asymptotic observer (2.8) provides an estimate of the state variables that are not available for direct measurement, and can also influence the response of the closed-loop system (2.2), (2.8) – (2.10) to external disturbances by the tunable elements selection. The observer's state vector is also fed to the input of the dynamic corrector, the main purpose of which is to compensate for external disturbances.

The search of the tunable elements, which is the essence of the multipurpose synthesis problem, can be formalized as an optimization problem. One of the main advantages of the multipurpose approach is the ability to search for tunable elements relatively independently of each other [5–9]. Individual elements of the multipurpose structure can also be turned on and off depending on the current operating mode.

Let us consider sequentially the tasks of searching the tunable elements of a multipurpose structure (2.8) – (2.10) in accordance with the requirements in the above mentioned operating modes.

1) Basic control law synthesis.

Basic control law is defined by the equation

$$\mathbf{u} = -\mathbf{K}_{\upsilon}\boldsymbol{\upsilon} - \mathbf{K}_{e}\mathbf{e}. \tag{2.11}$$

The desired dynamics quality of the plant proper motion is ensured by the choice of the $\mathbf{K}_{\upsilon}$ and $\mathbf{K}_{e}$ matrices. Taking into account (2.2) and (2.6), proper motion dynamics can be described by the system

$$\begin{aligned} \dot{\boldsymbol{\upsilon}} &= \mathbf{A}\boldsymbol{\upsilon} + \mathbf{B}\mathbf{u}, \\ \dot{\mathbf{e}} &= \mathbf{L}_{s}(\mathbf{e}, \mathbf{Z}_{c})\boldsymbol{\upsilon}. \end{aligned} \tag{2.12}$$

Theorem 2.1. *Feedback (2.11) ensures the stability of the zero equilibrium position* $\boldsymbol{\upsilon}_0 = \mathbf{0}$, $\mathbf{e}_0 = \mathbf{0}$ *of the system (2.12) with* $\mathbf{K}_e = \mu\mathbf{L}_s^{\mathrm{T}}$, $\mu > 0$, $\mathbf{K}_{\upsilon} \succ 0$.

Proof. Consider the quadratic form

$$V = \frac{\mu}{2}\mathbf{e}^{\mathrm{T}}\mathbf{e} + \frac{1}{2}\boldsymbol{\upsilon}^{\mathrm{T}}(\mathbf{B}^{-1})^{\mathrm{T}}\boldsymbol{\upsilon} \geq 0.$$

Note from the problem formulation that $\mathbf{B}^{-1} \succ 0$, and $V = 0$ only with simultaneous $\mathbf{e} = \mathbf{0}$ and $\boldsymbol{\upsilon} = \mathbf{0}$. Calculating the quadratic form derivative with respect to the system (2.12), we obtain

$$\dot{V}\big|_{(11),(12)} = \mu \dot{\mathbf{e}}^{\mathrm{T}} \mathbf{e} + \boldsymbol{\upsilon}^{\mathrm{T}} \mathbf{B}^{-1} \dot{\boldsymbol{\upsilon}} = \mu \boldsymbol{\upsilon}^{\mathrm{T}} \mathbf{L}_s^{\mathrm{T}} \mathbf{e} + \boldsymbol{\upsilon}^{\mathrm{T}} \mathbf{B}^{-1} \mathbf{A} \boldsymbol{\upsilon} + \boldsymbol{\upsilon}^{\mathrm{T}} \mathbf{u} =$$

$$= \boldsymbol{\upsilon}^{\mathrm{T}} \mathbf{B}^{-1} \mathbf{A} \boldsymbol{\upsilon} + \boldsymbol{\upsilon}^{\mathrm{T}} (\mu \mathbf{L}_s^{\mathrm{T}} \mathbf{e} + \mathbf{u}).$$

If we accept

$$\mathbf{u} = -\mu \mathbf{L}_s^{\mathrm{T}} \mathbf{e} - \mathbf{K}_{\upsilon} \boldsymbol{\upsilon}, \tag{2.13}$$

where $\mathbf{K}_{\upsilon} \succ 0$ – arbitrary positive definite matrix, we get

$$\dot{V}\big|_{(11),(12)} = \boldsymbol{\upsilon}^{\mathrm{T}} \mathbf{B}^{-1} \mathbf{A} \boldsymbol{\upsilon} - \boldsymbol{\upsilon}^{\mathrm{T}} \mathbf{K}_{\upsilon} \boldsymbol{\upsilon} \le 0,$$

Because the matrix $\mathbf{B}^{-1}\mathbf{A} = -\mathbf{D}$ is negative definite.

Thus, according to Lyapunov's theorem, the control law (2.13) ensures the stability of the zero equilibrium position $\boldsymbol{\upsilon}_0 = \mathbf{0}$, $\mathbf{e}_0 = \mathbf{0}$ of the closed-loop system (2.12), (2.13). ■

Note that in this case no restrictions are imposed on the matrix $\mathbf{K}_{\upsilon}$ other than positive definiteness. This property can be used to satisfy specified requirements for the plant dynamics.

2) Asymptotic observer synthesis.

Next, we turn to the problem of finding tunable elements of an asymptotic observer. Let us consider the dynamics of the estimation error vectors $\boldsymbol{\varepsilon}_{\upsilon} = \boldsymbol{\upsilon} - \mathbf{z}_{\upsilon}$, $\mathbf{e}_s = \mathbf{e} - \mathbf{z}_e$, which, according to (2.2), (2.6), (2.8) satisfy the system

$$\begin{aligned} \dot{\boldsymbol{\varepsilon}}_{\upsilon} &= (\mathbf{A} - \mathbf{H}_{\upsilon}) \boldsymbol{\varepsilon}_{\upsilon}, \\ \dot{\mathbf{e}}_s &= \mathbf{L}_s(\mathbf{e}, \mathbf{Z}_c) \boldsymbol{\varepsilon}_{\upsilon} - \mathbf{H}_e \mathbf{e}_s. \end{aligned} \tag{2.14}$$

Theorem 2.2. *Asymptotic stability of the zero equilibrium position* $\boldsymbol{\varepsilon}_{\upsilon 0} = \mathbf{0}$, $\mathbf{e}_{s0} = \mathbf{0}$ *of the system (2.14) is ensured with* $\mathbf{A} - \mathbf{H}_{\upsilon} \prec 0$ *and* $\mathbf{H}_e \succ 0$.

Proof. Equilibrium position of the system (2.14) is defined by

$$(\mathbf{A}-\mathbf{H}_{\upsilon})\boldsymbol{\varepsilon}_{\upsilon 0}=\mathbf{0},$$
$$\mathbf{L}_{s}(\mathbf{e},\mathbf{Z}_{c})\boldsymbol{\varepsilon}_{\upsilon 0}-\mathbf{H}_{e}\mathbf{e}_{s0}=\mathbf{0}.$$

Obviously, in this case the system has a zero equilibrium position $\boldsymbol{\varepsilon}_{\upsilon 0}=\mathbf{0}$, $\mathbf{e}_{s0}=\mathbf{0}$. Let us consider the first equation of system (2.14). Global asymptotic stability of the zero equilibrium position is guaranteed under the condition that the matrix $\mathbf{A}-\mathbf{H}_{\upsilon}$ is Hurwitz.

Let us consider the second equation of system (2.14). Since there is global asymptotic stability of the zero equilibrium position $\boldsymbol{\varepsilon}_{\upsilon}=\mathbf{0}$, and components of the matrix $\mathbf{L}_{s}(\mathbf{e},\mathbf{Z}_{c})$ are restricted, then we can conclude that the term $\mathbf{L}_{s}(\mathbf{e},\mathbf{Z}_{c})\boldsymbol{\varepsilon}_{\upsilon}\to\mathbf{0}$ with $t\to+\infty$. According to the cascade systems theorem [75], global asymptotic stability of the zero equilibrium position for the vector $\mathbf{e}_{s}$ is ensured if the matrix $\mathbf{H}_{e}\succ 0$ is positive definite. ■

Thus, in addition to the specified requirements, no restrictions are imposed on the tunable elements of the asymptotic observer. Therefore, just as for the basic control law, observer matrices can be selected taking into account the requirements for dynamics:

1) quality of the closed-loop system dynamics with the basic control law (2.11) and with a control signal on the state of the observer $\mathbf{u}=-\mathbf{K}_{\upsilon}\mathbf{z}_{\upsilon}-\mathbf{K}_{e}\mathbf{z}_{e}$ in the proper motion operating mode should be as identical as possible, while it is accepted that in the case of the basic law (2.11) the quality of the dynamics may be slightly better;

2) L2-norm value of the error vector $\mathbf{e}(t)$ should not exceed the specified value in the operating mode with constant external disturbance.

3) Dynamic corrector synthesis.

Let us now consider the problem of searching for tunable elements of a dynamic corrector. First of all, we prove the following theorem.

Theorem 2.3. *Multipurpose regulator (2.8) – (2.10) ensures stability of the zero equilibrium position* $\boldsymbol{\upsilon}_0 = \mathbf{0}$, $\mathbf{e}_0 = \mathbf{0}$ *of the system (2.12), if the matrices* $\mathbf{K}_\upsilon$ *and* $\mathbf{H}_e$ *are positive definite,* $\mathbf{K}_e = \mu \mathbf{L}_s^{\mathrm{T}}$, *and matrices* $\boldsymbol{\alpha}$ *and* $\mathbf{A} - \mathbf{H}_\upsilon$ *are Hurwitz.*

Proof. Consider the equations of the closed-loop system (2.14), (2.8) – (2.10) in the proper motion operating mode:

$$\begin{aligned}
\dot{\boldsymbol{\varepsilon}}_\upsilon &= (\mathbf{A} - \mathbf{H}_\upsilon)\boldsymbol{\varepsilon}_\upsilon, \\
\dot{\mathbf{e}}_s &= \mathbf{L}_s(\mathbf{e}, \mathbf{Z}_c)\boldsymbol{\varepsilon}_\upsilon - \mathbf{H}_e\mathbf{e}_s. \\
\dot{\mathbf{z}}_\upsilon &= \mathbf{A}\mathbf{z}_\upsilon + \mathbf{B}\mathbf{u} + \mathbf{H}_\upsilon\boldsymbol{\varepsilon}_\upsilon, \\
\dot{\mathbf{z}}_e &= \mathbf{L}_s(\mathbf{e}, \mathbf{Z}_c)\mathbf{z}_\upsilon + \mathbf{H}_e\mathbf{e}_s, \\
\dot{\mathbf{p}} &= \boldsymbol{\alpha}\mathbf{p} + \boldsymbol{\beta}_\upsilon\boldsymbol{\varepsilon}_\upsilon + \boldsymbol{\beta}_e\mathbf{e}_s, \\
\boldsymbol{\zeta} &= \boldsymbol{\gamma}\mathbf{p} + \boldsymbol{\mu}_\upsilon\boldsymbol{\varepsilon}_\upsilon + \boldsymbol{\mu}_e\mathbf{e}_s, \\
\mathbf{u} &= -\mathbf{K}_\upsilon\mathbf{z}_\upsilon - \mathbf{K}_e\mathbf{z}_e + \boldsymbol{\zeta}.
\end{aligned} \tag{2.15}$$

Excluding the variables $\mathbf{u}$ and $\boldsymbol{\zeta}$, we obtain

$$\begin{aligned}
\dot{\boldsymbol{\varepsilon}}_\upsilon &= (\mathbf{A} - \mathbf{H}_\upsilon)\boldsymbol{\varepsilon}_\upsilon, \\
\dot{\mathbf{e}}_s &= \mathbf{L}_s(\mathbf{e}, \mathbf{Z}_c)\boldsymbol{\varepsilon}_\upsilon - \mathbf{H}_e\mathbf{e}_s, \\
\dot{\mathbf{z}}_\upsilon &= (\mathbf{A} - \mathbf{B}\mathbf{K}_\upsilon)\mathbf{z}_\upsilon - \mathbf{B}\mathbf{K}_e\mathbf{z}_e + \mathbf{B}\boldsymbol{\gamma}\mathbf{p} + (\mathbf{B}\boldsymbol{\mu}_\upsilon + \mathbf{H}_\upsilon)\boldsymbol{\varepsilon}_\upsilon + \mathbf{B}\boldsymbol{\mu}_e\mathbf{e}_s, \\
\dot{\mathbf{z}}_e &= \mathbf{L}_s(\mathbf{e}, \mathbf{Z}_c)\mathbf{z}_\upsilon + \mathbf{H}_e\mathbf{e}_s, \\
\dot{\mathbf{p}} &= \boldsymbol{\alpha}\mathbf{p} + \boldsymbol{\beta}_\upsilon\boldsymbol{\varepsilon}_\upsilon + \boldsymbol{\beta}_e\mathbf{e}_s,
\end{aligned}$$

which can be represented in the matrix form as

$$\begin{pmatrix} \dot{\boldsymbol{\varepsilon}}_\upsilon \\ \dot{\mathbf{e}}_s \\ \dot{\mathbf{z}}_\upsilon \\ \dot{\mathbf{z}}_e \\ \dot{\mathbf{p}} \end{pmatrix} = \begin{pmatrix} \mathbf{A} - \mathbf{H}_\upsilon & \mathbf{0} & \mathbf{0} & \mathbf{0} & \mathbf{0} \\ \mathbf{L}_s(\mathbf{e}, \mathbf{Z}_c) & -\mathbf{H}_e & \mathbf{0} & \mathbf{0} & \mathbf{0} \\ \mathbf{B}\boldsymbol{\mu}_\upsilon + \mathbf{H}_\upsilon & \mathbf{B}\boldsymbol{\mu}_e & \mathbf{A} - \mathbf{B}\mathbf{K}_\upsilon & -\mathbf{B}\mathbf{K}_e & \mathbf{B}\boldsymbol{\gamma} \\ \mathbf{0} & \mathbf{H}_e & \mathbf{L}_s(\mathbf{e}, \mathbf{Z}_c) & \mathbf{0} & \mathbf{0} \\ \boldsymbol{\beta}_\upsilon & \boldsymbol{\beta}_e & \mathbf{0} & \mathbf{0} & \boldsymbol{\alpha} \end{pmatrix} \begin{pmatrix} \boldsymbol{\varepsilon}_\upsilon \\ \mathbf{e}_s \\ \mathbf{z}_\upsilon \\ \mathbf{z}_e \\ \mathbf{p} \end{pmatrix}. \tag{2.16}$$

Characteristic polynomial of the closed-loop system (2.16) is equal to

$$\Delta(s) = \det\begin{pmatrix} \mathbf{E}s - \mathbf{A} + \mathbf{H}_\upsilon & \mathbf{0} \\ -\mathbf{L}_s(\mathbf{e}, \mathbf{Z}_c) & \mathbf{E}s + \mathbf{H}_e \end{pmatrix} \det\begin{pmatrix} \mathbf{E}s - \mathbf{A} + \mathbf{B}\mathbf{K}_\upsilon & \mathbf{B}\mathbf{K}_e \\ -\mathbf{L}_s(\mathbf{e}, \mathbf{Z}_c) & \mathbf{E}s \end{pmatrix} \det(\mathbf{E}s - \boldsymbol{\alpha}) =$$

$$= \Delta_o(s)\Delta_b(s)\Phi(s),$$

where

- $\Delta_o(s)$ is the characteristic polynomial of the asymptotic observer (2.8);

- $\Delta_b(s)$ is the characteristic polynomial of the system (2.12), closed by the basic control law (2.11);
- $\Phi(s)$ is the characteristic polynomial of the dynamic corrector.

Polynomial $\Delta_o(s)$ is asymptotically stable according to the theorem 2.2. Stability of the polynomial $\Delta_b(s)$ follows from the theorem 2.1. Polynomial $\Phi(s)$ is asymptotically stable because the matrix $\boldsymbol{\alpha}$ is Hurwitz according to the formulation of the theorem 2.3. Thus, closed-loop system (2.15) is stable. ■

From Theorem 2.3 it follows that the only mandatory requirement for a dynamic corrector is the Hurwitz property of the matrix $\boldsymbol{\alpha}$. Let us now turn to the issue of ensuring astatism of the closed-loop system (2.2), (2.6), (2.8) – (2.10). We will assume that external disturbances are constant: $\mathbf{d}(t) = \mathbf{d}_0$, $\mathbf{d}_c(t) = \mathbf{d}_{c0}$. Let us represent the dynamic corrector (2.9) in tf-form:

$$\boldsymbol{\zeta} = \mathbf{F}_\upsilon(s)(\boldsymbol{\upsilon} - \mathbf{z}_\upsilon) + \mathbf{F}_e(s)(\mathbf{e} - \mathbf{z}_e), \tag{2.17}$$

where s is the Laplace variable, $\mathbf{F}_\upsilon(s) = \boldsymbol{\gamma}\left(\mathbf{E}_{n_p} s - \boldsymbol{\alpha}\right)^{-1}\boldsymbol{\beta}_\upsilon + \boldsymbol{\mu}_\upsilon$ and $\mathbf{F}_e(s) = \boldsymbol{\gamma}\left(\mathbf{E}_{n_p} s - \boldsymbol{\alpha}\right)^{-1}\boldsymbol{\beta}_e + \boldsymbol{\mu}_e$ are the corrector transfer matrices.

Theorem 2.4. *The closed system (2.2), (2.6), (2.8) – (2.10) is astatic with respect to the vectors* $\boldsymbol{\upsilon}$ *and* $\mathbf{e}$ *for any constant disturbances* $\mathbf{d}(t) = \mathbf{d}_0$ *and* $\mathbf{d}_c(t) = \mathbf{d}_{c0}$, *if the transfer matrices of the dynamic corrector satisfy the conditions*

$$\begin{aligned} &\mathbf{F}_\upsilon(0) = -\mathbf{B}^{-1}\mathbf{H}_\upsilon, \\ &\mathbf{F}_e(0) = \mathbf{B}^{-1}(\mathbf{B}\mathbf{K}_\upsilon\mathbf{T} - \mathbf{A}\mathbf{T} - \mathbf{B}\mathbf{K}_e), \\ &\mathbf{T} = -(\mathbf{L}_0^{\mathrm{T}}\mathbf{L}_0)^{-1}\mathbf{L}_0^{\mathrm{T}}\mathbf{H}_e, \end{aligned} \tag{2.18}$$

where $\mathbf{L}_0 = \mathbf{L}_s(\mathbf{e}_0, \mathbf{Z}_{c0})$ *is the value of the interaction matrix in the equilibrium position.*

Proof. According to (2.17) the closed-loop system equations can be represented as

$$\begin{aligned}
\dot{\boldsymbol{\varepsilon}}_{\upsilon} &= \mathbf{A}\boldsymbol{\varepsilon}_{\upsilon} - \mathbf{H}_{\upsilon}\boldsymbol{\varepsilon}_{\upsilon} + \mathbf{d}_0, \\
\dot{\mathbf{e}}_s &= \mathbf{L}_s(\mathbf{e}, \mathbf{Z}_c)\boldsymbol{\varepsilon}_{\upsilon} - \mathbf{H}_e\mathbf{e}_s + \mathbf{d}_{c0,} \\
\dot{\mathbf{z}}_{\upsilon} &= \mathbf{A}\mathbf{z}_{\upsilon} + \mathbf{H}_{\upsilon}\boldsymbol{\varepsilon}_{\upsilon} - \mathbf{B}\mathbf{K}_e\mathbf{z}_e - \mathbf{B}\mathbf{K}_{\upsilon}\mathbf{z}_{\upsilon} + \mathbf{B}\mathbf{F}_{\upsilon}(s)\boldsymbol{\varepsilon}_{\upsilon} + \mathbf{B}\mathbf{F}_e(s)\mathbf{e}_s, \\
\dot{\mathbf{z}}_e &= \mathbf{L}_s(\mathbf{e}, \mathbf{Z}_c)\mathbf{z}_{\upsilon} + \mathbf{H}_e\mathbf{e}_s.
\end{aligned}$$

Let us calculate the equilibrium position for this system. As a result we get

$$\begin{aligned}
&\mathbf{A}\boldsymbol{\varepsilon}_{\upsilon 0} - \mathbf{H}_{\upsilon}\boldsymbol{\varepsilon}_{\upsilon 0} + \mathbf{d}_0 = \mathbf{0}, \\
&\mathbf{L}_0\boldsymbol{\varepsilon}_{\upsilon 0} - \mathbf{H}_e\mathbf{e}_{s0} + \mathbf{d}_{c0} = \mathbf{0}, \\
&\mathbf{A}\mathbf{z}_{\upsilon 0} + \mathbf{H}_{\upsilon}\boldsymbol{\varepsilon}_{\upsilon 0} - \mathbf{B}\mathbf{K}_e\mathbf{z}_{e0} - \mathbf{B}\mathbf{K}_{\upsilon}\mathbf{z}_{\upsilon 0} + \mathbf{B}\mathbf{F}_{\upsilon}(0)\boldsymbol{\varepsilon}_{\upsilon 0} + \mathbf{B}\mathbf{F}_e(0)\mathbf{e}_{s0} = \mathbf{0}, \\
&\mathbf{L}_0\mathbf{z}_{\upsilon 0} + \mathbf{H}_e\mathbf{e}_{s0} = \mathbf{0},
\end{aligned} \tag{2.19}$$

where $\boldsymbol{\varepsilon}_{\upsilon 0}$, $\mathbf{e}_{s0}$, $\mathbf{z}_{\upsilon 0}$, $\mathbf{z}_{e0}$ are the the values of the corresponding variables in the equilibrium position. From the first two equations of the system (2.19) it is clear that the estimation error vectors $\boldsymbol{\varepsilon}_{\upsilon 0}$, $\mathbf{e}_{s0}$ and external disturbances $\mathbf{d}_0$, $\mathbf{d}_{c0}$ are directly related to each other. In this regard, vectors $\boldsymbol{\varepsilon}_{\upsilon 0}$ and $\mathbf{e}_{s0}$ can be considered further as external disturbances.

From the last equation of system (2.19) we obtain

$$\mathbf{z}_{\upsilon 0} = -(\mathbf{L}_0^{\mathrm{T}}\mathbf{L}_0)^{-1}\mathbf{L}_0^{\mathrm{T}}\mathbf{H}_e\mathbf{e}_{s0}. \tag{2.20}$$

Introducing auxiliary matrix $\mathbf{T} = -(\mathbf{L}_0^{\mathrm{T}}\mathbf{L}_0)^{-1}\mathbf{L}_0^{\mathrm{T}}\mathbf{H}_e$ and substituting (2.20) into the third equation of the system (2.19), we get the relation

$$\mathbf{B}\mathbf{K}_e\mathbf{e}_0 = (\mathbf{A}\mathbf{T} - \mathbf{B}\mathbf{K}_{\upsilon}\mathbf{T} + \mathbf{B}\mathbf{F}_e(0) + \mathbf{B}\mathbf{K}_e)\mathbf{e}_{s0} + \left[\mathbf{H}_{\upsilon} + \mathbf{B}\mathbf{F}_{\upsilon}(0)\right]\boldsymbol{\varepsilon}_{\upsilon 0}.$$

Thus, in order to ensure condition (2.7) in the presence of constant external disturbances, i.e. to fulfill the property of astatism, it is necessary that the multipliers of the vectors $\mathbf{e}_{s0}$ and $\boldsymbol{\varepsilon}_{\upsilon 0}$ are equal to zero, which is ensured by the conditions (2.18). ■

Now consider the operating mode in the presence of a polyharmonic disturbance in the form $d(t) = \sum_{i=1}^{N_{\omega}} A_i \sin(\omega_i t)$, where N_{ω} – number of harmonics. We will assume that in this mode the motions of the system are small enough to replace the matrix $\mathbf{L}_s(\mathbf{e}, \mathbf{Z}_c)$ with constant value $\mathbf{L}_0 = \mathbf{L}_s(\mathbf{e}_0, \mathbf{Z}_{c0})$, corresponding to the equi-

librium position. Then the equations of the multi-purpose controller (2.8) – (2.10) are taking the form

$$\begin{aligned}\dot{\mathbf{z}}_\upsilon &= \mathbf{A}\mathbf{z}_\upsilon + \mathbf{B}\mathbf{u} + \mathbf{H}_\upsilon\boldsymbol{\varepsilon}_\upsilon,\\ \dot{\mathbf{z}}_e &= \mathbf{L}_0\mathbf{z}_\upsilon + \mathbf{H}_e\mathbf{e}_s,\\ \mathbf{u} &= -\mathbf{K}_\upsilon\mathbf{z}_\upsilon - \mathbf{K}_e\mathbf{z}_e + \boldsymbol{\zeta}.\end{aligned}$$

Excluding the third equation:

$$\begin{aligned}\dot{\mathbf{z}}_\upsilon &= \mathbf{A}\mathbf{z}_\upsilon - \mathbf{B}\mathbf{K}_\upsilon\mathbf{z} - \mathbf{B}\mathbf{K}_e\mathbf{z}_e + \mathbf{B}\boldsymbol{\zeta} + \mathbf{H}_\upsilon\boldsymbol{\varepsilon}_\upsilon,\\ \dot{\mathbf{z}}_e &= \mathbf{L}_0\mathbf{z}_\upsilon + \mathbf{H}_e\mathbf{e}_s,\end{aligned}$$

or in matrix form:

$$\begin{pmatrix}\dot{\mathbf{z}}_\upsilon\\ \dot{\mathbf{z}}_e\end{pmatrix} = \mathbf{A}_s\begin{pmatrix}\mathbf{z}_\upsilon\\ \mathbf{z}_e\end{pmatrix} + \mathbf{B}_s\begin{pmatrix}\boldsymbol{\varepsilon}_\upsilon\\ \mathbf{e}_s\\ \boldsymbol{\zeta}\end{pmatrix}, \tag{2.21}$$

where

$$\mathbf{A}_s = \begin{pmatrix}\mathbf{A}-\mathbf{B}\mathbf{K}_\upsilon & -\mathbf{B}\mathbf{K}_e\\ \mathbf{L}_0 & \mathbf{0}\end{pmatrix},\ \mathbf{B}_s = \begin{pmatrix}\mathbf{H}_\upsilon & \mathbf{0} & \mathbf{B}\\ \mathbf{0} & \mathbf{H}_e & \mathbf{0}\end{pmatrix}.$$

Let us represent (2.21) in tf-form:

$$\begin{pmatrix}\mathbf{z}_\upsilon\\ \mathbf{z}_e\end{pmatrix} = \mathbf{P}(s)\begin{pmatrix}\boldsymbol{\varepsilon}_\upsilon\\ \mathbf{e}_s\\ \boldsymbol{\zeta}\end{pmatrix}, \tag{2.22}$$

where

$$\mathbf{P}(s) = (\mathbf{E}s - \mathbf{A}_s)^{-1}\mathbf{B}_s = \begin{pmatrix}\mathbf{P}_{11}(s) & \mathbf{P}_{12}(s) & \mathbf{P}_{13}(s)\\ \mathbf{P}_{21}(s) & \mathbf{P}_{22}(s) & \mathbf{P}_{23}(s)\end{pmatrix}.$$

Theorem 2.5. *Filtering polyharmonic disturbance with frequencies* ω_i, $i = \overline{1, N_\omega}$ *in the control channel is ensured by the conditions*

$$\begin{aligned}\mathbf{F}_\upsilon(j\omega_i) &= -\mathbf{F}^{-1}(j\omega_i)[\mathbf{K}_\upsilon\mathbf{P}_{11}(j\omega_i) + \mathbf{K}_e\mathbf{P}_{21}(j\omega_i)],\\ \mathbf{F}_e(j\omega_i) &= -\mathbf{F}^{-1}(j\omega_i)[\mathbf{K}_\upsilon\mathbf{P}_{12}(j\omega_i) + \mathbf{K}_e\mathbf{P}_{22}(j\omega_i)],\end{aligned} \tag{2.23}$$

where $\mathbf{F}(j\omega_i) = \mathbf{K}_\upsilon\mathbf{P}_{13}(j\omega_i) + \mathbf{K}_e\mathbf{P}_{23}(j\omega_i) - \mathbf{E}$.

Proof. Let us substitute (2.22) into the equation of the control signal:

$$\mathbf{u} = -\mathbf{K}_\upsilon(\mathbf{P}_{11}\boldsymbol{\varepsilon}_\upsilon + \mathbf{P}_{12}\mathbf{e}_s + \mathbf{P}_{13}\boldsymbol{\zeta}) - \mathbf{K}_e(\mathbf{P}_{21}\boldsymbol{\varepsilon}_\upsilon + \mathbf{P}_{22}\mathbf{e}_s + \mathbf{P}_{23}\boldsymbol{\zeta}) + \boldsymbol{\zeta} =$$
$$= -(\mathbf{K}_\upsilon\mathbf{P}_{11} + \mathbf{K}_e\mathbf{P}_{21})\boldsymbol{\varepsilon}_\upsilon - (\mathbf{K}_\upsilon\mathbf{P}_{12} + \mathbf{K}_e\mathbf{P}_{22})\mathbf{e}_s - (\mathbf{K}_\upsilon\mathbf{P}_{13} + \mathbf{K}_e\mathbf{P}_{23} - \mathbf{E})\boldsymbol{\zeta}.$$

Taking into account $\mathbf{F}(s) = \mathbf{K}_\upsilon\mathbf{P}_{13}(s) + \mathbf{K}_e\mathbf{P}_{23}(s) - \mathbf{E}$ we obtain

$$\begin{aligned}\mathbf{u} &= -(\mathbf{K}_\upsilon\mathbf{P}_{11} + \mathbf{K}_e\mathbf{P}_{21})\boldsymbol{\varepsilon}_\upsilon - (\mathbf{K}_\upsilon\mathbf{P}_{12} + \mathbf{K}_e\mathbf{P}_{22})\mathbf{e}_s - \mathbf{F}\boldsymbol{\zeta} = \\ &= -(\mathbf{K}_\upsilon\mathbf{P}_{11} + \mathbf{K}_e\mathbf{P}_{21})\boldsymbol{\varepsilon}_\upsilon - (\mathbf{K}_\upsilon\mathbf{P}_{12} + \mathbf{K}_e\mathbf{P}_{22})\mathbf{e}_s - \mathbf{F}(\mathbf{F}_\upsilon\boldsymbol{\varepsilon}_\upsilon + \mathbf{F}_e\mathbf{e}_s) = \\ &= -(\mathbf{K}_\upsilon\mathbf{P}_{11} + \mathbf{K}_e\mathbf{P}_{21} + \mathbf{F}\mathbf{F}_\upsilon)\boldsymbol{\varepsilon}_\upsilon - (\mathbf{K}_\upsilon\mathbf{P}_{12} + \mathbf{K}_e\mathbf{P}_{22} + \mathbf{F}\mathbf{F}_e)\mathbf{e}_s.\end{aligned} \qquad (2.24)$$

Multipliers of $\boldsymbol{\varepsilon}_\upsilon$ and $\mathbf{e}_s$ in the right part of the (2.24) represent transfer matrices from the corresponding inputs to the output control signal. Thus, to ensure filtering properties across frequencies ω_i, $i = \overline{1, N_\omega}$ it is necessary that these transfer functions are equal to zero:

$$\mathbf{K}_\upsilon\mathbf{P}_{11}(j\omega_i) + \mathbf{K}_e\mathbf{P}_{21}(j\omega_i) + \mathbf{F}(j\omega_i)\mathbf{F}_\upsilon(j\omega_i) = 0,$$
$$\mathbf{K}_\upsilon\mathbf{P}_{12}(j\omega_i) + \mathbf{K}_e\mathbf{P}_{22}(j\omega_i) + \mathbf{F}(j\omega_i)\mathbf{F}_e(j\omega_i) = 0,$$

from which we obtain the conditions (2.23). ■

Now let us consider the problem of the synthesis of the dynamic corrector transfer matrices $\mathbf{F}_\upsilon = \begin{pmatrix}\mathbf{F}_{\upsilon 1} & \mathbf{F}_{\upsilon 2} & \dots & \mathbf{F}_{\upsilon 6}\end{pmatrix}^T$ and $\mathbf{F}_e = \begin{pmatrix}\mathbf{F}_{e1} & \mathbf{F}_{e2} & \dots & \mathbf{F}_{e6}\end{pmatrix}^T$ that satisfy the conditions of astatism (2.18) and disturbance filtering (2.23). To do this, we rewrite conditions (2.18) and (2.23) in the following form:

$$\mathbf{F}_\upsilon(0) = \mathbf{F}_\upsilon^0 = \begin{pmatrix}\mathbf{F}_{\upsilon 1}^0 & \mathbf{F}_{\upsilon 2}^0 & \dots & \mathbf{F}_{\upsilon 6}^0\end{pmatrix}^T,$$
$$\mathbf{F}_\upsilon(j\omega_i) = \mathbf{F}_{\upsilon i}^* = \begin{pmatrix}\mathbf{F}_{\upsilon i1}^* & \mathbf{F}_{\upsilon i2}^* & \dots & \mathbf{F}_{\upsilon i6}^*\end{pmatrix}^T,$$
$$\mathbf{F}_e(0) = \mathbf{F}_e^0 = \begin{pmatrix}\mathbf{F}_{e1}^0 & \mathbf{F}_{e2}^0 & \dots & \mathbf{F}_{e6}^0\end{pmatrix}^T,$$
$$\mathbf{F}_e(j\omega_i) = \mathbf{F}_{ei}^* = \begin{pmatrix}\mathbf{F}_{ei1}^* & \mathbf{F}_{ei2}^* & \dots & \mathbf{F}_{ei6}^*\end{pmatrix}^T,$$

where $\mathbf{F}_\upsilon^0$, $\mathbf{F}_{\upsilon i}^*$, $\mathbf{F}_e^0$ and $\mathbf{F}_{ei}^*$ are constant matrices. Next, we present the reasoning for synthesizing the transfer matrix $\mathbf{F}_\upsilon$, because for matrix $\mathbf{F}_e$ the procedure is completely similar.

Each component of the $\mathbf{F}_\upsilon$ corrector with transfer matrix $\mathbf{F}_{\upsilon k}(s)$, $k = \overline{1,6}$, can be described in the tf-form by the equation

$$\boldsymbol{\zeta}_{\upsilon k} = \mathbf{F}_{\upsilon k}(s)\boldsymbol{\varepsilon}_\upsilon,$$

or in state space

$$\dot{\mathbf{p}}_{\upsilon k} = \boldsymbol{\alpha}_{\upsilon k}\mathbf{p}_{\upsilon k} + \boldsymbol{\beta}_{\upsilon k}\boldsymbol{\varepsilon}_{\upsilon},$$
$$\boldsymbol{\zeta}_{\upsilon k} = \boldsymbol{\gamma}_{\upsilon k}\mathbf{p}_{\upsilon k} + \boldsymbol{\mu}_{\upsilon k}\boldsymbol{\varepsilon}_{\upsilon},$$

where $\mathbf{p}_{\upsilon k} \in E^{2N_\omega}$ – corrector state vector. In this case, the transfer matrix $\mathbf{F}_{\upsilon k}(s)$ is equal to $\mathbf{F}_{\upsilon k}(s) = \boldsymbol{\gamma}_{\upsilon k}(\mathbf{E}_{n_p}s - \boldsymbol{\alpha}_{\upsilon k})^{-1}\boldsymbol{\beta}_{\upsilon k} + \boldsymbol{\mu}_{\upsilon k}$. Taking into account the notations

$$\mathbf{R}_{\upsilon ik} = \mathrm{Re}\,\mathbf{F}^*_{\upsilon ik},$$
$$\mathbf{I}_{\upsilon ik} = \mathrm{Im}\,\mathbf{F}^*_{\upsilon ik},$$
$$i = \overline{1, N_\omega}, k = \overline{1,6},$$

conditions (2.18) and (2.23) can be rewritten as

$$\begin{aligned} &-\boldsymbol{\gamma}_{\upsilon k}\boldsymbol{\alpha}^{-1}_{\upsilon k}\boldsymbol{\beta}_{\upsilon k} + \boldsymbol{\mu}_{\upsilon k} = \mathbf{F}^0_{\upsilon k},\\ &\boldsymbol{\gamma}_{\upsilon k}(\mathbf{E}_{2N_\omega} j\omega_i - \boldsymbol{\alpha}_{\upsilon k})^{-1}\boldsymbol{\beta}_{\upsilon k} + \boldsymbol{\mu}_{\upsilon k} = \mathbf{R}_{\upsilon ik} + \mathbf{I}_{\upsilon ik} j,\\ &i = \overline{1, N_\omega}, k = \overline{1,6}. \end{aligned} \qquad (2.25)$$

Let us choose arbitrary Hurwitz matrices $\boldsymbol{\alpha}_{\upsilon k}$ and arbitrary vectors $\boldsymbol{\gamma}_{\upsilon k}$. Introducing the notations

$$\boldsymbol{\alpha}^R_{\upsilon ik} = \mathrm{Re}(\mathbf{E}_{2N_\omega} j\omega_i - \boldsymbol{\alpha}_{\upsilon k})^{-1},$$
$$\boldsymbol{\alpha}^I_{\upsilon ik} = \mathrm{Im}(\mathbf{E}_{2N_\omega} j\omega_i - \boldsymbol{\alpha}_{\upsilon k})^{-1},$$

and subtracting the first equation of the system (2.25) from the second one, we obtain

$$\boldsymbol{\gamma}_{\upsilon k}(\boldsymbol{\alpha}^R_{\upsilon ik} + \boldsymbol{\alpha}^{-1}_{\upsilon k})\boldsymbol{\beta}_{\upsilon k} = \mathbf{R}_{\upsilon ik} - \mathbf{F}^0_{\upsilon k},$$
$$\boldsymbol{\gamma}_{\upsilon k}\boldsymbol{\alpha}^I_{\upsilon ik}\boldsymbol{\beta}_{\upsilon k} = \mathbf{I}_{\upsilon ik},$$
$$i = \overline{1, N_\omega}, k = \overline{1,6},$$

which can be written as

$$\mathbf{A}_{\upsilon k}\boldsymbol{\beta}_{\upsilon k} = \mathbf{B}_{\upsilon k}, \qquad (2.26)$$

where

$$\mathbf{A}_{\upsilon k}=\begin{pmatrix}\boldsymbol{\gamma}_{\upsilon k}(\boldsymbol{\alpha}_{\upsilon 1k}^{R}+\boldsymbol{\alpha}_{\upsilon k}^{-1})\\ \boldsymbol{\gamma}_{\upsilon k}\boldsymbol{\alpha}_{\upsilon 1k}^{I}\\ \cdots\\ \boldsymbol{\gamma}_{\upsilon k}(\boldsymbol{\alpha}_{\upsilon N_\omega k}^{R}+\boldsymbol{\alpha}_{\upsilon k}^{-1})\\ \boldsymbol{\gamma}_{\upsilon k}\boldsymbol{\alpha}_{\upsilon N_\omega k}^{I}\end{pmatrix},\mathbf{B}_{\upsilon k}=\begin{pmatrix}\mathbf{R}_{\upsilon 1k}-\mathbf{F}_{\upsilon k}^{0}\\ \mathbf{I}_{\upsilon 1k}\\ \cdots\\ \mathbf{R}_{\upsilon N_\omega k}-\mathbf{F}_{\upsilon k}^{0}\\ \mathbf{I}_{\upsilon N_\omega k}\end{pmatrix},k=\overline{1,6}. \qquad (2.27)$$

Thus, the vector $\boldsymbol{\beta}_{\upsilon k}$ can be found as a result of solving the linear system (2.26). Next, substituting $\boldsymbol{\beta}_{\upsilon k}$ into the first equation of the system (2.25), we calculate $\boldsymbol{\mu}_{\upsilon k}$ using the formula

$$\boldsymbol{\mu}_{\upsilon k}=\mathbf{F}_{\upsilon k}^{0}+\boldsymbol{\gamma}_{\upsilon k}\boldsymbol{\alpha}_{\upsilon k}^{-1}\boldsymbol{\beta}_{\upsilon k},\ k=\overline{1,6}. \qquad (2.28)$$

The resulting matrices $\boldsymbol{\alpha}_{\upsilon k}$, $\boldsymbol{\beta}_{\upsilon k}$, $\boldsymbol{\gamma}_{\upsilon k}$, $\boldsymbol{\mu}_{\upsilon k}$, $k=\overline{1,6}$ determine the dynamic corrector, which provides filtering at frequencies ω_i, $i=\overline{1,N_\omega}$ and the astatism of the closed-loop system.

In accordance with the above reasoning, let us formulate the algorithm for the multipurpose regulator (2.8) – (2.10) synthesis.

Algorithm № 1 (multipurpose regulator synthesis)

1) Fix the values of the μ coefficient and matrix $\mathbf{K}_\upsilon$ for the basic control law (2.11). These values can be found, for example, from the perspective of minimizing the time constant of the transient process in a closed system.

2) Set the values of the matrices $\mathbf{H}_\upsilon$ and $\mathbf{H}_e$ of the asymptotic observer (2.8) to ensure the fastest convergence of estimates to the actual values of the plant state variables.

3) Calculate the values $\mathbf{F}_\upsilon(0)$ and $\mathbf{F}_e(0)$ of the dynamic corrector transfer matrices in accordance with the conditions (2.18) to ensure astatism of the closed-loop system.

4) Set the frequencies ω_i, $i=\overline{1,N_\omega}$ of the external polyharmonic disturbance and calculate the corresponding values $\mathbf{F}_\upsilon(j\omega_i)$ and $\mathbf{F}_e(j\omega_i)$ of the dynamic corrector transfer matrices.

5) Fix the Hurwitz matrices $\boldsymbol{\alpha}_{\upsilon k}$, $\boldsymbol{\gamma}_{\upsilon k}$ and $\boldsymbol{\alpha}_{ek}$, $\boldsymbol{\gamma}_{ek}$ of the dynamic correctors, $k=\overline{1,6}$. In particular, we can take $\boldsymbol{\gamma}_{\upsilon k}=\begin{pmatrix}0 & \dots & 0 & 1\end{pmatrix}$, set the eigenvalue λ of multiplicity $2N_{\omega}$, and calculate the corresponding Frobenius form for matrices $\boldsymbol{\alpha}_{\upsilon k}$ with $\mathrm{Re}(\lambda)<0$. Define matrices $\boldsymbol{\alpha}_{ek}$ and $\boldsymbol{\gamma}_{ek}$ in the same way.

6) Calculate matrices $\mathbf{A}_{\upsilon k}$ and in accordance with formulas (2.27). From the linear system (2.26) find the vector $\boldsymbol{\beta}_{\upsilon k}$. Calculate the vector $\boldsymbol{\mu}_{\upsilon k}$ using formula (2.28). Similarly, find the vectors $\boldsymbol{\beta}_{ek}$ and $\boldsymbol{\mu}_{ek}$.

2.3. Constant Delay Compensation

Let us introduce the constant delay h to the control channel and to the disturbance channel of the system (2.2). Also, for convenience, we will assume that the matrix $\mathbf{B}$ is taken into account in the term $\mathbf{d}$. As a result, we obtain a system of the form

$$\begin{aligned}\dot{\boldsymbol{\upsilon}}(t)&=\mathbf{A}\boldsymbol{\upsilon}(t)+\mathbf{B}\mathbf{u}(t-h)+\mathbf{d}(t-h),\\ \dot{\boldsymbol{\eta}}(t)&=\mathbf{R}\big(\boldsymbol{\eta}(t)\big)\boldsymbol{\upsilon}(t).\end{aligned}$$

As noted in the previous chapter, delay, usually, affects the controlled motion dynamics in a negative way. Let us set the problem of taking into account the delay to preserve the same dynamic properties as in the closed-loop system (2.2), (2.6), (2.8) – (2.10). As in the previous chapter, we will use the compensation approach, which consists of estimating the system velocity vector prediction using the Cauchy formula

$$\boldsymbol{\upsilon}(t+h)=e^{\mathbf{A}h}\,\boldsymbol{\upsilon}(t)+e^{\mathbf{A}h}\int_{t}^{t+h}e^{-\mathbf{A}(\tau-t)}\big[\mathbf{B}\mathbf{u}(\tau-h)+\mathbf{d}(\tau-h)\big]\,d\tau. \qquad (2.29)$$

Equation (2.29), in turn, is more convenient to use in the form of a dynamic system [10]

$$\begin{aligned}\dot{\mathbf{z}}_p&=\mathbf{A}\mathbf{z}+\mathbf{B}\mathbf{u}+\mathbf{d},\\ \boldsymbol{\upsilon}(t+h)&=\mathbf{z}_p(t)+e^{\mathbf{A}h}\big[\boldsymbol{\upsilon}(t)-\mathbf{z}_p(t-h)\big].\end{aligned} \qquad (2.30)$$

Taking into account (2.30), we can transform the controller (2.8) – (2.10) for the delay compensation, in a way that preserves the original transfer matrix of the closed-loop system. Note that in this case, asymptotic observers evaluate the system state prediction by the amount of delay. Here it is also required to have an estimation of the prediction of the moving plant position $\mathbf{z}_\eta$ through the future velocity estimation $\mathbf{z}_\upsilon$. Let us denote the velocity prediction $\boldsymbol{\upsilon}(t+h)$ as $\boldsymbol{\lambda}$ variable. As a result, we obtain a multipurpose regulator with delay compensation in the form

$$\begin{aligned}
&\dot{\mathbf{z}}_p = \mathbf{A}\mathbf{z}_p + \mathbf{B}\mathbf{u} + \mathbf{d},\\
&\dot{\mathbf{z}}_\upsilon = \mathbf{A}\mathbf{z}_\upsilon + \mathbf{B}\mathbf{u} + \mathbf{H}_\upsilon(\lambda - \mathbf{z}_\upsilon),\\
&\dot{\mathbf{z}}_\eta = \mathbf{R}(\mathbf{z}_\eta)\mathbf{z}_\upsilon,\\
&\dot{\mathbf{z}}_e = \mathbf{L}(\mathbf{e},\mathbf{Z})\mathbf{z}_\upsilon + \mathbf{H}_e(\mathbf{e} - \mathbf{z}_e),\\
&\dot{\mathbf{p}} = \boldsymbol{\alpha}\mathbf{p} + \boldsymbol{\beta}_\upsilon(\boldsymbol{\lambda} - \mathbf{z}_\upsilon) + \boldsymbol{\beta}_e(\mathbf{e} - \mathbf{z}_e),\\
&\boldsymbol{\zeta} = \boldsymbol{\gamma}\mathbf{p} + \boldsymbol{\mu}_\upsilon(\boldsymbol{\lambda} - \mathbf{z}_\upsilon) + \boldsymbol{\mu}_e(\mathbf{e} - \mathbf{z}_e),\\
&\boldsymbol{\lambda} = \mathbf{z}_p + e^{\mathbf{A}h}(\boldsymbol{\upsilon} - \mathbf{z}_p(t-h)),\\
&\mathbf{u} = -\mathbf{K}_e\mathbf{z}_e - \mathbf{K}_\upsilon\mathbf{z}_\upsilon + \boldsymbol{\zeta}.
\end{aligned} \tag{2.31}$$

Note that the regulator (2.31), indeed, is nothing more than a transformation of the original regulator (2.8) – (2.10) without taking into account the delay, and uses the same synthesized set of adjustable elements. In other words, if a multipurpose regulator is synthesized without taking into account the delay, which satisfies all the stated requirements, then for the constant delay compensation there is no need to carry out additional synthesis of any elements of the multipurpose structure; it is enough to use a transformed controller in the form (2.31).

Thus, it is possible to formulate an algorithm for the multipurpose regulator synthesis for the constant delay h compensation.

Algorithm № 2 (multipurpose delay compensating regulator synthesis)

1) Synthesize the basic controller (2.8) – (2.10) for a closed-loop system without delay in accordance with Algorithm 1.

2) Add equations (2.30) to the resulting controller to calculate the system velocity prediction by the amount of delay, as well as the observer equation to estimate the position $\mathbf{z}_\eta$ of the moving object.

3) Replace all occurrences of the velocity $\boldsymbol{\upsilon}$ in the basic controller with the predicted value $\boldsymbol{\lambda}$.

2.4. Positioning the Mobile Robot Relative to the Visual Marker

Let us consider a mobile robot with the omni-wheeled chassis (Fig. 2.2), which ensures that the system is fully-actuated when moving in a plane. We will assume that the control in this case is the forces and moment acting on the chassis when the wheels move. Let us assume that in the control channel (as well as in the external disturbance channel) there is a constant transport delay h. The mathematical model of the robot dynamics is described by a system of equations [82]

$$\begin{aligned} \dot{\boldsymbol{\upsilon}}(t) &= \mathbf{A}\boldsymbol{\upsilon}(t) + \mathbf{B}\mathbf{u}(t-h) + \mathbf{d}(t-h), \\ \dot{\boldsymbol{\eta}}(t) &= \mathbf{R}\big(\boldsymbol{\eta}(t)\big)\boldsymbol{\upsilon}(t), \end{aligned} \tag{2.32}$$

where $\boldsymbol{\upsilon} = (v, v_n, \omega)^{\mathrm{T}}$ is the velocity vector: v – longitudinal linear velocity, v_n – linear normal velocity, ω – angular velocity; $\mathbf{u} = (u_v, u_{vn}, u_\omega)^{\mathrm{T}}$ – control actions vector: u_v – longitudinal traction force, u_{vn} – normal traction force, u_ω – rotating momentum; $\boldsymbol{\eta} = (x, y, \varphi)^{\mathrm{T}}$ – center of mass position and robot's heading angle; $\mathbf{d}$ – external disturbances vector; $\mathbf{A}$ – diagonal matrix of the friction coefficients; $\mathbf{B}$ – diagonal matrix of the control coefficients. The only nonlinearity of system (2.32) is described by the rotation matrix

$$\mathbf{R}(\boldsymbol{\eta}) = \mathbf{R}(\varphi) = \begin{pmatrix} \cos(\varphi) & -\sin(\varphi) & 0 \\ \sin(\varphi) & \cos(\varphi) & 0 \\ 0 & 0 & 1 \end{pmatrix}.$$

Basic issues of accounting for delay based on a compensation approach in the tasks of mobile robot control were first described in [48, 49], and a multipurpose approach to the stabilizing feedback synthesis for such robots is presented in

the article [47]. Issues of visual positioning with multipurpose feedback without taking delay into account are addressed in [41, 44, 45, 87, 95], and articles [42, 86] develop the results obtained for delay compensation.

Let us assume that a video camera is rigidly fixed in the geometric center of the robot, oriented in the direction of the robot's motion. In the camera's field of view there is always a certain visual marker, in the image plane represented by a set of points $\mathbf{s} = (x_i, y_i)$, $i = \overline{1, N}$, which in turn are projections of marker points (X_i, Y_i, Z_i), $i = \overline{1, N}$ in the camera reference frame. Let us set the task of positioning the robot relative to the marker in such a way that the projections of the marker points on the image are in the desired position. In this case, it is necessary to compensate for constant and polyharmonic external disturbances, as well as delay.

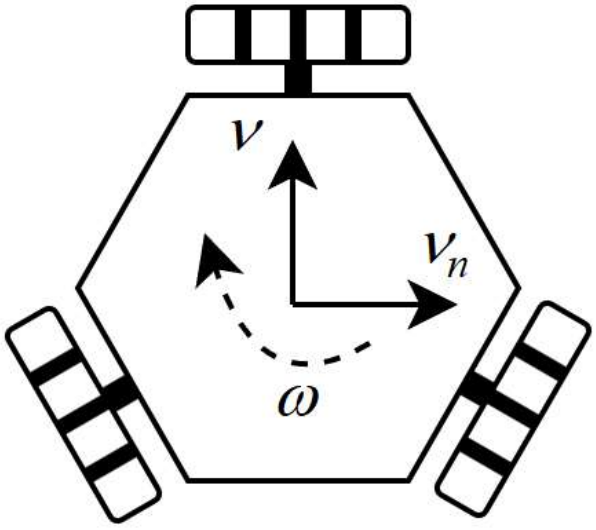

Fig. 2.2. Omni-wheeled robot model.

Note that in this case the interaction matrix $\mathbf{L}_s(\mathbf{s}, \mathbf{Z}_c)$ is much simpler:

$$\mathbf{L}(x_i, y_i, Z_i) = \begin{pmatrix} \frac{x_i}{Z_i} & -\frac{1}{Z_i} & -(1+x_i^2) \\ \frac{y_i}{Z_i} & 0 & -x_i y_i \end{pmatrix}.$$

Let us consider the application of the multipurpose regulator in various operating modes by experimenting with a computer model implemented in the Matlab-Simulink environment. For initial conditions, we will assume that the robot is located at the origin of reference frame and is directed in the direction of the Ox axis, and the center of the square-shaped visual marker is located at the point $(1.9601 \quad -0.3973)$ and rotated by an angle of 0.2 rad. The control goal is to achieve the position of the robot at which the distance to the marker is 1 m, and the angle between the heading angle of the robot and the vector directed from the center of the marker to the center of the robot is zero. This position corresponds to a point $(0.9801 \quad -0.1987)$. Let us take the corner points of the marker as the set of points of interest. Let us accept the following values for the parameters of the system and the multipurpose regulator:

$$\mathbf{A} = \text{diag}([-0.2587 \quad -0.2654 \quad -0.7333]),$$

$$\mathbf{B} = \text{diag}([0.5140 \quad 0.5140 \quad 66.7]),$$

$$\mathbf{H}_v = 10\mathbf{E}_3,\ \mathbf{H}_e = 10\mathbf{E}_8,\ \mu = 4,$$

$$\mathbf{K}_v = \text{diag}([62.7442 \quad 2.6878 \quad 0.9891]).$$

Let us first consider the simplest situation in which there is no external disturbance and delay; accordingly, the dynamic corrector is turned off and delay compensation is not applied. Fig. 2.3 demonstrates the dynamics of the system in this case – the left plot shows the trajectory of the corner points of the marker in the image plane, and the right plot shows the dynamics of the robot's position. As it can be seen, the desired marker position is reached in about 10 seconds and the robot stops.

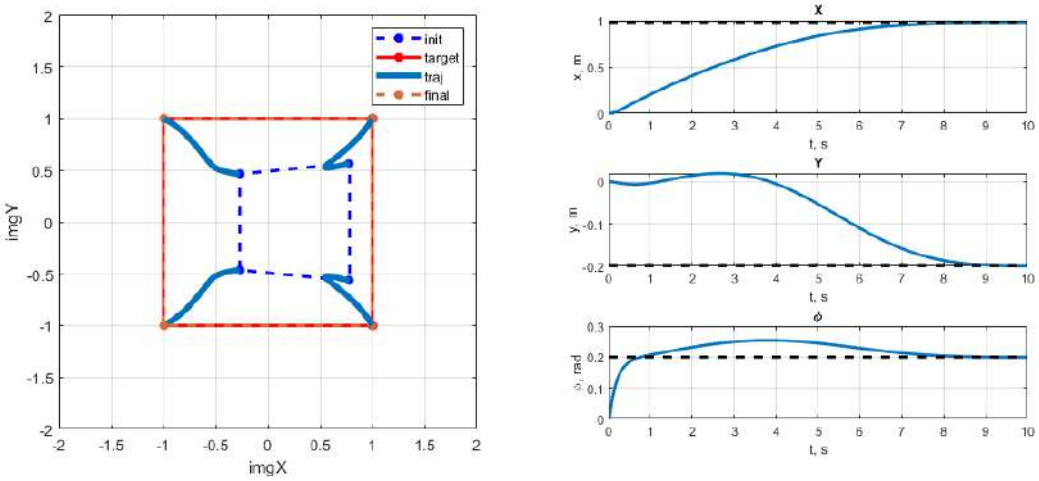

Fig. 2.3. Dynamics of the points on the image plane (left) and the robot motion in the absence of the delay and external disturbance (right).

Now consider the case when the robot is already in the desired position, but it is affected by a constant external disturbance $\mathbf{d} = [0.4 \quad 0.2 \quad 0.1]^T$. The dynamics of the system for this situation is presented in Fig. 2.4. One can notice that the robot deviates from the initial position and cannot return back.

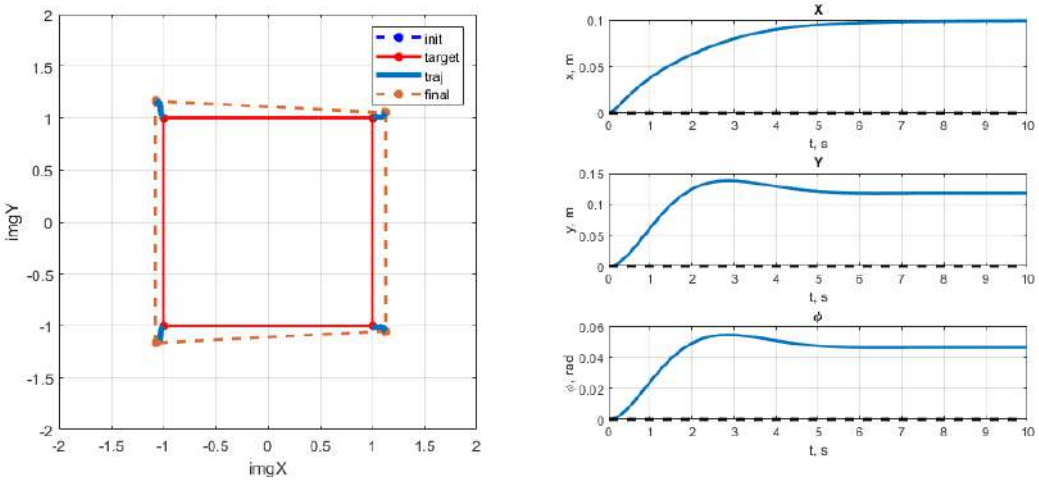

Fig. 2.4. Dynamics of robot motion in the presence of constant external disturbance with the dynamic corrector turned off.

Now we will apply the dynamic corrector synthesized in accordance with the procedure described in paragraph 2.2 for a constant disturbance compensation, as well as a polyharmonic disturbance consisting of three frequencies

$\omega_1 = 31.4159\,\mathrm{s}^{-1}$, $\omega_2 = 37.6991\,\mathrm{s}^{-1}$ and $\omega_3 = 43.9823\,\mathrm{s}^{-1}$. For $\boldsymbol{\alpha}_{\upsilon k}$ matrices we take matrices in the Frobenius form with eigenvalues $\lambda = -6$ of multiplicity 6. As it can be seen from Fig. 2.5, in this case the presence of a corrector allows the robot to return to its initial position under the influence of a constant external disturbance.

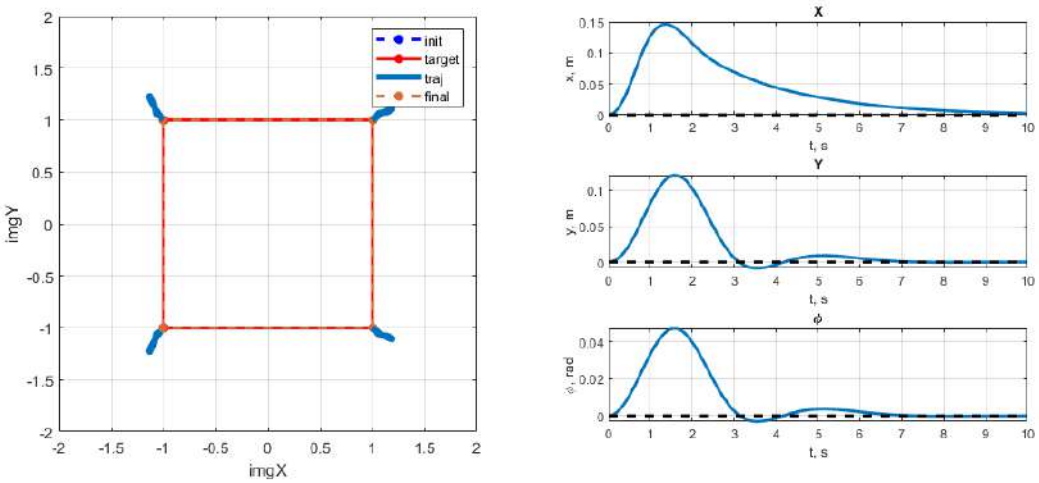

Fig. 2.5. Dynamics of robot motion in the presence of a constant external disturbance with the dynamic corrector turned on.

Finally, let us consider the influence of polyharmonic external disturbance in the form

$$w(t) = \sin(\omega_1 t) + \sin(\omega_2 t) + \sin(\omega_3 t),$$
$$\mathbf{d}(t) = \begin{pmatrix} 0.4w(t) & 0.2w(t) & 0.1w(t) \end{pmatrix}^{\mathrm{T}},$$

while the dynamic corrector will be turned on only after 5 seconds of the experiment. The dynamics of the system for this case are presented in Fig. 2.6 and Fig. 2.7. It can be seen that turning on the corrector does not have a noticeable effect on the dynamics of the system, while the intensity of the control signal decreases almost to zero.

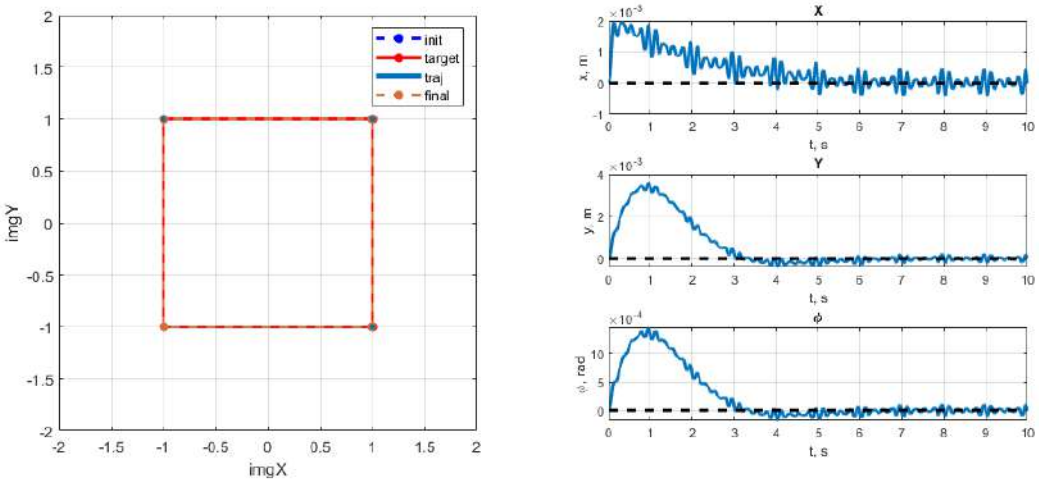

Fig. 2.6. Dynamics of robot motion in the presence of polyharmonic disturbance.

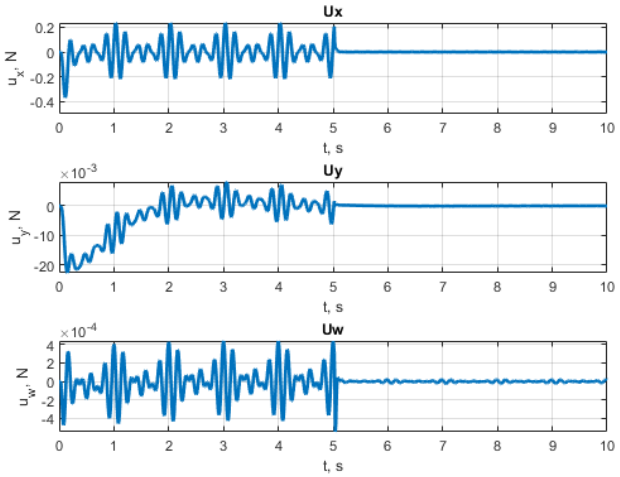

Fig. 2.7. Control signal in the presence of polyharmonic disturbance.

Now let us apply a constant delay $h = 0.06$ s to the system. Let us consider the first case when the robot moves towards a visual marker without external disturbance and with the dynamic corrector turned off. As it can be seen from Fig. 2.8, there is a noticeable deterioration in the quality of the dynamics along the heading angle, and oscillatory processes begin. A further increase in delay makes the system unstable.

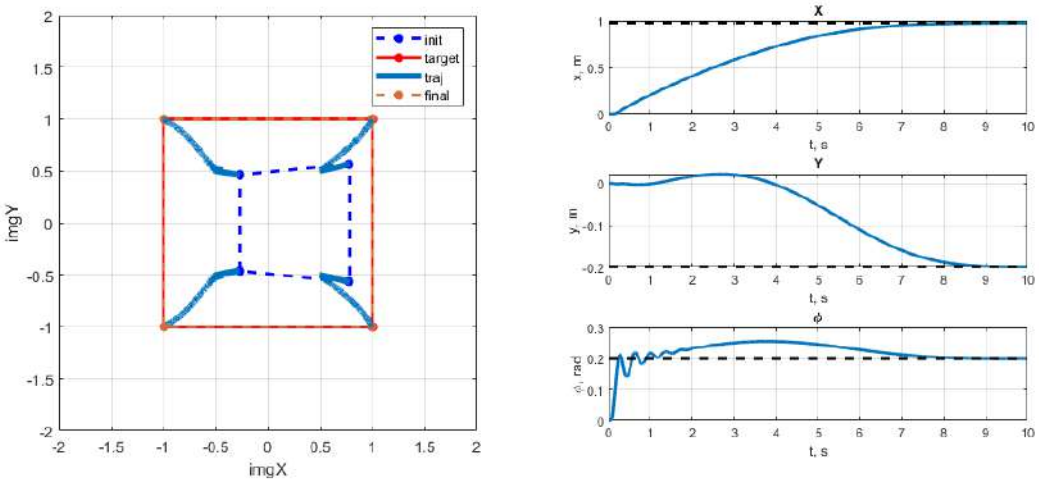

Fig. 2.8. Dynamics of robot motion in the presence of constant delay.

Let us transform the multipurpose regulator for the constant delay compensation in accordance with the previous paragraph. Analysis of Fig. 2.9 allows us to conclude that in this case the dynamics of the robot practically matches the case without the presence of delay.

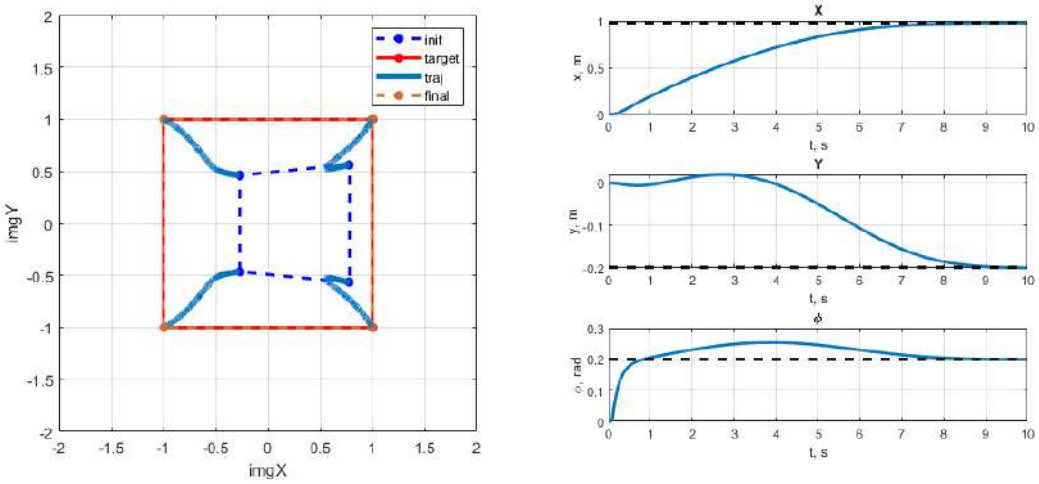

Fig. 2.9. Dynamics of robot motion with constant delay compensation.

Let us also not that the dynamics of the system in the presence of a constant or polyharmonic external disturbance in the case of delay compensation is also almost identical to the corresponding cases without delay, as it can be seen from Fig. 2.10, 2.11 and 2.12.

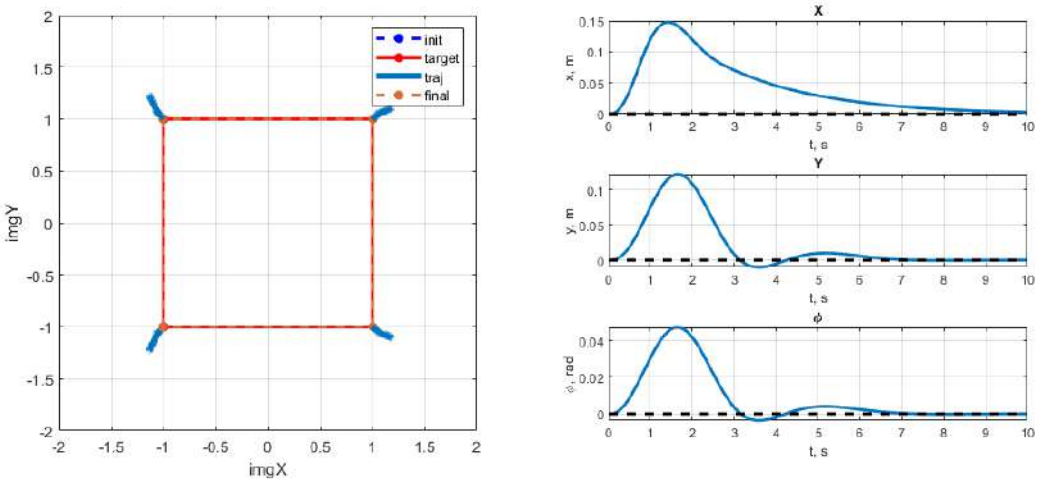

Fig. 2.10. Dynamics of robot motion in the presence of a constant external disturbance with the corrector turned on and with constant delay compensation.

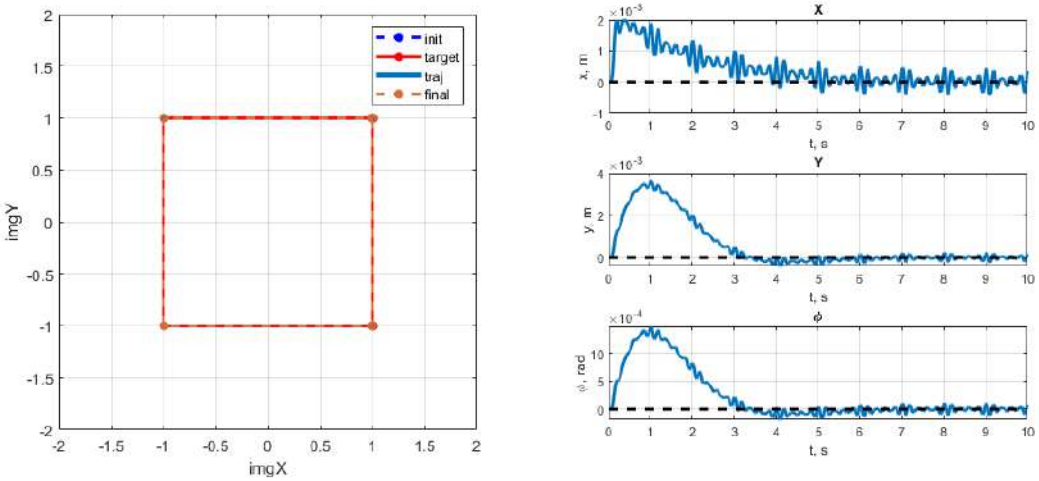

Fig. 2.11. Dynamics of robot motion in the presence of a polyharmonic external disturbance with the corrector turned on and with constant delay compensation.

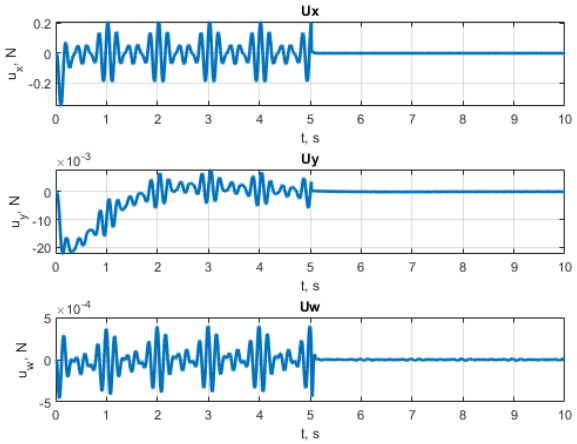

Fig. 2.12. Control signal in the presence of a polyharmonic external disturbance with the corrector turned on and with constant delay compensation.

Thus, the multipurpose regulator in this task is indeed an effective tool for stabilizing and compensating for external disturbances, and delay compensating transformation allows to obtain the dynamics of the system, which coincides with the dynamics in case without the delay.

2.5. Positioning the Underactuated Robot Relative to the Visual Marker

Now let us consider a similar problem using the example of an underactuated robot. Assume that the plant is a differential drive mobile robot, which is controlled by setting the voltages on the electric motors of two driving wheels (Fig. 2.13). As before, we assume that there is a constant transport delay h in the control channel and the external disturbance channel. The mathematical model of the robot dynamics is described by a system of equations [59]

$$\begin{aligned} \dot{\boldsymbol{\upsilon}}(t) &= \mathbf{A}\boldsymbol{\upsilon}(t) + \mathbf{B}\mathbf{u}(t-h) + \mathbf{d}(t-h), \\ \dot{\boldsymbol{\eta}}(t) &= \mathbf{R}\big(\boldsymbol{\eta}(t)\big)\boldsymbol{\upsilon}(t), \end{aligned} \tag{2.33}$$

where $\boldsymbol{\upsilon} = (v, \omega)^{\mathrm{T}}$ – velocity vector: v – linear velocity, ω – angular velocity; $\mathbf{u} = (u_v, u_\omega)^{\mathrm{T}}$ – control actions vector: u_v – drives voltage sum, u_ω – drives voltage difference; $\boldsymbol{\eta} = (x, y, \varphi)^{\mathrm{T}}$ – center of mass position and the robot's heading angle; $\mathbf{d}$ – external disturbance vector; $\mathbf{A}$ – diagonal matrix of the friction coefficients; $\mathbf{B}$ – diagonal matrix of the control coefficients. The only nonlinearity of system (2.33) is described by the rotation matrix

$$\mathbf{R}(\boldsymbol{\eta}) = \mathbf{R}(\varphi) = \begin{pmatrix} \sin(\varphi) & 0 \\ \cos(\varphi) & 0 \\ 0 & 1 \end{pmatrix}.$$

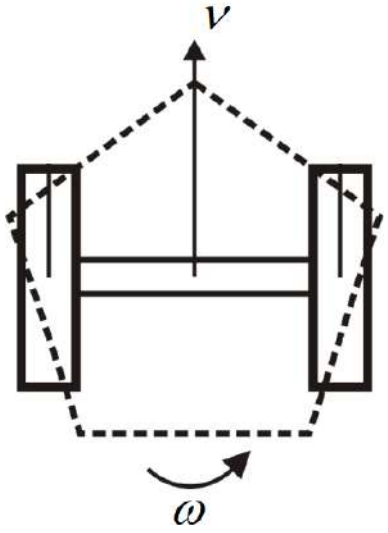

Fig. 2.13. Differential drive robot model.

Interaction matrix $\mathbf{L}_s(s, \mathbf{Z}_c)$ in this case is also rather simple:

$$\mathbf{L}(x_i, y_i, Z_i) = \begin{pmatrix} \frac{x_i}{Z_i} & -(1+x_i^2) \\ \frac{y_i}{Z_i} & -x_i y_i \end{pmatrix}.$$

As in the previous paragraph, we set the problem of positioning the robot relative to a square-shaped visual marker. The initial conditions and the desired position also the same. Let us accept the following values for the parameters of the system and the multipurpose regulator:

$$\mathbf{A} = -\mathbf{E}_{2\text{x}2},\ \mathbf{B} = \mathbf{E}_{2\text{x}2},$$

$$\mathbf{H}_v = 100\mathbf{E}_{3\text{x}3},\ \mathbf{H}_e = 100\mathbf{E}_{8\text{x}8},$$

$$\mathbf{K}_v = diag([8 \quad 2]),\ \mu = 4.$$

Let us first consider the simplest situation in which there is no external disturbance and delay; accordingly, the dynamic corrector is turned off and delay compensation is not applied. Fig. 2.14 demonstrates the dynamics of the system in this case. As it can be seen, the desired marker position is reached in about 3 seconds and the robot stops.

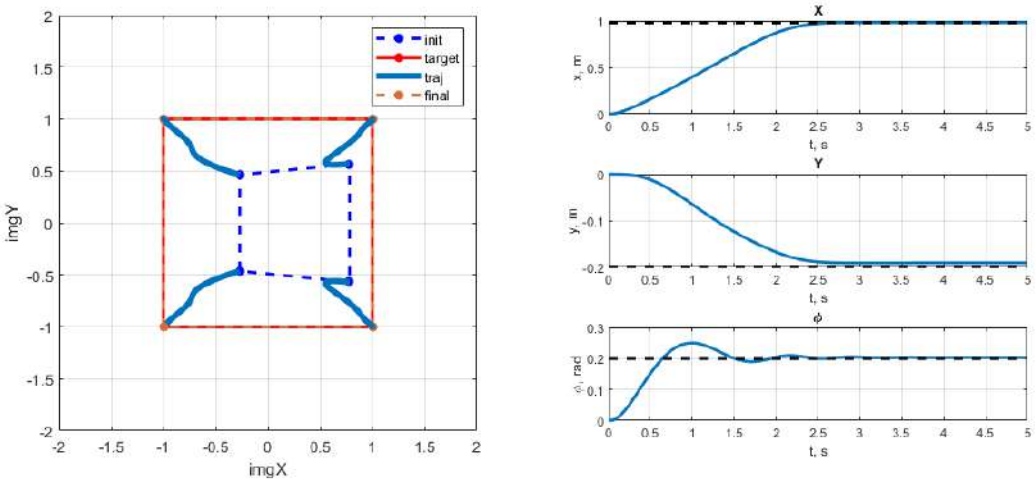

Fig. 2.14. Dynamics of the system in the absence of external disturbances and delay.

Next, we apply a constant external disturbance $\mathbf{d} = (2 \quad 1)^{\mathrm{T}}$ with the dynamic corrector turned off in a case when the robot is already in the desired position. From Fig. 2.15 it is clear that in this case the robot is displaced and cannot compensate the displacement, since the closed-loop system does not have astatism.

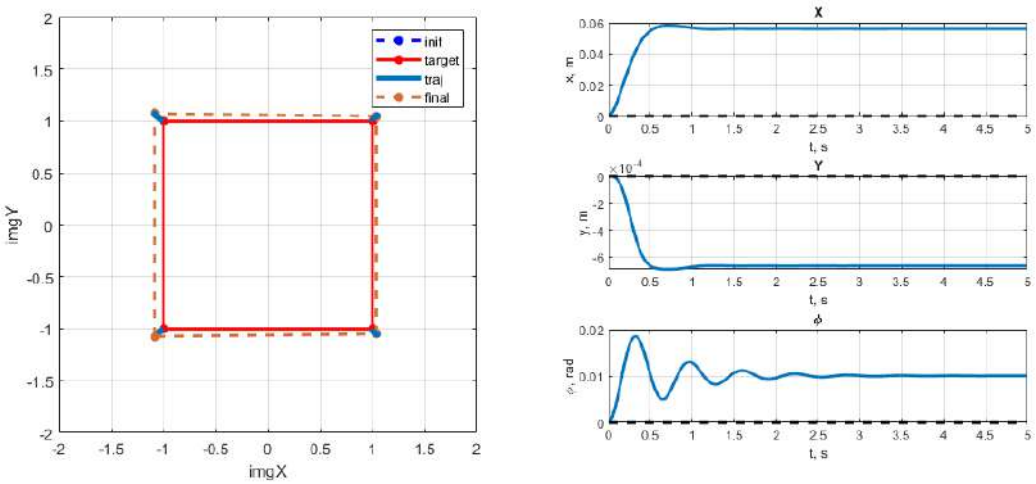

Fig. 2.15. Dynamics of the system in the presence of external disturbance.

As before, we synthesize a dynamic corrector to compensate simultaneously for constant disturbance and polyharmonic disturbance with three frequencies $\omega_1 = 31.4159 \ \ \mathrm{s}^{-1}$, $\omega_2 = 37.6991 \ \ \mathrm{s}^{-1}$ and $\omega_3 = 43.9823 \ \ \mathrm{s}^{-1}$. For matrices $\boldsymbol{\alpha}_{\upsilon k}$ we will take matrices in Frobenius form with eigenvalues $\lambda = -2.8$ of multiplicity 4.

The dynamics of the system with the corrector turned on are shown in Fig. 2.16. It can be seen that in this case the robot returns to its initial position.

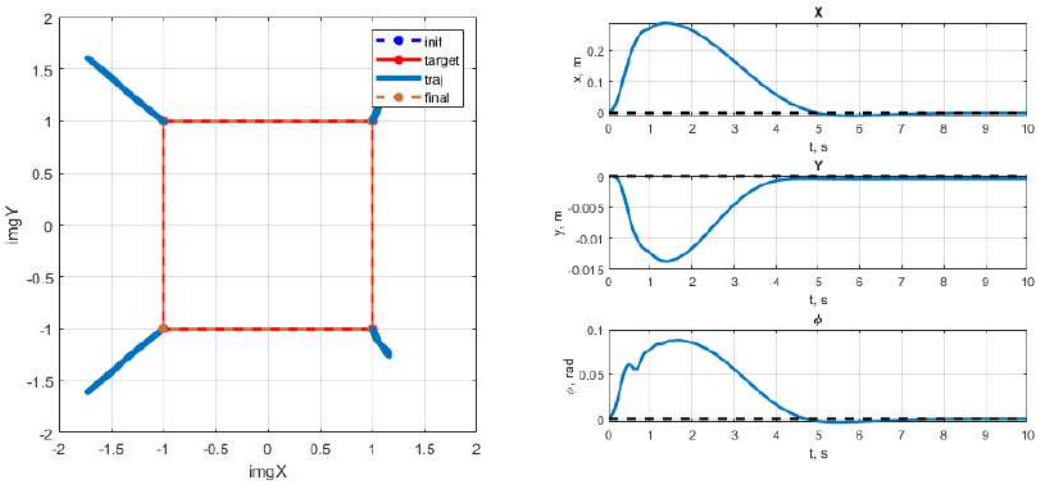

Fig. 2.16. Dynamics of points in the image plane in the presence of external disturbance with the dynamic corrector turned on.

Now consider the influence of a polyharmonic disturbance in the form

$$w(t) = \sin(\omega_1 t) + \sin(\omega_2 t) + \sin(\omega_3 t),$$
$$\mathbf{d}(t) = \begin{pmatrix} 2w(t) & w(t) \end{pmatrix}^{\mathrm{T}},$$

while the dynamic corrector remains turned off for the first 5 s. From Fig. 2.17 and 2.18 it is clear that after turning on the corrector, the control intensity is significantly reduced, without having a noticeable effect on the dynamics of the robot's motion.

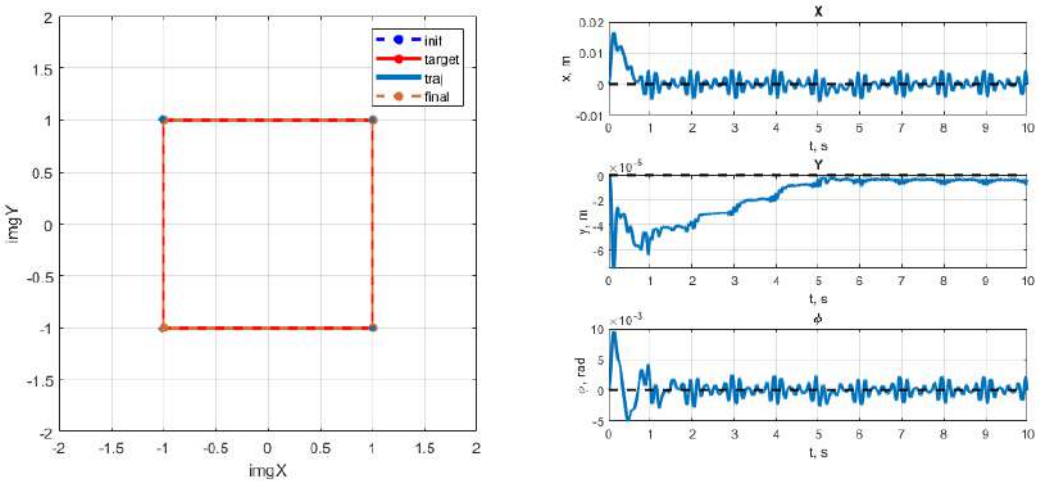

Fig. 2.17. Dynamics of the system in the presence of polyharmonic disturbance.

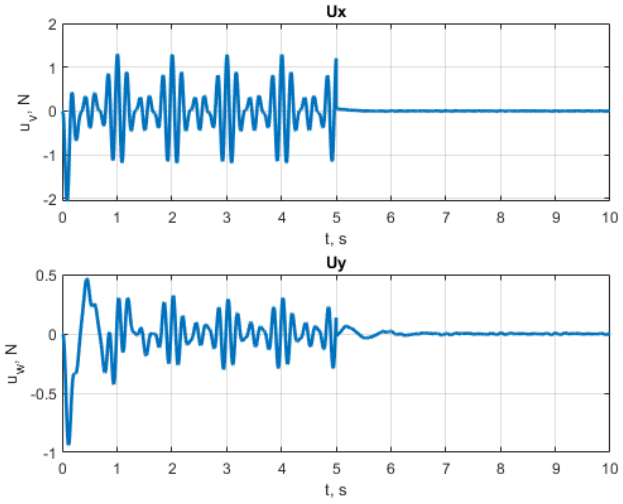

Fig. 2.18. Control signal dynamics in the presence of polyharmonic disturbance.

Let us return again to the original task of moving to a visual marker and apply a constant delay $h = 0.04$ s to the system. Fig. 2.19 shows the dynamics of the system in this case, from which it can be seen that the system becomes unstable with respect to the heading angle.

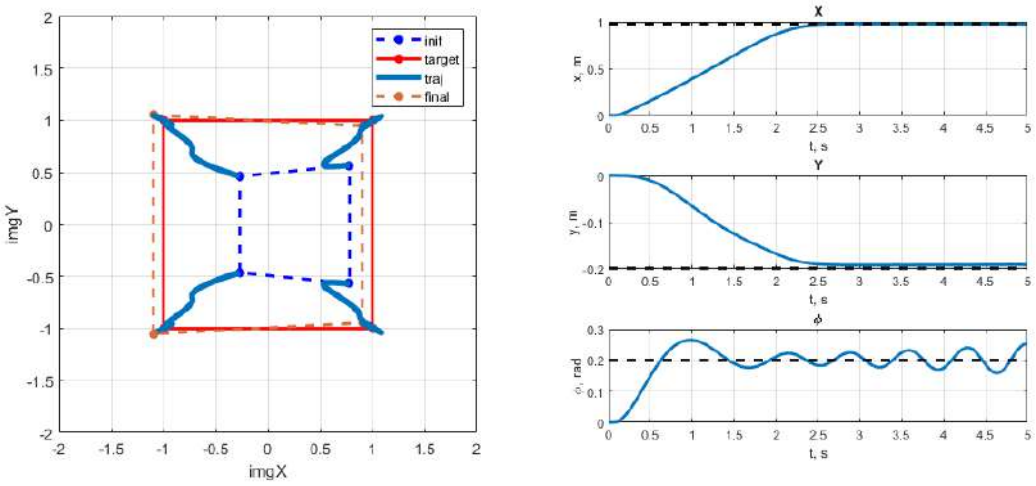

Fig. 2.19. System dynamics in the presence of constant delay.

As in the previous paragraph, we will apply a delay-compensating transformation of the regulator. Fig. 2.20, 2.21, 2.22 and 2.23 demonstrate that the use of a transformed regulator allows to obtain dynamics almost identical to the case without delay in all operating modes – without external disturbance and with constant and polyharmonic external disturbance using a dynamic corrector.

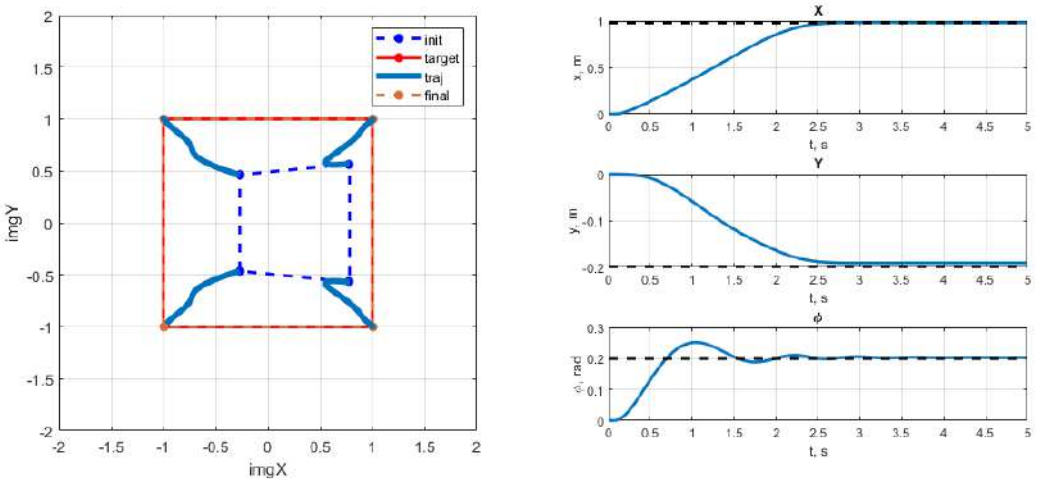

Fig. 2.20. System dynamics in the presence of a constant delay using a compensating regulator.

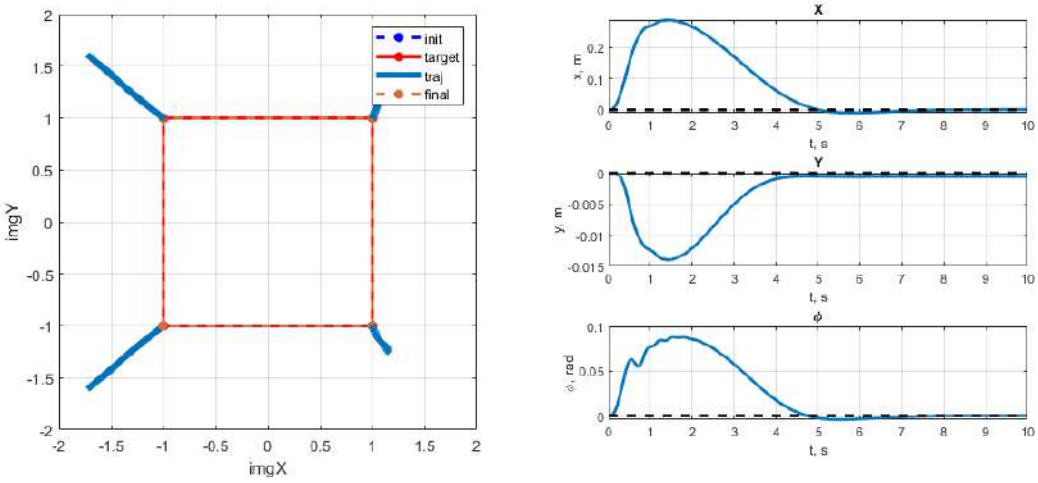

Fig. 2.21. System dynamics in the presence of a constant external disturbance.

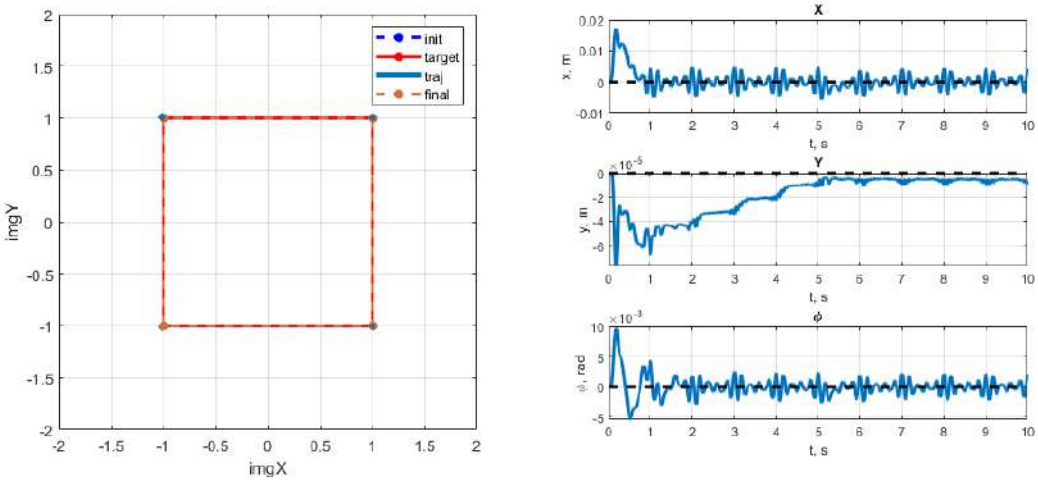

Fig. 2.22. System dynamics in the presence of polyharmonic disturbance.

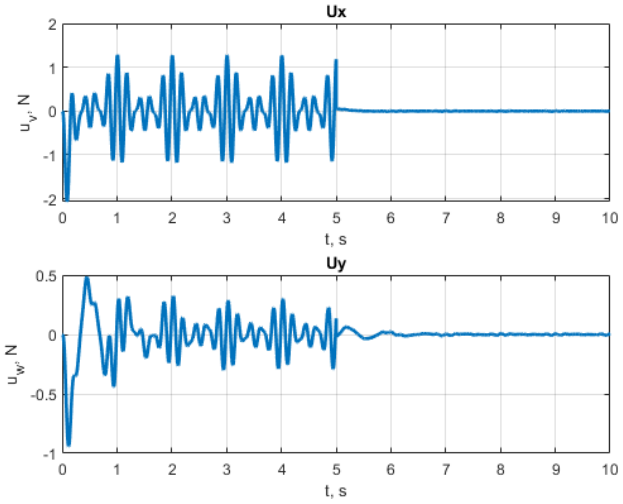

Fig. 2.23. Control signal dynamics in the presence of polyharmonic disturbance.

Thus, the presented approach can also be used for the underactuated systems, at least for a certain subset of positions.

2.6. Conclusions

The results of the experiments with a computer model allow to conclude that multipurpose regulators can be effectively used in tasks of visual positioning of moving objects. At the same time, all the advantages of such regulators are retained: independence of the synthesis of adjustable elements and the ability to disable individual elements of the multipurpose structure of the control law.

As in the previous chapter, it is shown that the presence of delay negatively affects the quality of the dynamics of controlled motion. A special transformation of the multipurpose regulator makes it possible to compensate for the delay, preserving the dynamic characteristics of a closed-loop system synthesized without taking into account the delay. Provided that the external disturbance is available for direct measurement, the compensating controller also works along with the dynamic corrector turned on.

Chapter 3. Multipurpose Control of the Nonlinear Systems Based on the Feedback Linearization

Currently, robotic manipulator arms are an integral part of automated production, replacing human labor where accuracy and speed of work are required [55]. Of particular interest when solving problems of controlling such objects is the fact that mathematical models of the dynamics of such robots contain significant nonlinearities. In this case, an approach called feedback linearization [69] is often used to get rid of nonlinearity.

This chapter describes the combination of multipurpose control structure usage with compensation approach presented in previous chapters, as well as feedback linearization in the problem of stabilizing a given position of nonlinear control objects taking into account external disturbances and delays. It is worth noting that there are alternative methods for taking into account delay, for example, the use of asymptotic observers of a special type [88] or the continuous pole placement method [80, 89], however, the procedure for designing a controller in this case is quite complex and does not always guarantee the stability of a closed-loop system.

Paragraph 3.1 provides formulation of the problem. Paragraph 3.2 is devoted to the feedback linearization method in the given problem. Paragraph 3.3 introduces a multipurpose regulator for a linearized system, as well as a procedure for synthesizing such a controller. Paragraph 3.4 describes the transformation of a multipurpose regulator for constant delay compensation. Finally, paragraph 3.5 is devoted to the results of experiments with a computer model of a two-link robotic manipulator arm in various operating modes.

3.1. Problem Formulation

Let us consider a nonlinear mathematical model of the dynamics of an arbitrary control object taking into account the constant delay in the control channel and in the external disturbance channel in the form

$$\mathbf{M}[\boldsymbol{\theta}(t)]\ddot{\boldsymbol{\theta}}(t) + \mathbf{C}[\boldsymbol{\theta}(t), \dot{\boldsymbol{\theta}}(t)] + \mathbf{g}[\boldsymbol{\theta}(t)] = \boldsymbol{\tau}(t-h) + \boldsymbol{\tau}_e(t-h), \qquad (3.1)$$

where $\boldsymbol{\theta} \in E^n$ – generalized coordinates vector, $\mathbf{M} = \mathbf{M}^{\mathrm{T}}$ – positive definite symmetric inertia matrix, $\mathbf{C}$ – Coriolis and centripetal forces vector, $\mathbf{g}$ – gravitational forces vector, $\boldsymbol{\tau} \in E^n$ – control torque vector, $\boldsymbol{\tau}_e \in E^n$ – external disturbance vector, t – current time, h – constant delay.

We will assume that the control goal is to stabilize the current position $\boldsymbol{\theta}$ of the control object in a given position $\boldsymbol{\theta}_d$, i.e. ensuring condition

$$\lim_{t \to +\infty} \boldsymbol{\theta}(t) = \boldsymbol{\theta}_d . \tag{3.2}$$

Let us consider various operating modes in which special requirements for system dynamics are set.

1) In the absence of external disturbances, the system is in *the proper motion mode*, where the main requirements for the quality of dynamics, in addition to condition (3.2), may include restrictions on the settling time and overshoot.

2) In case $\boldsymbol{\tau}_e(t) = \boldsymbol{\tau}_{e0}$ the system is in the *forced motion under the influence of a constant external disturbance mode*. We will assume that in this mode the desired position $\boldsymbol{\theta}_d$ corresponds to the initial position $\boldsymbol{\theta}_0$, while restrictions are set on the maximum deviation of the current state $\boldsymbol{\theta}(t)$ from the given position $\boldsymbol{\theta}_d$, and the control goal is to ensure astatism of the system taking into account these restrictions.

3) In the *forced motion under the influence of a periodic external disturbance mode*, it is necessary to minimize the intensity of the response of the control signal to a polyharmonic disturbance with known frequencies, without deteriorating the quality of stabilization. In this mode we will also accept $\boldsymbol{\theta}_d = \boldsymbol{\theta}_0$.

3.2. Feedback Linearization

Let us first consider a simpler problem of stabilizing the plant current position in the proper motion mode (i.e. in the absence of external disturbance), and also without taking into account the delay. Then the mathematical model will take the form

$$\mathbf{M}(\boldsymbol{\theta})\ddot{\boldsymbol{\theta}} + \mathbf{C}(\boldsymbol{\theta},\dot{\boldsymbol{\theta}}) + \mathbf{g}(\boldsymbol{\theta}) = \boldsymbol{\tau}. \tag{3.3}$$

Before introducing the multipurpose control structure, let us consider the following problem. The matrices $\mathbf{M}(\boldsymbol{\theta})$, $\mathbf{C}(\boldsymbol{\theta},\dot{\boldsymbol{\theta}})$ and $\mathbf{g}(\boldsymbol{\theta})$ in equations (3.3) are generally nonlinear. In this regard, let us linearize the system (3.3) by generating a control signal in such a way that gets rid of nonlinearities.

Resolving (3.3) with respect to the highest derivative, we obtain

$$\ddot{\boldsymbol{\theta}} = \mathbf{M}^{-1}(\boldsymbol{\theta})(\boldsymbol{\tau} - \mathbf{C}(\boldsymbol{\theta},\dot{\boldsymbol{\theta}}) - \mathbf{g}(\boldsymbol{\theta})). \tag{3.4}$$

Next, we reduce (3.4) to a system of first-order ODEs. Let us introduce the vector $\boldsymbol{\omega}(t) = \dot{\boldsymbol{\theta}}(t)$. Then system (3.4) can be represented in the form

$$\begin{aligned} \dot{\boldsymbol{\theta}} &= \boldsymbol{\omega}, \\ \dot{\boldsymbol{\omega}} &= \mathbf{M}^{-1}(\boldsymbol{\theta})(\boldsymbol{\tau} - \mathbf{C}(\boldsymbol{\theta},\boldsymbol{\omega}) - \mathbf{g}(\boldsymbol{\theta})). \end{aligned} \tag{3.5}$$

Let us represent the control signal in the form

$$\boldsymbol{\tau} = \mathbf{C}(\boldsymbol{\theta},\boldsymbol{\omega}) + \mathbf{g}(\boldsymbol{\theta}) + \mathbf{M}(\boldsymbol{\theta})\mathbf{u}, \tag{3.6}$$

where $\mathbf{u} = \mathbf{u}(t)$ is some vector function. Substituting (3.6) into (3.5), we obtain a linear time-invariant (LTI) system

$$\begin{aligned} \dot{\boldsymbol{\theta}} &= \boldsymbol{\omega}, \\ \dot{\boldsymbol{\omega}} &= \mathbf{u}, \end{aligned} \tag{3.7}$$

for which $\mathbf{u}$ is a control signal.

The asymptotic stability of system (3.7) can be achieved by synthesizing the vector $\mathbf{u}$ in the form

$$\mathbf{u} = -\mathbf{K}_\theta\boldsymbol{\theta} - \mathbf{K}_\omega\boldsymbol{\omega}, \tag{3.8}$$

where $\mathbf{K}_\theta$ and $\mathbf{K}_\omega$ are arbitrary matrices that ensure the Hurwitz property of the matrix

$$\begin{pmatrix} \mathbf{0} & \mathbf{E} \\ -\mathbf{K}_\theta & -\mathbf{K}_\omega \end{pmatrix},$$

as well as the required quality of the closed-loop system dynamics. For example, if a quadratic quality functional is given, then the matrices $\mathbf{K}_\theta$ and $\mathbf{K}_\omega$ can be found as a solution to the LQR synthesis problem.

3.3. Multipurpose Regulator Synthesis

Now consider the general case for an arbitrary operating mode in which external disturbances may be present. Let us consider the issue of regulator synthesis for generating a control signal in a linearized system (3.7), taking into account the requirements for dynamics in various motion modes. To begin with, we will assume that there given an arbitrary linear system in the form

$$\begin{aligned} \dot{\mathbf{x}} &= \mathbf{A}\mathbf{x} + \mathbf{B}\mathbf{u} + \mathbf{d}, \\ \mathbf{y} &= \mathbf{C}\mathbf{x}, \end{aligned} \tag{3.9}$$

where $\mathbf{x}$ – system state vector, $\mathbf{y}$ – measurement vector, $\mathbf{d} = \mathbf{d}(t)$ – external disturbance vector, $\mathbf{A}$, $\mathbf{B}$ and $\mathbf{C}$ – constant matrices. To stabilize system (3.9) taking into account the specified requirements, we will generate a control signal using a multipurpose regulator in the form

$$\begin{aligned} \dot{\mathbf{z}} &= \mathbf{A}\mathbf{z} + \mathbf{B}\mathbf{u} + \mathbf{H}(\mathbf{y} - \mathbf{C}\mathbf{z}), \\ \dot{\mathbf{p}} &= \boldsymbol{\alpha}\mathbf{p} + \boldsymbol{\beta}(\mathbf{y} - \mathbf{C}\mathbf{z}), \\ \boldsymbol{\xi} &= \boldsymbol{\gamma}\mathbf{p} + \boldsymbol{\mu}(\mathbf{y} - \mathbf{C}\mathbf{z}), \\ \mathbf{u} &= -\mathbf{K}\mathbf{z} + \boldsymbol{\xi}. \end{aligned} \tag{3.10}$$

The first equation of the system (3.10) is an asymptotic observer whose task is to model the dynamics of the original control object. The output of the observer is used in the dynamic corrector, represented by the second and third equations of the system (3.10). The corrector is used to compensate for external disturbances in various operating modes. For example, it can be used to ensure astatism in the output $\mathbf{y}$ of a control object in the presence of a constant external disturbance, or to minimize the intensity of the control signal in response to a polyharmonic disturbance. Finally, the last equation of the regulator (3.10) is a control signal that is directly fed to the input of the linear system (3.9).

Let us turn to the problem of the multipurpose regulator synthesis. The adjustable elements of structure (3.10) are the matrix $\mathbf{H}$ of the asymptotic observer, the matrix $\mathbf{K}$ of the control law and the matrices $\boldsymbol{\alpha}$, $\boldsymbol{\beta}$, $\boldsymbol{\gamma}$, $\boldsymbol{\mu}$ of the

dynamic corrector. Let us consider the equations of the closed-loop system (3.9) – (3.10) without external disturbance, excluding the variables $\mathbf{y}$, $\boldsymbol{\xi}$, $\mathbf{u}$:

$$\begin{aligned}
\dot{\mathbf{x}} &= \mathbf{A}\mathbf{x} - \mathbf{B}\mathbf{K}\mathbf{z} + \mathbf{B}\boldsymbol{\gamma}\mathbf{p} + \mathbf{B}\boldsymbol{\mu}\mathbf{C}(\mathbf{x} - \mathbf{z}),\\
\dot{\mathbf{z}} &= \mathbf{A}\mathbf{z} - \mathbf{B}\mathbf{K}\mathbf{z} + \mathbf{B}\boldsymbol{\gamma}\mathbf{p} + \mathbf{B}\boldsymbol{\mu}\mathbf{C}(\mathbf{x} - \mathbf{z}) + \mathbf{H}\mathbf{C}(\mathbf{x} - \mathbf{z}),\\
\dot{\mathbf{p}} &= \boldsymbol{\alpha}\mathbf{p} + \boldsymbol{\beta}\mathbf{C}(\mathbf{x} - \mathbf{z}),
\end{aligned}$$

or in the matrix form:

$$\begin{pmatrix} \dot{\mathbf{x}} \\ \dot{\mathbf{z}} \\ \dot{\mathbf{p}} \end{pmatrix} = \begin{pmatrix} \mathbf{A} + \mathbf{B}\boldsymbol{\mu}\mathbf{C} & -\mathbf{B}\mathbf{K} - \mathbf{B}\boldsymbol{\mu}\mathbf{C} & \mathbf{B}\boldsymbol{\gamma} \\ \mathbf{B}\boldsymbol{\mu}\mathbf{C} + \mathbf{H}\mathbf{C} & \mathbf{A} - \mathbf{B}\mathbf{K} - \mathbf{B}\boldsymbol{\mu}\mathbf{C} - \mathbf{H}\mathbf{C} & \mathbf{B}\boldsymbol{\gamma} \\ \boldsymbol{\beta}\mathbf{C} & -\boldsymbol{\beta}\mathbf{C} & \boldsymbol{\alpha} \end{pmatrix} \begin{pmatrix} \mathbf{x} \\ \mathbf{z} \\ \mathbf{p} \end{pmatrix}. \qquad (3.11)$$

The characteristic polynomial of system (3.11) is equal to

$$\Delta(s) = \det \begin{pmatrix} \mathbf{E}s - \mathbf{A} - \mathbf{B}\boldsymbol{\mu}\mathbf{C} & \mathbf{B}\mathbf{K} + \mathbf{B}\boldsymbol{\mu}\mathbf{C} & -\mathbf{B}\boldsymbol{\gamma} \\ -\mathbf{B}\boldsymbol{\mu}\mathbf{C} - \mathbf{H}\mathbf{C} & \mathbf{E}s - \mathbf{A} + \mathbf{B}\mathbf{K} + \mathbf{B}\boldsymbol{\mu}\mathbf{C} + \mathbf{H}\mathbf{C} & -\mathbf{B}\boldsymbol{\gamma} \\ -\boldsymbol{\beta}\mathbf{C} & \boldsymbol{\beta}\mathbf{C} & \mathbf{E}s - \boldsymbol{\alpha} \end{pmatrix}.$$

Adding the second column to the first one, we obtain

$$\Delta(s) = \det \begin{pmatrix} \mathbf{E}s - \mathbf{A} + \mathbf{B}\mathbf{K} & \mathbf{B}\mathbf{K} + \mathbf{B}\boldsymbol{\mu}\mathbf{C} & -\mathbf{B}\boldsymbol{\gamma} \\ \mathbf{E}s - \mathbf{A} + \mathbf{B}\mathbf{K} & \mathbf{E}s - \mathbf{A} + \mathbf{B}\mathbf{K} + \mathbf{B}\boldsymbol{\mu}\mathbf{C} + \mathbf{H}\mathbf{C} & -\mathbf{B}\boldsymbol{\gamma} \\ \mathbf{0} & \boldsymbol{\beta}\mathbf{C} & \mathbf{E}s - \boldsymbol{\alpha} \end{pmatrix}.$$

Next, subtracting the first row from the second one, we get

$$\Delta(s) = \det \begin{pmatrix} \mathbf{E}s - \mathbf{A} + \mathbf{B}\mathbf{K} & \mathbf{B}\mathbf{K} + \mathbf{B}\boldsymbol{\mu}\mathbf{C} & -\mathbf{B}\boldsymbol{\gamma} \\ \mathbf{0} & \mathbf{E}s - \mathbf{A} + \mathbf{H}\mathbf{C} & \mathbf{0} \\ \mathbf{0} & \boldsymbol{\beta}\mathbf{C} & \mathbf{E}s - \boldsymbol{\alpha} \end{pmatrix}.$$

According to the property of the quasi-triangular matrix determinant, we can write

$$\begin{aligned}
\Delta(s) &= \det(\mathbf{E}s - \mathbf{A} + \mathbf{B}\mathbf{K}) \det \begin{pmatrix} \mathbf{E}s - \mathbf{A} + \mathbf{H}\mathbf{C} & \mathbf{0} \\ \boldsymbol{\beta}\mathbf{C} & \mathbf{E}s - \boldsymbol{\alpha} \end{pmatrix} = \\
&= \det(\mathbf{E}s - \mathbf{A} + \mathbf{B}\mathbf{K}) \det(\mathbf{E}s - \mathbf{A} + \mathbf{H}\mathbf{C}) \det(\mathbf{E}s - \boldsymbol{\alpha}) = \Delta_b(s)\Delta_o(s)\Phi(s),
\end{aligned}$$

where $\Delta_b(s)$, $\Delta_o(s)$ and $\Phi(s)$ – characteristic polynomials of the system (3.9), closed by the basic control law, of the asymptotic observer and of the dynamic corrector, correspondingly. Thus, in the general case, to ensure the asymptotic stability of the closed-loop system (3.9) – (3.10), the following conditions must be met:

1) matrix $\mathbf{K}$ of the control law must ensure that matrix $\mathbf{A}-\mathbf{BK}$ is Hurwitz;
2) matrix $\mathbf{H}$ of the asymptotic observer must ensure that matrix $\mathbf{A}-\mathbf{HC}$ is Hurwitz;
3) matrix $\boldsymbol{\alpha}$ of the dynamic corrector must be Hurwitz.

Further refinement of the values of the adjustable elements depends on the specific requirements for the quality of the controlled motion dynamics.

Let us consider, in particular, the issues of ensuring astatism and minimization of the control signal response to a polyharmonic disturbance in the corresponding modes. Let us return to the linearized system (3.7). Despite the fact that precise measurements of the variables $\boldsymbol{\theta}$ and $\boldsymbol{\omega}$ are used to the nonlinearities compensation, we will assume that the output of the linearized system is the vector $\mathbf{y}=\boldsymbol{\theta}$. It will be shown below that this is sufficient for the efficient operation of a multipurpose regulator, which in this case can be represented as

$$\begin{aligned}
&\dot{\mathbf{z}}_\theta = \mathbf{z}_\omega + \mathbf{H}_\theta(\boldsymbol{\theta}-\mathbf{z}_\theta),\\
&\dot{\mathbf{z}}_\omega = \mathbf{u} + \mathbf{H}_\omega(\boldsymbol{\theta}-\mathbf{z}_\theta),\\
&\dot{\mathbf{p}} = \boldsymbol{\alpha}\mathbf{p} + \boldsymbol{\beta}(\boldsymbol{\theta}-\mathbf{z}_\theta),\\
&\boldsymbol{\xi} = \boldsymbol{\gamma}\mathbf{p} + \boldsymbol{\mu}(\boldsymbol{\theta}-\mathbf{z}_\theta),\\
&\mathbf{u} = -\mathbf{K}_\theta(\mathbf{z}_\theta-\boldsymbol{\theta}_d) - \mathbf{K}_\omega\mathbf{z}_\omega + \boldsymbol{\xi},
\end{aligned} \tag{3.12}$$

where $\mathbf{z}_\theta$ and $\mathbf{z}_\omega$ – state vector of the corresponding asymptotic observers for the variables $\boldsymbol{\theta}$ and $\boldsymbol{\omega}$. Tunable elements of the regulator (3.12) are matrices $\mathbf{H}_\theta$, $\mathbf{H}_\omega$, $\mathbf{K}_\theta$, $\mathbf{K}_\omega$, $\boldsymbol{\alpha}$, $\boldsymbol{\beta}$, $\boldsymbol{\gamma}$, $\boldsymbol{\mu}$. From the considerations given above for the regulator (3.10) it follows that:

1) matrices $\mathbf{K}_\theta$ and $\mathbf{K}_\omega$ of the basic control law must ensure the Hurwitz property of the matrix

$$\mathbf{K}_b = \begin{pmatrix} \mathbf{0} & \mathbf{E} \\ -\mathbf{K}_\theta & -\mathbf{K}_\omega \end{pmatrix};$$

2) matrices $\mathbf{H}_\theta$ and $\mathbf{H}_\omega$ of the asymptotic observer are set from the similar reasoning, providing the Hurwitz property of the matrix

$$\mathbf{H}_o = \begin{pmatrix} -\mathbf{H}_\theta & \mathbf{E} \\ -\mathbf{H}_\omega & \mathbf{0} \end{pmatrix};$$

3) matrix $\boldsymbol{\alpha}$ of the dynamic corrector must be Hurwitz.

Next, we turn to the issue of dynamic corrector synthesis to ensure astatism of a closed-loop system in the presence of a constant external disturbance. The corrector can be represented in tf-form as

$$\boldsymbol{\xi} = \mathbf{F}(s)(\boldsymbol{\theta} - \mathbf{z}_\theta),$$

where s – Laplace variable, $\mathbf{F}(s) = \boldsymbol{\gamma}(\mathbf{E}s - \boldsymbol{\alpha})^{-1}\boldsymbol{\beta} + \boldsymbol{\mu}$ – corrector transfer matrix.

The presence of an external disturbance in equation (3.3) leads to the fact that, actually, as a result of feedback linearization, instead of (3.7), we obtain the system

$$\begin{aligned} \dot{\boldsymbol{\theta}} &= \boldsymbol{\omega}, \\ \dot{\boldsymbol{\omega}} &= \mathbf{u} + \mathbf{d}, \end{aligned} \tag{3.13}$$

where $\mathbf{d}(t) = \mathbf{M}^{-1}[\boldsymbol{\theta}(t)]\boldsymbol{\tau}_e(t)$.

In the considered mode of motion, the external disturbance is constant or slowly changing, i.e. we can assume that $\mathbf{d}(t) = \mathbf{d}_0$.

Theorem 3.1. *Closed-loop system (3.13), (3.12) is astatic with respect to any constant disturbance* $\mathbf{d}(t) = \mathbf{d}_0$, *if the transfer matrix of the dynamic corrector satisfies the condition*

$$\mathbf{F}(0) = -\mathbf{K}_\theta - \mathbf{K}_\omega\mathbf{H}_\theta - \mathbf{H}_\omega. \tag{3.14}$$

Proof. The dynamics equations of the closed-loop system (3.13), (3.12) can be written as

$$\begin{aligned} \dot{\boldsymbol{\theta}} &= \boldsymbol{\omega}, \\ \dot{\boldsymbol{\omega}} &= \mathbf{u} + \mathbf{d}_0, \\ \dot{\mathbf{z}}_\theta &= \mathbf{z}_\omega + \mathbf{H}_\theta\boldsymbol{\varepsilon}_\theta, \\ \dot{\mathbf{z}}_\omega &= \mathbf{u} + \mathbf{H}_\omega\boldsymbol{\varepsilon}_\theta, \\ \boldsymbol{\xi} &= \mathbf{F}(s)\boldsymbol{\varepsilon}_\theta, \\ \mathbf{u} &= -\mathbf{K}_\theta(\mathbf{z}_\theta - \boldsymbol{\theta}_d) - \mathbf{K}_\omega\mathbf{z}_\omega + \boldsymbol{\xi}, \end{aligned}$$

where $\boldsymbol{\varepsilon}_\theta = \boldsymbol{\theta} - \mathbf{z}_\theta$. Subtracting the third and fourth equations from the first two, introducing the notation $\boldsymbol{\varepsilon}_\omega = \boldsymbol{\omega} - \mathbf{z}_\omega$, and excluding the vectors $\mathbf{u}$ and ξ, we get

$$\begin{aligned}
&\dot{\boldsymbol{\varepsilon}}_\theta = \boldsymbol{\varepsilon}_\omega - \mathbf{H}_\theta \boldsymbol{\varepsilon}_\theta, \\
&\dot{\boldsymbol{\varepsilon}}_\omega = -\mathbf{H}_\omega \boldsymbol{\varepsilon}_\theta + \mathbf{d}_0, \\
&\dot{\mathbf{z}}_\theta = \mathbf{z}_\omega + \mathbf{H}_\theta \boldsymbol{\varepsilon}_\theta, \\
&\dot{\mathbf{z}}_\omega = -\mathbf{K}_\theta(\mathbf{z}_\theta - \boldsymbol{\theta}_d) - \mathbf{K}_\omega \mathbf{z}_\omega + \mathbf{F}(s)\boldsymbol{\varepsilon}_\theta + \mathbf{H}_\omega \boldsymbol{\varepsilon}_\theta,
\end{aligned} \tag{3.15}$$

Consider the equilibrium position of the system (3.15):

$$\begin{aligned}
&\boldsymbol{\varepsilon}_{\omega 0} - \mathbf{H}_\theta \boldsymbol{\varepsilon}_{\theta 0} = \mathbf{0}, \\
&-\mathbf{H}_\omega \boldsymbol{\varepsilon}_{\theta 0} + \mathbf{d}_0 = \mathbf{0}, \\
&\mathbf{z}_{\omega 0} + \mathbf{H}_\theta \boldsymbol{\varepsilon}_{\theta 0} = \mathbf{0}, \\
&-\mathbf{K}_\theta(\mathbf{z}_{\theta 0} - \boldsymbol{\theta}_d) - \mathbf{K}_\omega \mathbf{z}_{\omega 0} + (\mathbf{F}(0) + \mathbf{H}_\omega)\boldsymbol{\varepsilon}_{\theta 0} = \mathbf{0},
\end{aligned} \tag{3.16}$$

where $\boldsymbol{\varepsilon}_{\omega 0}$, $\boldsymbol{\varepsilon}_{\theta 0}$, $\mathbf{z}_{\omega 0}$ and $\mathbf{z}_{\theta 0}$ – steady values of the corresponding vectors. From the second equation (3.16) it is clear that $\mathbf{d}_0 = \mathbf{H}_\omega \boldsymbol{\varepsilon}_{\theta 0}$, i.e. the steady error vector $\boldsymbol{\varepsilon}_{\theta 0}$ and external disturbance vector $\mathbf{d}_0$ are directly related to each other. Hence we can further consider the vector $\boldsymbol{\varepsilon}_{\theta 0}$ as the external disturbance

From the third equation of (3.16) we obtain that $\mathbf{z}_{\omega 0} = -\mathbf{H}_\theta \boldsymbol{\varepsilon}_{\theta 0}$. Substituting this equality into the last equation of system (3.16) we get

$$-\mathbf{K}_\theta(\mathbf{z}_{\theta 0} - \boldsymbol{\theta}_d) + \mathbf{K}_\omega \mathbf{H}_\theta \boldsymbol{\varepsilon}_{\theta 0} + (\mathbf{F}(0) + \mathbf{H}_\omega)\boldsymbol{\varepsilon}_{\theta 0} = 0,$$

or, substituting $\mathbf{z}_{\theta 0} = \boldsymbol{\theta}_0 - \boldsymbol{\varepsilon}_{\theta 0}$, where $\boldsymbol{\theta}_0$ – steady value of the $\boldsymbol{\theta}$:

$$\mathbf{K}_\theta(\boldsymbol{\theta}_0 - \boldsymbol{\theta}_d) = (\mathbf{K}_\theta + \mathbf{K}_\omega \mathbf{H}_\theta + \mathbf{F}(0) + \mathbf{H}_\omega)\boldsymbol{\varepsilon}_{\theta 0},$$

from which it follows that in order for the equality $\boldsymbol{\theta}_0 = \boldsymbol{\theta}_d$ to hold in the equilibrium position, it is necessary to ensure that the multiplier of $\boldsymbol{\varepsilon}_{\theta 0}$ is equal to zero, i.e.

$$\mathbf{K}_\theta + \mathbf{K}_\omega \mathbf{H}_\theta + \mathbf{F}(0) + \mathbf{H}_\omega = 0,$$

which is equivalent to the condition (3.14). ■

Thus, if the dynamic corrector transfer matrix satisfies condition (3.14), then the closed-loop system (3.13), (3.12) has the property of astatism with respect to external disturbance $\mathbf{d}_0$.

Now let us turn to the problem of the dynamic corrector synthesis in the presence of the polyharmonic disturbance in the form

$$w(t) = \sum_{i=1}^{N_\omega} A_i \sin(\omega_i t),$$
$$\mathbf{d}(t) = \mathbf{a} w(t),$$

where N_ω – number of harmonics, A_i – constant amplitudes, ω_i – frequencies, $\mathbf{a}$ – constant coefficients vector. Consider the multipurpose regulator in the form

$$\begin{aligned} \dot{\mathbf{z}}_\theta &= \mathbf{z}_\omega + \mathbf{H}_\theta \boldsymbol{\varepsilon}_\theta, \\ \dot{\mathbf{z}}_\omega &= \mathbf{u} + \mathbf{H}_\omega \boldsymbol{\varepsilon}_\theta, \\ \boldsymbol{\xi} &= \mathbf{F}(s) \boldsymbol{\varepsilon}_\theta, \\ \mathbf{u} &= -\mathbf{K}_\theta \mathbf{z}_\theta - \mathbf{K}_\omega \mathbf{z}_\omega + \boldsymbol{\xi}. \end{aligned} \tag{3.17}$$

Substituting the expression for the control signal $\mathbf{u}$ into the second equation of the (3.17), we obtain

$$\begin{aligned} \dot{\mathbf{z}}_\theta &= \mathbf{z}_\omega + \mathbf{H}_\theta \boldsymbol{\varepsilon}_\theta, \\ \dot{\mathbf{z}}_\omega &= -\mathbf{K}_\theta \mathbf{z}_\theta - \mathbf{K}_\omega \mathbf{z}_\omega + \boldsymbol{\xi} + \mathbf{H}_\omega \boldsymbol{\varepsilon}_\theta, \end{aligned}$$

or in matrix form:

$$\begin{pmatrix} \dot{\mathbf{z}}_\theta \\ \dot{\mathbf{z}}_\omega \end{pmatrix} = \begin{pmatrix} \mathbf{0} & \mathbf{E} \\ -\mathbf{K}_\theta & -\mathbf{K}_\omega \end{pmatrix} \begin{pmatrix} \mathbf{z}_\theta \\ \mathbf{z}_\omega \end{pmatrix} + \begin{pmatrix} \mathbf{H}_\theta & \mathbf{0} \\ \mathbf{H}_\omega & \mathbf{E} \end{pmatrix} \begin{pmatrix} \boldsymbol{\varepsilon}_\theta \\ \boldsymbol{\xi} \end{pmatrix}. \tag{3.18}$$

Introducing notations

$$\mathbf{A}_s = \begin{pmatrix} \mathbf{0} & \mathbf{E} \\ -\mathbf{K}_\theta & -\mathbf{K}_\omega \end{pmatrix}, \ \mathbf{B}_s = \begin{pmatrix} \mathbf{H}_\theta & \mathbf{0} \\ \mathbf{H}_\omega & \mathbf{E} \end{pmatrix},$$

let us represent (3.18) in the tf-form:

$$\begin{pmatrix} \mathbf{z}_\theta \\ \mathbf{z}_\omega \end{pmatrix} = \mathbf{P}(s) \begin{pmatrix} \boldsymbol{\varepsilon}_\theta \\ \boldsymbol{\xi} \end{pmatrix}, \tag{3.19}$$

where

$$\mathbf{P}(s) = (\mathbf{E}s - \mathbf{A}_s)^{-1} \mathbf{B}_s = \begin{pmatrix} \mathbf{P}_{11}(s) & \mathbf{P}_{12}(s) \\ \mathbf{P}_{21}(s) & \mathbf{P}_{22}(s) \end{pmatrix}.$$

Theorem 3.2. *Filtration of the polyharmonic disturbance with frequencies* ω_i, $i = \overline{1, N_\omega}$ *in the control channel is ensured with*

$$\mathbf{F}(j\omega_i) = -\mathbf{T}^{-1}(j\omega_i)[\mathbf{K}_\theta \mathbf{P}_{11}(j\omega_i) + \mathbf{K}_\omega \mathbf{P}_{21}(j\omega_i)], \tag{3.20}$$

where $\mathbf{T}(j\omega_i) = \mathbf{K}_\theta \mathbf{P}_{12}(j\omega_i) + \mathbf{K}_\omega \mathbf{P}_{22}(j\omega_i) - \mathbf{E}$.

Proof. From (3.19) it follows that

$$\begin{aligned} \mathbf{z}_\theta &= \mathbf{P}_{11}\boldsymbol{\varepsilon}_\theta + \mathbf{P}_{12}\boldsymbol{\xi}, \\ \mathbf{z}_\omega &= \mathbf{P}_{21}\boldsymbol{\varepsilon}_\theta + \mathbf{P}_{22}\boldsymbol{\xi}. \end{aligned} \tag{3.21}$$

Substituting (3.21) into the expression for the control signal in (3.17), we obtain

$$\begin{aligned} &\mathbf{u} = -\mathbf{K}_\theta(\mathbf{P}_{11}\boldsymbol{\varepsilon}_\theta + \mathbf{P}_{12}\boldsymbol{\xi}) - \mathbf{K}_\omega(\mathbf{P}_{21}\boldsymbol{\varepsilon}_\theta + \mathbf{P}_{22}\boldsymbol{\xi}) + \boldsymbol{\xi} = \\ &= -(\mathbf{K}_\theta \mathbf{P}_{11} + \mathbf{K}_\omega \mathbf{P}_{21})\boldsymbol{\varepsilon}_\theta - (\mathbf{K}_\theta \mathbf{P}_{12} + \mathbf{K}_\omega \mathbf{P}_{22} - \mathbf{E})\boldsymbol{\xi}. \end{aligned}$$

Let us introduce the notation $\mathbf{T}(s) = \mathbf{K}_\theta \mathbf{P}_{12}(s) + \mathbf{K}_\omega \mathbf{P}_{22}(s) - \mathbf{E}$, then

$$\begin{aligned} &\mathbf{u} = -(\mathbf{K}_\theta \mathbf{P}_{11} + \mathbf{K}_\omega \mathbf{P}_{21})\boldsymbol{\varepsilon}_\theta - \mathbf{T}\boldsymbol{\xi} = \\ &= -(\mathbf{K}_\theta \mathbf{P}_{11} + \mathbf{K}_\omega \mathbf{P}_{21})\boldsymbol{\varepsilon}_\theta - \mathbf{TF}\boldsymbol{\varepsilon}_\theta = \\ &= -(\mathbf{K}_\theta \mathbf{P}_{11} + \mathbf{K}_\omega \mathbf{P}_{21} + \mathbf{TF})\boldsymbol{\varepsilon}_\theta. \end{aligned} \tag{3.22}$$

The expression $\mathbf{G}(s) = -[\mathbf{K}_\theta \mathbf{P}_{11}(s) + \mathbf{K}_\omega \mathbf{P}_{21}(s) + \mathbf{T}(s)\mathbf{F}(s)]$ from the (3.22) is the transfer matrix from the input $\boldsymbol{\varepsilon}_\theta$ to the output $\mathbf{u}$. To ensure minimization of the response of the control signal to a polyharmonic disturbance with frequencies ω_i, $i = \overline{1, N_\omega}$, it is necessary to provide the condition $\mathbf{G}(j\omega_i) = 0$ by the choice of the transfer matrix $\mathbf{F}(s)$ of the dynamic corrector, from where we obtain the conditions (3.20). ■

Finally, let us discuss the issue of synthesizing the dynamic corrector transfer matrix $\mathbf{F}(s) = \begin{pmatrix} \mathbf{F}_1(s) & \mathbf{F}_2(s) & \dots & \mathbf{F}_n(s) \end{pmatrix}^{\mathrm{T}}$, which satisfies the conditions (3.14) and (3.20), i.e. ensuring the closed-loop system astatism and polyharmonic external disturbance filtration. Let us introduce the notations

$$\begin{aligned} &\mathbf{F}(0) = \mathbf{F}^0 = \begin{pmatrix} \mathbf{F}_1^0 & \mathbf{F}_2^0 & \dots & \mathbf{F}_n^0 \end{pmatrix}^{\mathrm{T}}, \\ &\mathbf{F}(j\omega_i) = \mathbf{F}_i^* = \begin{pmatrix} \mathbf{F}_{i1}^* & \mathbf{F}_{i2}^* & \dots & \mathbf{F}_{in}^* \end{pmatrix}^{\mathrm{T}}, \\ &i = \overline{1, N_\omega}, \end{aligned}$$

where $\mathbf{F}^0$ and $\mathbf{F}_i^*$ – constant matrices. Each individual component of the dynamic corrector corresponding to a generalized coordinate with an index $k=\overline{1,n}$, can be described by the equation

$$\xi_k = \mathbf{F}_k(s)\boldsymbol{\varepsilon}_\theta,$$

which can be represented in state space as

$$\begin{aligned} \dot{\mathbf{p}}_k &= \boldsymbol{\alpha}_k \mathbf{p}_k + \boldsymbol{\beta}_k \boldsymbol{\varepsilon}_\theta, \\ \xi_k &= \boldsymbol{\gamma}_k \mathbf{p}_k + \boldsymbol{\mu}_k \boldsymbol{\varepsilon}_\theta. \end{aligned} \tag{3.23}$$

Here $\mathbf{p}_k \in E^{2N_\omega}$ – state vector of the corresponding component of the dynamic corrector. Note that, taking into account (3.23), the transfer matrix $\mathbf{F}_k(s)$ can be represented as $\mathbf{F}_k(s) = \boldsymbol{\gamma}_k(\mathbf{E}_{2N_\omega} s - \boldsymbol{\alpha}_k)^{-1}\boldsymbol{\beta}_k + \boldsymbol{\mu}_k$.

Thus, conditions (3.14) and (3.20) can be rewritten as

$$\begin{aligned} &-\boldsymbol{\gamma}_k \boldsymbol{\alpha}_k^{-1}\boldsymbol{\beta}_k + \boldsymbol{\mu}_k = \mathbf{F}_k^0, \\ &\boldsymbol{\gamma}_k(\mathbf{E}_{2N_\omega} j\omega_i - \boldsymbol{\alpha}_k)^{-1}\boldsymbol{\beta}_k + \boldsymbol{\mu}_k = \mathbf{R}_{ik} + \mathbf{I}_{ik} j, \\ &i=\overline{1,N_\omega}, k=\overline{1,n}, \end{aligned} \tag{3.24}$$

where

$$\begin{aligned} \mathbf{R}_{ik} &= \operatorname{Re}\mathbf{F}_{ik}^*, \\ \mathbf{I}_{ik} &= \operatorname{Im}\mathbf{F}_{ik}^*. \end{aligned}$$

Let us define in an arbitrary way non-zero vectors $\boldsymbol{\gamma}_k$ with dimensions $1\times 2n$ and Hurwitz matrices $\boldsymbol{\alpha}_k$ with dimensions $2n\times 2n$. Note that in this case the matrices $\mathbf{E}_{2N_\omega} j\omega_i - \boldsymbol{\alpha}_k$ from (3.24) are non-singular. Let us subtract the first equation (3.24) from the second one and pick out the real and imaginary parts, then

$$\begin{aligned} &\boldsymbol{\gamma}_k(\boldsymbol{\alpha}_{ik}^R + \boldsymbol{\alpha}_k^{-1})\boldsymbol{\beta}_k = \mathbf{R}_{ik} - \mathbf{F}_k^0, \\ &\boldsymbol{\gamma}_k \boldsymbol{\alpha}_{ik}^I \boldsymbol{\beta}_k = \mathbf{I}_{ik}, \\ &i=\overline{1,N_\omega}, k=\overline{1,n}, \end{aligned} \tag{3.25}$$

where

$$\boldsymbol{\alpha}_{ik}^{R} = \mathrm{Re}(\mathbf{E}_{2N_\omega} j\omega_i - \boldsymbol{\alpha}_k)^{-1},$$
$$\boldsymbol{\alpha}_{ik}^{I} = \mathrm{Im}(\mathbf{E}_{2N_\omega} j\omega_i - \boldsymbol{\alpha}_k)^{-1}.$$

Let us introduce the notations

$$\mathbf{A}_k = \begin{pmatrix} \boldsymbol{\gamma}_k(\boldsymbol{\alpha}_{1k}^{R} + \boldsymbol{\alpha}_k^{-1}) \\ \boldsymbol{\gamma}_k \boldsymbol{\alpha}_{1k}^{I} \\ \cdots \\ \boldsymbol{\gamma}_k(\boldsymbol{\alpha}_{N_\omega k}^{R} + \boldsymbol{\alpha}_k^{-1}) \\ \boldsymbol{\gamma}_k \boldsymbol{\alpha}_{N_\omega k}^{I} \end{pmatrix}, \ \mathbf{B}_k = \begin{pmatrix} \mathbf{R}_{1k} - \mathbf{F}_k^0 \\ \mathbf{I}_{1k} \\ \cdots \\ \mathbf{R}_{N_\omega k} - \mathbf{F}_k^0 \\ \mathbf{I}_{N_\omega k} \end{pmatrix}, \ k = \overline{1,n}, \tag{3.26}$$

then (3.25) can be represented as linear system

$$\mathbf{A}_k \boldsymbol{\beta}_k = \mathbf{B}_k \tag{3.27}$$

with $2N_\omega \times n$ equations and $2N_\omega \times n$ variables for each fixed k. According to the fact that matrices $\mathbf{A}_k$ are non-singular, system (3.27) has a unique solution – the matrix $\boldsymbol{\beta}_k$. In turn, knowing $\boldsymbol{\beta}_k$, it is possible to calculate the matrix $\boldsymbol{\mu}_k$ by using the formula

$$\boldsymbol{\mu}_k = \mathbf{F}_k^0 + \boldsymbol{\gamma}_k \boldsymbol{\alpha}_k^{-1} \boldsymbol{\beta}_k, \ k = \overline{1,n}. \tag{3.28}$$

obtained from the first equation of the system (3.24).

Thus, the dynamic corrector, represented by the resulting matrices $\boldsymbol{\alpha}_k$, $\boldsymbol{\beta}_k$, $\boldsymbol{\gamma}_k$, $\boldsymbol{\mu}_k$, $k = \overline{1,n}$, provides astatism of the closed-loop system at the output $\boldsymbol{\theta}$ and filtration of the polyharmonic disturbance with frequencies ω_i, $i = \overline{1,N_\omega}$ in the control channel.

The above considerations allow us to formulate the following algorithm for the multipurpose regulator synthesis.

Algorithm № 1 (multipurpose regulator synthesis)

1) Set the values of the matrices $\mathbf{K}_\theta$ and $\mathbf{K}_\omega$ of the basic control law (3.8), ensuring the Hurwitz property of the matrix $\mathbf{K}_b$ and the required quality of the closed-loop system dynamics.

2) Fix the matrices $\mathbf{H}_\theta$ and $\mathbf{H}_\omega$ of the asymptotic observers that ensure the Hurwitz property of the matrix $\mathbf{H}_o$ and the desired degree of convergence of the errors between the estimates and the actual plant state.

3) Using the formulas from condition (3.14), calculate the corresponding value $\mathbf{F}(0) = \mathbf{F}^0$ of the corrector transfer matrix which ensures astatism of the closed-loop system with respect to the constant external disturbances.

4) Calculate the values $\mathbf{F}(j\omega_i)$ of the dynamic corrector transfer matrix corresponding to the given frequencies ω_i, $i = \overline{1, N_\omega}$ of the external polyharmonic disturbance.

5) Fix the Hurwitz matrices $\boldsymbol{\alpha}_k$ and vectors $\boldsymbol{\gamma}_k$, $k = \overline{1, n}$ of the corresponding the dynamic corrector components. In particular, matrices $\boldsymbol{\alpha}_k$ can be represented in Frobenius form by specifying eigenvalue λ with a negative real part and with multiplicity $2N_\omega$, and the row vector $\boldsymbol{\gamma}_k$ can be taken in the form $\boldsymbol{\gamma}_k = (0 \quad \ldots \quad 0 \quad 1)$.

6) Calculate the matrices $\mathbf{A}_k$ and $\mathbf{B}_k$, using formulas (3.26). Find the vectors $\boldsymbol{\beta}_k$ by solving the linear system (3.27). Using formula (3.28), calculate the vectors $\boldsymbol{\mu}_k$.

3.4. Constant Delay Compensation

Now let us return to the system with constant delay (3.1). The use of linearizing feedback (3.6) with a multipurpose regulator (3.12) in the presence of delay does not allow to ensure the desired quality of the controlled motion dynamics, and in certain cases can lead to complete loss of stability. First of all, the delay of the control signal $\boldsymbol{\tau}$ leads to the fact that the terms and multipliers compensating the nonlinearities cease to coincide with the actual values at the moment of action of the delayed control. Due to this, feedback linearization no longer works. In addition, even if linearization is successful, the term $\mathbf{u}$, which is

the control for the linear system, will also be delayed, which will lead to a deterioration in the control quality.

In this regard, to overcome these shortcomings, we will consider the compensation approach [73]. Its essence is to use the plant state prediction based on the amount of delay in the feedback:

$$\begin{aligned} \boldsymbol{\theta}_p(t) &= \boldsymbol{\theta}(t+h), \\ \boldsymbol{\omega}_p(t) &= \boldsymbol{\omega}(t+h). \end{aligned} \tag{3.29}$$

Let us reduce (3.1) to the system of first-order ODEs:

$$\begin{aligned} \dot{\boldsymbol{\theta}} &= \boldsymbol{\omega}, \\ \dot{\boldsymbol{\omega}} &= \mathbf{M}^{-1}(\boldsymbol{\theta})(\boldsymbol{\tau}(t-h) + \boldsymbol{\tau}_e(t-h) - \mathbf{C}(\boldsymbol{\theta},\boldsymbol{\omega}) - \mathbf{g}(\boldsymbol{\theta})), \end{aligned} \tag{3.30}$$

then, knowing the current values of the state variables $\boldsymbol{\theta}(t)$ and $\boldsymbol{\omega}(t)$, prediction (3.29) can be obtained by integrating right-hand sides of the system (3.30):

$$\begin{aligned} \boldsymbol{\theta}_p(t) &= \int_0^{t+h} \boldsymbol{\omega}(\delta)d\delta, \\ \boldsymbol{\omega}_p(t) &= \int_0^{t+h} \mathbf{M}^{-1}(\boldsymbol{\theta}(\delta))(\boldsymbol{\tau}(\delta-h) + \boldsymbol{\tau}_e(\delta-h) - \mathbf{C}(\boldsymbol{\theta}(\delta),\boldsymbol{\omega}(\delta)) - \mathbf{g}(\boldsymbol{\theta}(\delta)))d\delta. \end{aligned} \tag{3.31}$$

Transforming the integrals on the right-hand sides of (3.31), we obtain

$$\begin{aligned} \boldsymbol{\theta}_p(t) &= \int_0^{t} \boldsymbol{\omega}(\delta)d\delta + \int_t^{t+h} \boldsymbol{\omega}(\delta)d\delta, \\ \boldsymbol{\omega}_p(t) &= \int_0^{t} [...]d\delta + \int_t^{t+h} [...]d\delta. \end{aligned} \tag{3.32}$$

The first terms on the right-hand sides of (3.32) represent the current values $\boldsymbol{\theta}(t)$ and $\boldsymbol{\omega}(t)$, therefore

$$\begin{aligned} \boldsymbol{\theta}_p(t) &= \boldsymbol{\theta}(t) + \int_t^{t+h} \boldsymbol{\omega}(\delta)d\delta, \\ \boldsymbol{\omega}_p(t) &= \boldsymbol{\omega}(t) + \int_t^{t+h} \mathbf{M}^{-1}(\boldsymbol{\theta}(\delta))(\boldsymbol{\tau}(\delta-h) + \boldsymbol{\tau}_e(\delta-h) - \mathbf{C}(\boldsymbol{\theta}(\delta),\boldsymbol{\omega}(\delta)) - \mathbf{g}(\boldsymbol{\theta}(\delta)))d\delta. \end{aligned}$$

Next we denote $\sigma = \delta - h$, then

$$\begin{aligned}
&\boldsymbol{\theta}_p(t) = \boldsymbol{\theta}(t) + \int_{t-h}^{t} \boldsymbol{\omega}_p(\sigma) d\sigma, \\
&\boldsymbol{\omega}_p(t) = \boldsymbol{\omega}(t) + \int_{t-h}^{t} \Big[\mathbf{M}^{-1}(\boldsymbol{\theta}_p(\sigma))(\boldsymbol{\tau}(\sigma) + \boldsymbol{\tau}_e(\sigma) - \\
&- \mathbf{C}(\boldsymbol{\theta}_p(\sigma), \boldsymbol{\omega}_p(\sigma)) - \mathbf{g}(\boldsymbol{\theta}_p(\sigma))) \Big] d\sigma
\end{aligned} \tag{3.33}$$

Note that direct numerical solution of the integrals in the right-hand sides of (3.33) can cause certain difficulties, as indicated, for example, in [73]. In connection with this fact, we introduce the auxiliary dynamic system

$$\begin{aligned}
&\dot{\mathbf{q}} = \mathbf{w}, \\
&\dot{\mathbf{w}} = \mathbf{M}^{-1}(\mathbf{q})(\boldsymbol{\tau} + \boldsymbol{\tau}_e - \mathbf{C}(\mathbf{q}, \mathbf{w}) - \mathbf{g}(\mathbf{q})),
\end{aligned} \tag{3.34}$$

and besides in the time interval $t \in [-h, 0]$ the following conditions are met:

$$\begin{aligned}
&\mathbf{q}(t) = \boldsymbol{\theta}_0, \\
&\mathbf{w}(t) = \boldsymbol{\omega}_0, \\
&\boldsymbol{\tau}(t) = 0, \\
&\boldsymbol{\tau}_e(t) = 0.
\end{aligned}$$

Taking (3.34) into account, we can rewrite system (3.31) in the form

$$\begin{aligned}
&\boldsymbol{\theta}_p = \boldsymbol{\theta}(t) + \mathbf{q}(t) - \mathbf{q}(t-h), \\
&\boldsymbol{\omega}_p = \boldsymbol{\omega}(t) + \mathbf{w}(t) - \mathbf{w}(t-h).
\end{aligned} \tag{3.35}$$

Let us transform the linearizing feedback (3.6) and the multipurpose regulator (3.12), using the prediction according to the formulas (3.35):

$$\begin{aligned}
&\dot{\mathbf{q}} = \mathbf{w}, \\
&\dot{\mathbf{w}} = \mathbf{M}^{-1}(\mathbf{q})(\boldsymbol{\tau} + \boldsymbol{\tau}_e - \mathbf{C}(\mathbf{q}, \mathbf{w}) - \mathbf{g}(\mathbf{q})), \\
&\boldsymbol{\theta}_p = \boldsymbol{\theta} + \mathbf{q} - \mathbf{q}(t-h), \\
&\boldsymbol{\omega}_p = \boldsymbol{\omega} + \mathbf{w} - \mathbf{w}(t-h), \\
&\boldsymbol{\varepsilon}_{\theta p} = \boldsymbol{\theta}_p - \mathbf{z}_\theta, \\
&\dot{\mathbf{z}}_\theta = \mathbf{z}_\omega + \mathbf{H}_\theta \boldsymbol{\varepsilon}_{\theta p}, \\
&\dot{\mathbf{z}}_\omega = \mathbf{u} + \mathbf{H}_\omega \boldsymbol{\varepsilon}_{\theta p}, \\
&\mathbf{u} = -\mathbf{K}_\theta(\mathbf{z}_\theta - \boldsymbol{\theta}_d) - \mathbf{K}_\omega \mathbf{z}_\omega + \mathbf{F}(s)\boldsymbol{\varepsilon}_{\theta p}, \\
&\boldsymbol{\tau} = \mathbf{C}(\boldsymbol{\theta}_p, \boldsymbol{\omega}_p) + \mathbf{g}(\boldsymbol{\theta}_p) + \mathbf{M}(\boldsymbol{\theta}_p)\mathbf{u}.
\end{aligned} \tag{3.36}$$

System (3.36) is a regulator that compensates the constant delay in the feedback channel and external disturbance channel. Note that (3.36) is a transformation of the multipurpose regulator (3.12), preserving its transfer matrix. Thus, to synthesize a regulator (3.36), it is enough to synthesize a controller without delay (3.12), which satisfies all the requirements for dynamics in various operating modes, and then add the calculation of the prediction in accordance with (3.36). The disadvantage of this approach is the need to directly measure the external disturbance without the delay.

Taking into account the above considerations, we formulate the following algorithm.

Algorithm № 2 (multipurpose compensating regulator synthesis)

1) In accordance with algorithm № 1, synthesize the basic regulator (3.12) for a closed-loop system without delay.

2) To calculate the system state prediction by the value of the constant delay, add equations (3.34) and (3.35) to the synthesized regulator.

3) Replace all the occurrences of the current state measurements $\boldsymbol{\theta}$ and $\boldsymbol{\omega}$, accordingly, in the equation of the control signal $\boldsymbol{\tau}$ and in the equation of its linear part $\mathbf{u}$ with the predicted values $\boldsymbol{\theta}_p$ and $\boldsymbol{\omega}_p$.

3.5. Experimental Results

To test the performance of the described algorithms, a computer model was implemented in the Octave environment. A two-link manipulator was chosen as a plant (Fig. 3.1).

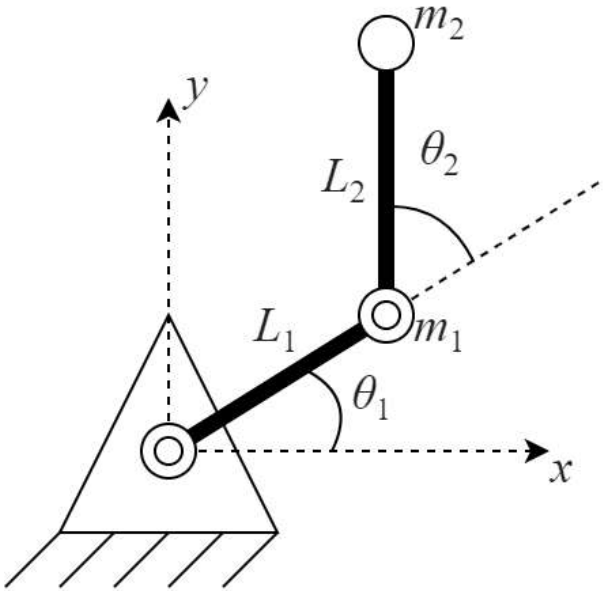

Fig. 3.1. Two-link manipulator.

The matrices of system (3.1) in this case has the values [77]

$$\mathbf{M}(\boldsymbol{\theta}) = \begin{bmatrix} m_1 L_1^2 + m_2 (L_1^2 + 2L_1 L_2 \cos\theta_2 + L_2^2) & m_2 (L_1 L_2 \cos\theta_2 + L_2^2) \\ m_2 (L_1 L_2 \cos\theta_2 + L_2^2) & m_2 L_2^2 \end{bmatrix},$$

$$\mathbf{C}(\boldsymbol{\theta}, \dot{\boldsymbol{\theta}}) = \begin{bmatrix} -m_2 L_1 L_2 \cos\theta_2 (2\dot{\theta}_1 \dot{\theta}_2 + \dot{\theta}_2^2) \\ m_2 L_1 L_2 \dot{\theta}_1^2 \sin\theta_2 \end{bmatrix},$$

$$\mathbf{g}(\boldsymbol{\theta}) = \begin{bmatrix} (m_1 + m_2) L_1 g \cos\theta_1 + m_2 g L_2 \cos(\theta_1 + \theta_2) \\ m_2 g L_2 \cos(\theta_1 + \theta_2) \end{bmatrix},$$

where m_1 and m_2 – point masses at the link ends, L_1 and L_2 – link lengths, g – gravitational acceleration, $\boldsymbol{\theta} = (\theta_1 \quad \theta_2)^{\mathrm{T}}$ – joint angles. Let us take $m_1 = m_2 = 1\text{kg}$, $L_1 = L_2 = 1\text{m}$, $g = 9.8\,\text{m/s}^2$.

For adjustable elements of the multipurpose regulator (3.12), we take the values

$$\mathbf{K}_\theta = \begin{pmatrix} 8 & 0 \\ 0 & 8 \end{pmatrix}, \mathbf{K}_\omega = \begin{pmatrix} 8 & 0 \\ 0 & 8 \end{pmatrix},$$

$$\mathbf{H}_\theta = \begin{pmatrix} 16 & 0 \\ 0 & 16 \end{pmatrix}, \mathbf{H}_\omega = \begin{pmatrix} 32 & 0 \\ 0 & 32 \end{pmatrix}.$$

The matrices $\boldsymbol{\alpha}_k$ of the dynamic corrector were taken as Frobenius matrices with eigenvalue $\lambda = -3$ of multiplicity 6. The values $\boldsymbol{\gamma}_k$ were chosen as vectors

$\boldsymbol{\gamma}_k = \begin{pmatrix} 0 & 0 & 0 & 0 & 0 & 1 \end{pmatrix}$. A constant disturbance in the corresponding mode was set in the form

$$\boldsymbol{\tau}_e(t) = \begin{pmatrix} 0.1 & 0.1 \end{pmatrix}^{\mathrm{T}} \tag{3.37}$$

Finally, in the periodic disturbance mode, the vector $\boldsymbol{\tau}_e$ was represented as

$$\begin{aligned} &\boldsymbol{\tau}_e(t) = \begin{pmatrix} w(t) & w(t) \end{pmatrix}^{\mathrm{T}}, \\ &w(t) = \sin(\omega_1 t) + \sin(\omega_2 t) + \sin(\omega_3 t), \end{aligned} \tag{3.38}$$

with $\omega_1 = 31.416\ \mathrm{s}^{-1}$, $\omega_2 = 37.699\ \mathrm{s}^{-1}$ and $\omega_3 = 43.982\ \mathrm{s}^{-1}$.

3.5.1. System without the delay

First, let us consider the mode without external disturbance and delay with the dynamic corrector turned off. Let us take $\boldsymbol{\theta}_0 = (0 \quad 0)^{\mathrm{T}}$, $\boldsymbol{\omega}_0 = (0 \quad 0)^{\mathrm{T}}$ as the initial position. Assume that the desired position is $\boldsymbol{\theta}_d = (45 \quad 60)^{\mathrm{T}}$ degrees. The dynamics of the system in this mode is shown in Fig. 3.2. Note that the desired position has been achieved.

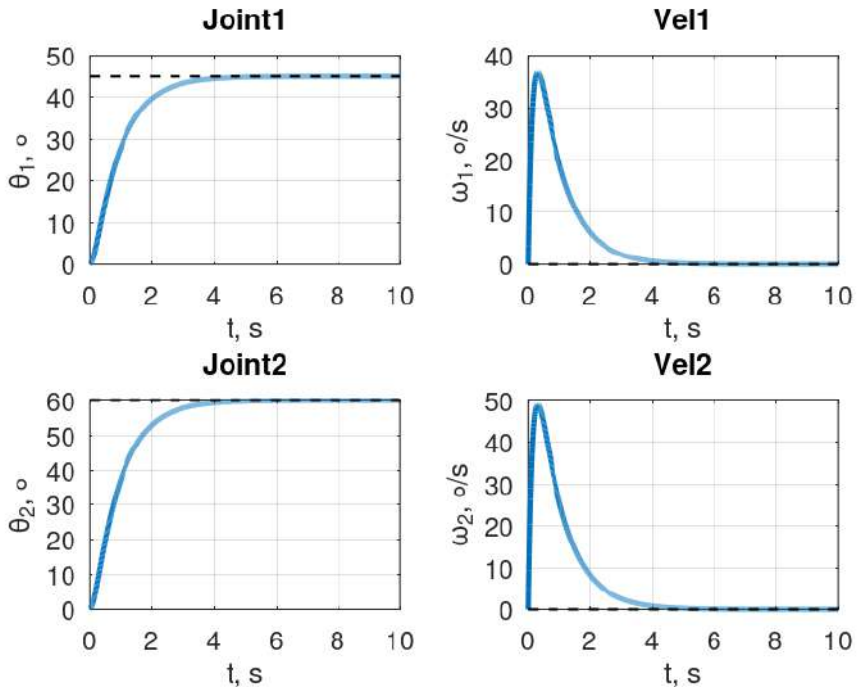

Fig. 3.2. Dynamics of the system without external disturbance and delay.

Now let us consider the influence of the external disturbance. Let us set the initial position corresponding to the desired one, i.e. $\boldsymbol{\theta}_0 = \boldsymbol{\theta}_d = (45 \quad 60)^{\mathrm{T}}$ degrees. Apply a constant disturbance (3.37) to the plant with the dynamic corrector turned off. As can be seen from Fig. 3.3, in this case the manipulator deviates from the desired position and cannot return to it. Thus, without a dynamic corrector, astatism is not ensured.

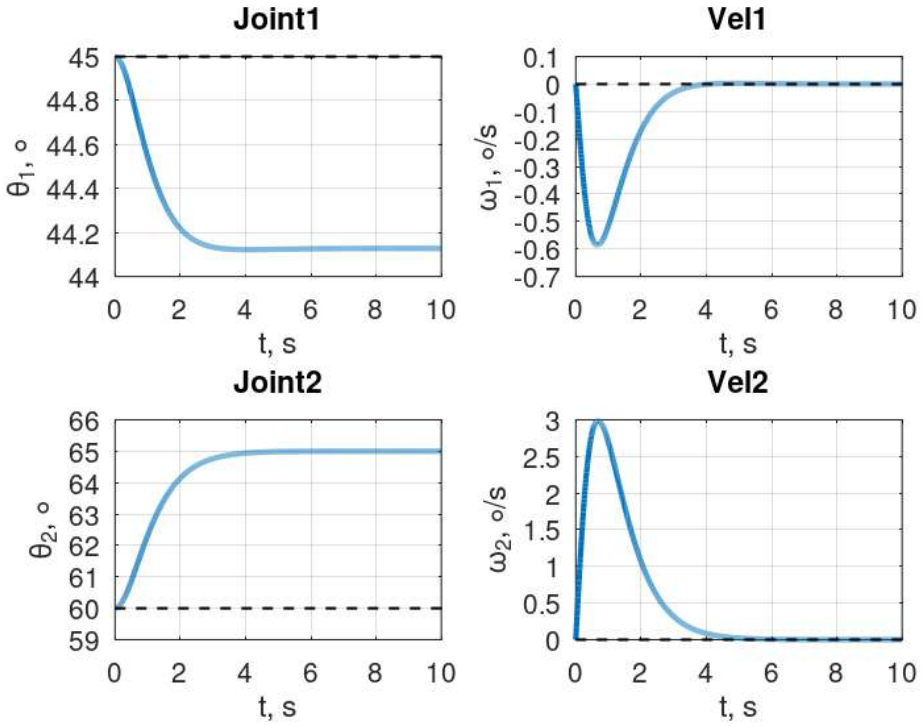

Fig. 3.3. Dynamics of a system without delay under the influence of a constant external disturbance.

Now, under the same conditions, let us turn on the dynamic corrector. The dynamics of the system presented in Fig. 3.4 demonstrates that the corrector actually provides astatism – after the initial deviation, the robot returns back to the desired position.

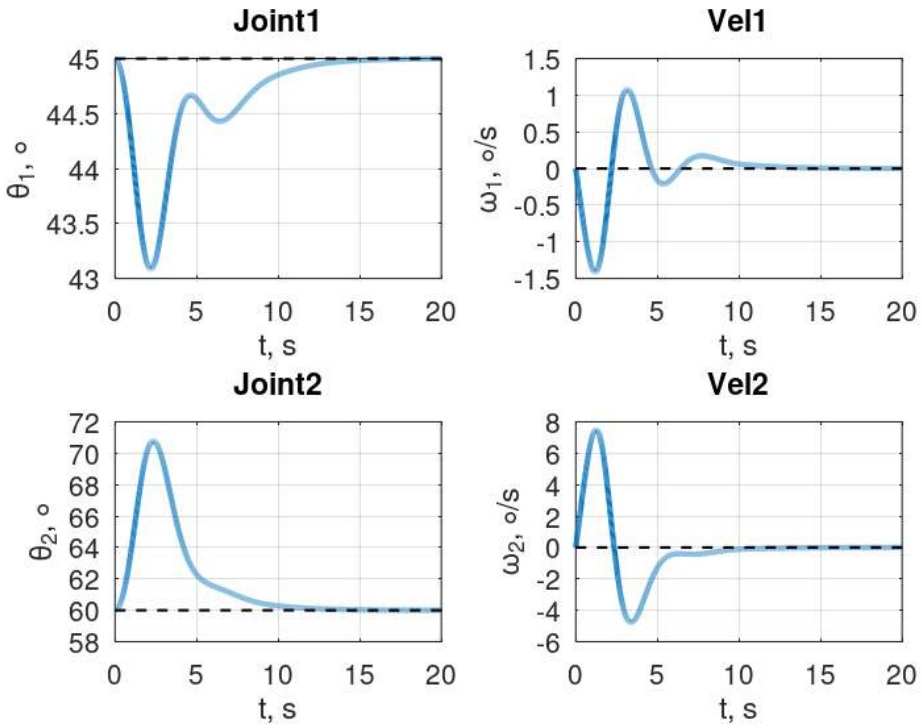

Fig. 3.4. Dynamics of a system without delay with constant external disturbance and enabled dynamic corrector.

Finally, let us consider the influence of polyharmonic disturbance (3.38). In this mode, for clarity, the dynamic corrector will be turned on only after 10s of system movement. From Fig. 3.5 it can be seen that the periodic disturbance also displaces the robot from the given position, but turning on the corrector brings it back, while the intensity of the $\boldsymbol{\theta}$ output oscillations does not change. However, from paying attention to the dynamics of the control signal $\boldsymbol{\tau}$ (Fig. 3.6), a decrease in the intensity of control action can be noted after turning on the corrector. Let us also note that the lack of complete compensation for periodic disturbances is explained by the fact that in reality in this case the influence of external disturbances on the linear part $\mathbf{u}$ of the control signal $\boldsymbol{\tau}$ is minimized.

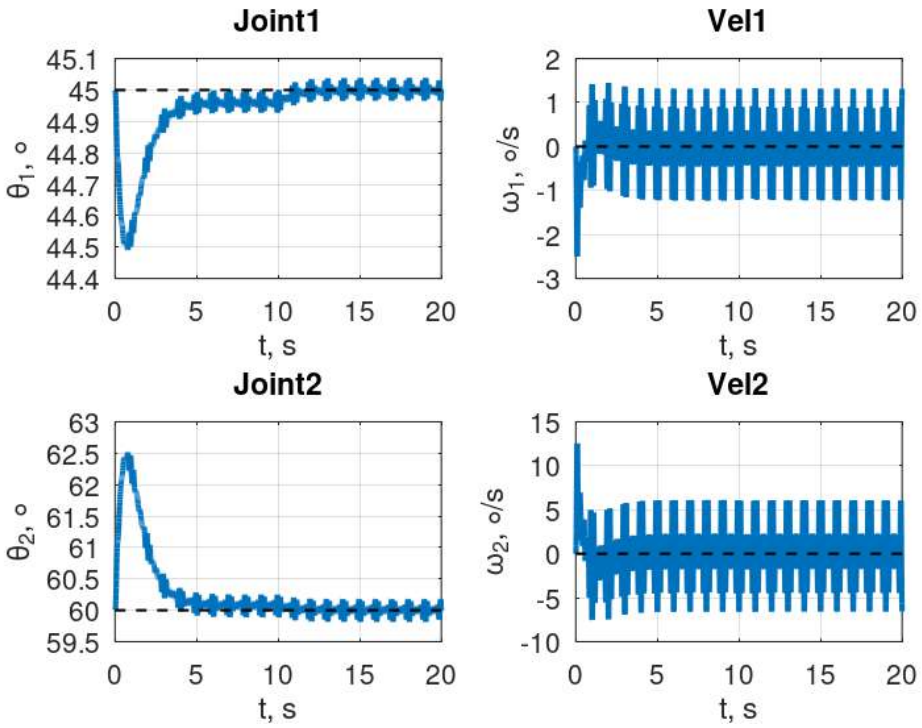

Fig. 3.5. Dynamics of a system without delay with a polyharmonic external disturbance and with a dynamic corrector enabled at the moment t = 10 s.

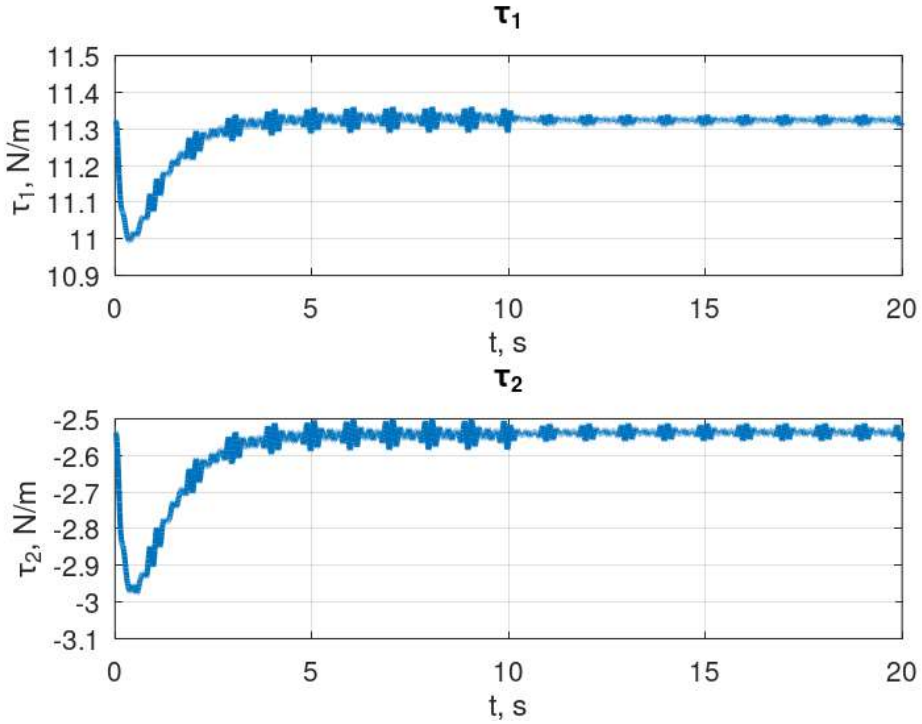

Fig. 3.6. Dynamics of the control signal $\boldsymbol{\tau}$ without delay with a polyharmonic external disturbance.

Fig. 3.7 shows the dynamics of the linear part $\mathbf{u}$ of the control signal $\boldsymbol{\tau}$ directly. It can be seen here that the influence of external disturbance is completely compensated by turning on the dynamic corrector, as expected.

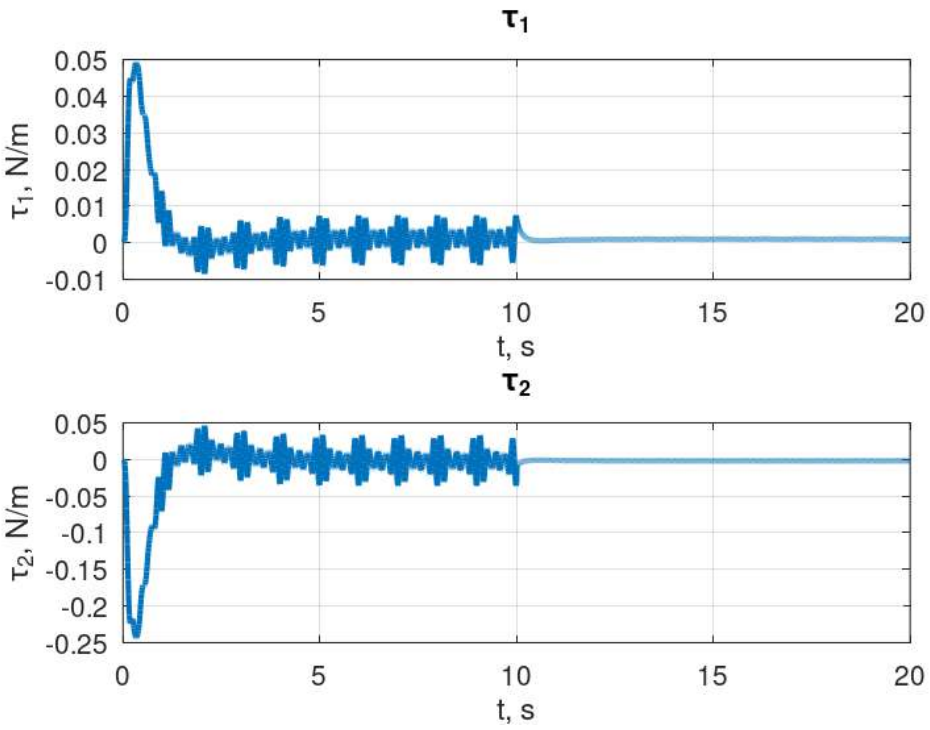

Fig. 3.7. Dynamics of the linear part $\mathbf{u}$ of the control signal $\boldsymbol{\tau}$ without delay with polyharmonic external disturbance

The influence of a periodic disturbance on the control signal $\boldsymbol{\tau}$ can be reduced by usage of outputs of asymptotic observers $\mathbf{z}_\theta$ and $\mathbf{z}_\omega$ instead of actual measurements $\boldsymbol{\theta}$ and $\boldsymbol{\omega}$ in the calculation of the values of matrices $\mathbf{M}$, $\mathbf{C}$ and $\mathbf{g}$ which compensate nonlinearities. An example of dynamics with this approach is shown in Fig. 3.8 and 3.9. It can be seen that the amplitude of oscillations of the joint angles $\boldsymbol{\theta}$ becomes slightly smaller, while a more significant decrease in the intensity of the control signal $\boldsymbol{\tau}$ is noticeable after turning on the corrector. The influence of the disturbance on the linear part $\mathbf{u}$ in this case is also completely compensated, as shown in Fig. 3.10.

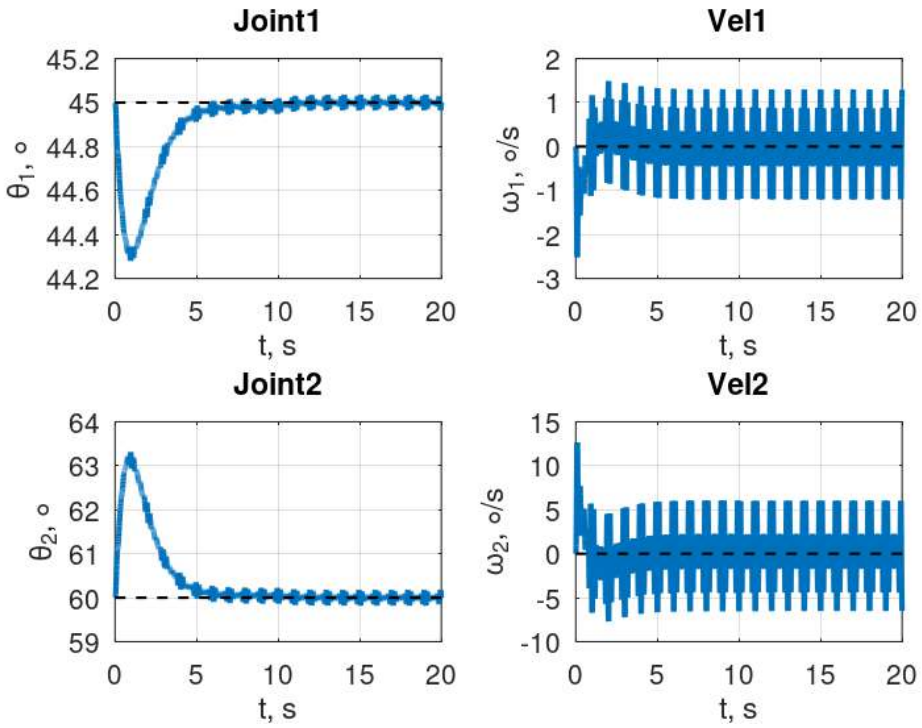

Fig. 3.8. System dynamics when using observer outputs to calculate matrices in the control signal.

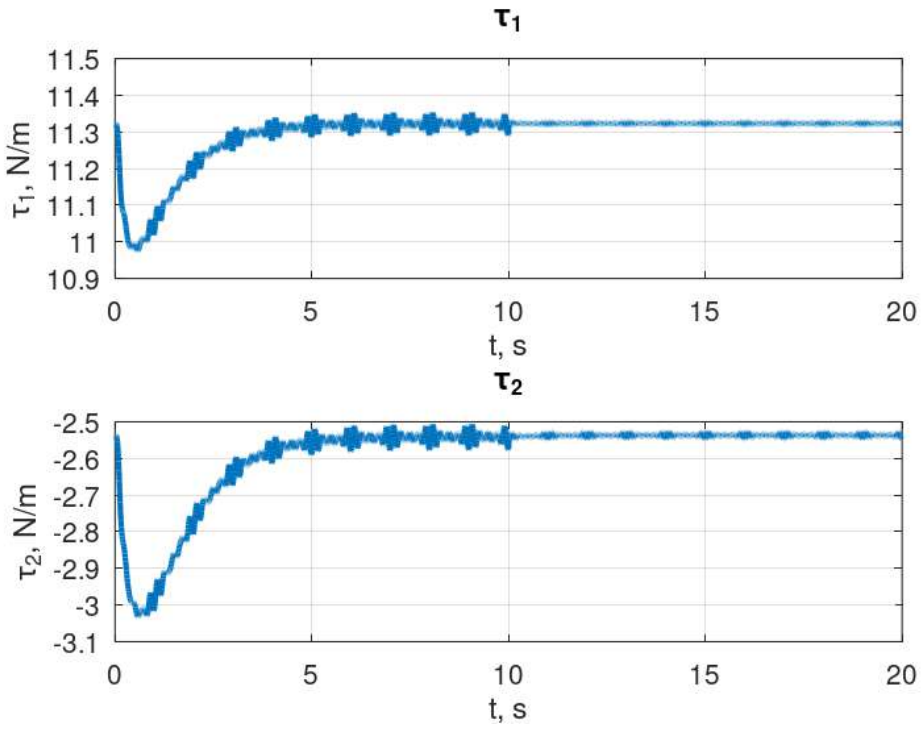

Fig. 3.9. Dynamics of the control signal τ when using observer outputs to calculate matrices in the control signal.

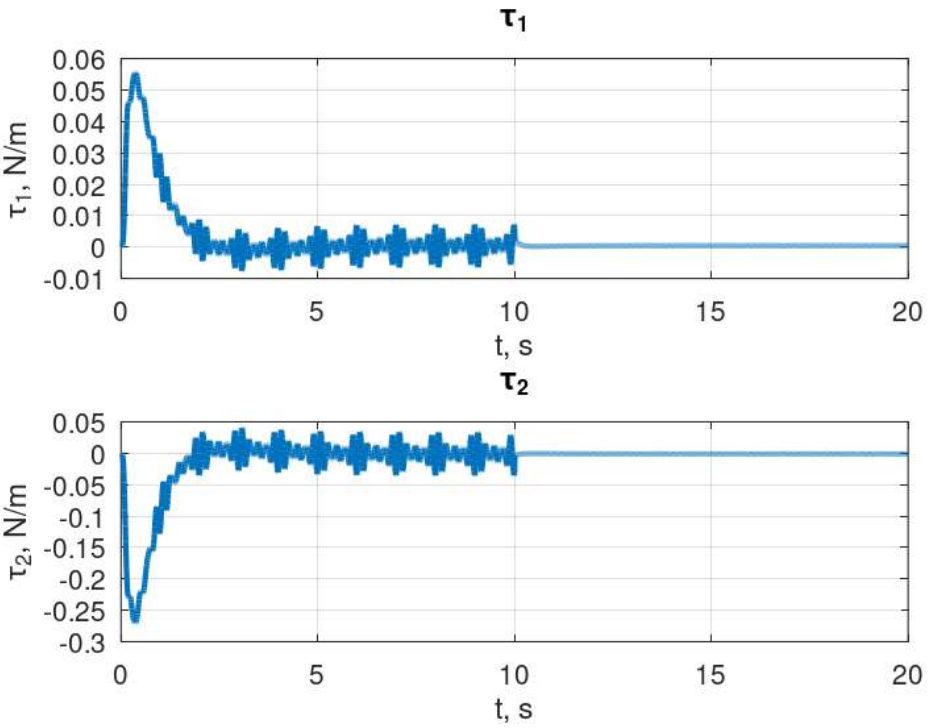

Fig. 3.10. Dynamics of the linear part $\mathbf{u}$ of the control signal $\boldsymbol{\tau}$ when using observer outputs to calculate matrices in the control signal.

3.5.2. System with constant delay without the delay compensation

Now let us consider the effect of a constant delay $h = 0.1$s when using the same multipurpose regulator (3.12) without compensating transformation. Let us again turn to the proper motion mode in the absence of external disturbances. The dynamics of the system for this case are presented in Fig. 3.11. One can notice a significant deterioration in the quality of the dynamics. A further increase in the delay leads to instability of the system.

The influence of a constant external disturbance when the corrector is turned off, as in the case without delay, leads to a displacement of the manipulator from the specified position, while the dynamics also worsen (Fig. 3.12). Turning on the corrector under such conditions leads to instability of the system, as can be seen from Fig. 3.13. The operation of the corrector under the influence of periodic disturbances also leads to instability.

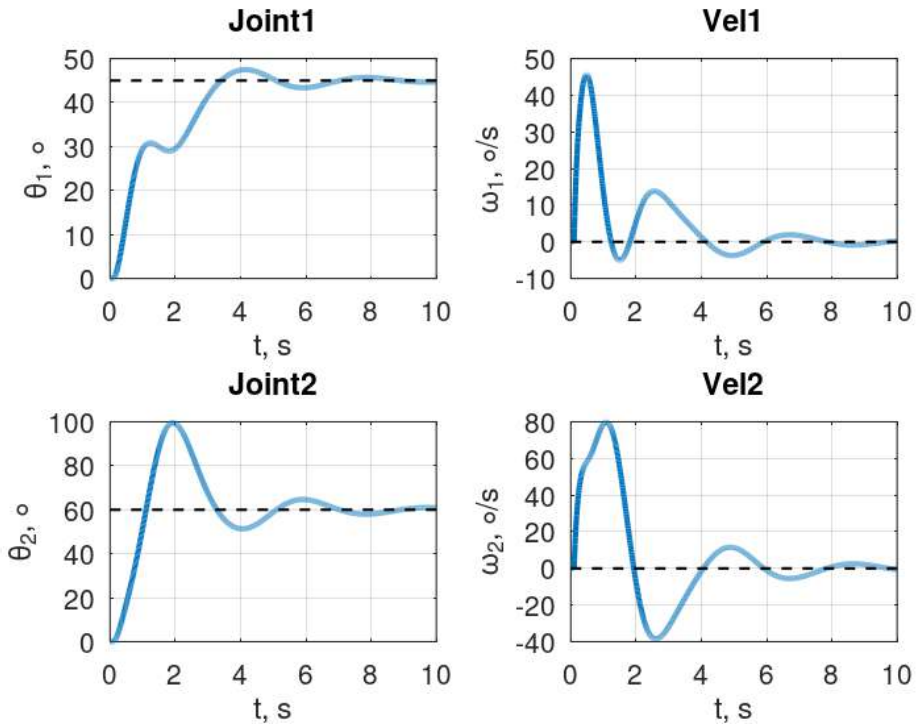

Fig. 3.11. Dynamics of a system without external disturbance with constant delay without compensation.

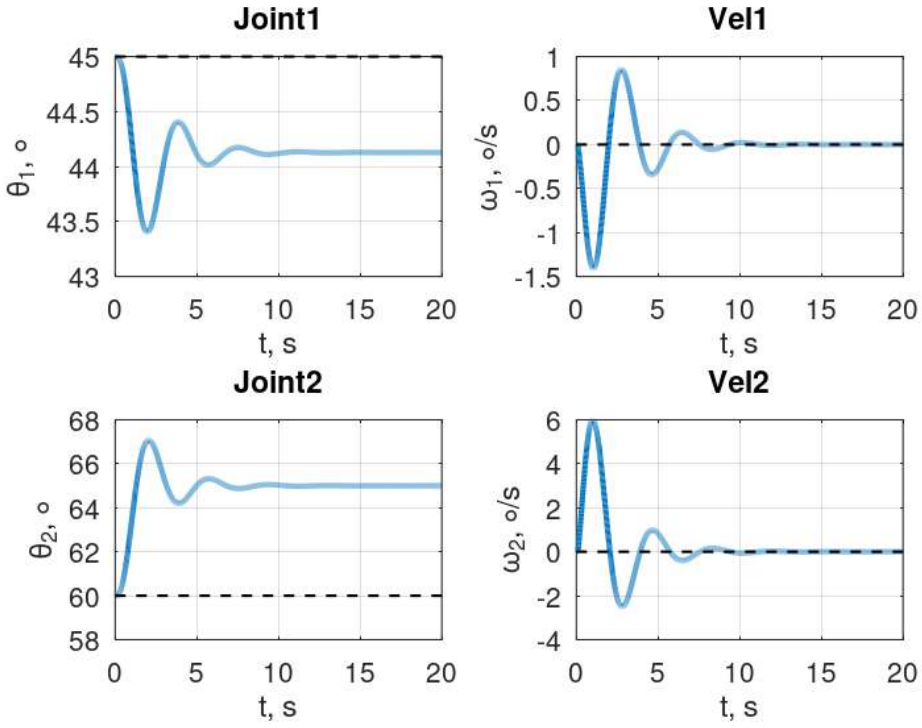

Fig. 3.12. Dynamics of a system under constant external disturbance and with constant delay without compensation and corrector.

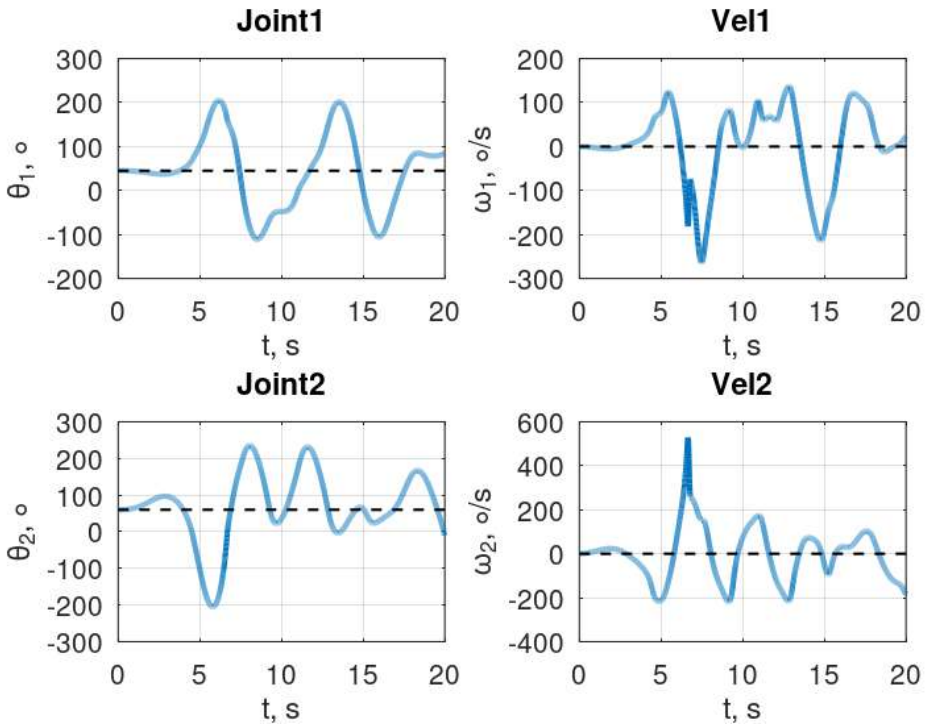

Fig. 3.13. Dynamics of the system with a constant external disturbance and an enabled corrector with a constant delay without compensation.

Let us demonstrate the operation of a dynamic corrector without loss of stability. To do this, we lower the delay value to $h = 0.05$ s, using the value $\lambda = -10$ as an eigenvalue for synthesizing the corrector matrices $\boldsymbol{\alpha}_k$. The dynamics of the system under the influence of a constant disturbance with the corrector turned on for this case is presented in Fig. 3.14. It can be seen that the corrector manages to ensure that the manipulator returns to the specified position, but the dynamics of the system is much worse than in the case without delay. When applying a periodic disturbance under similar conditions with the corrector turned on after 10 s, as can be seen from Fig. 3.15 and Fig. 3.16, changes in dynamics are insignificant.

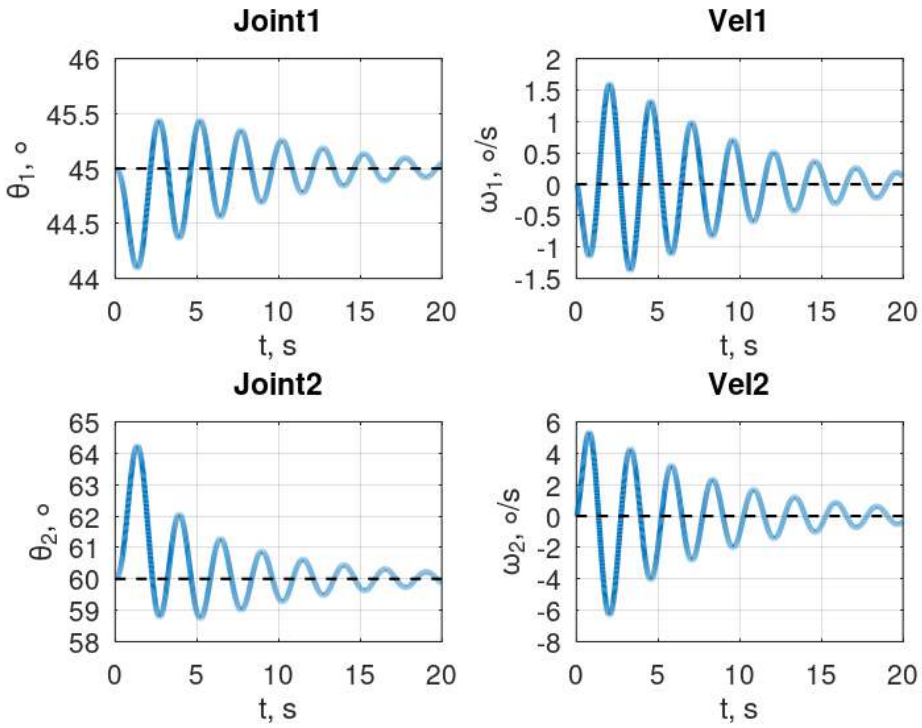

Fig. 3.14. Dynamics of the system with a constant external disturbance and a turned on corrector with reduced delay.

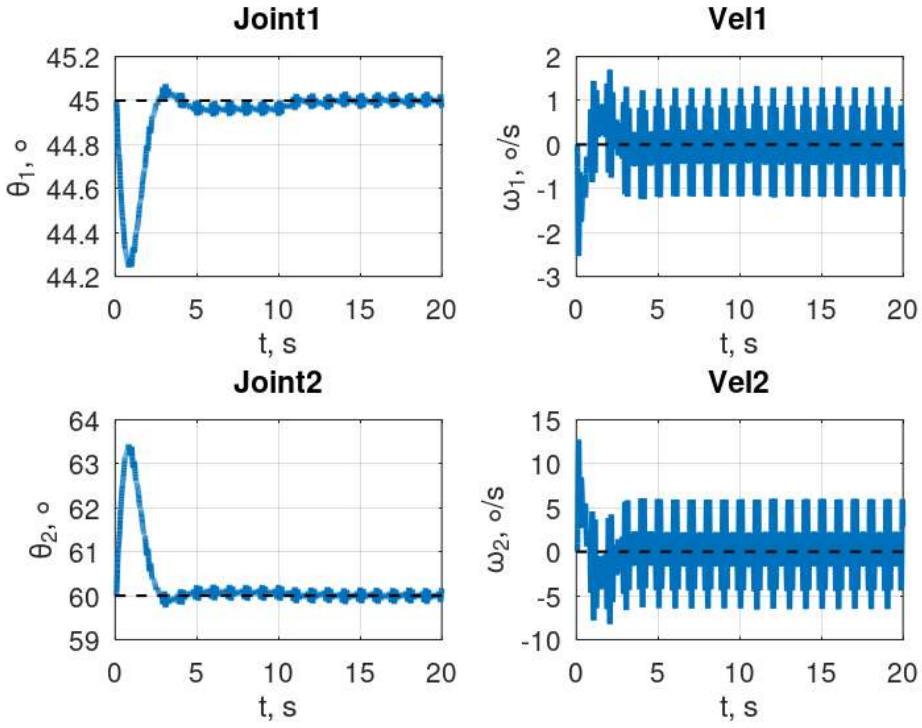

Fig. 3.15. Dynamics of a system under periodic external disturbance with reduced delay.

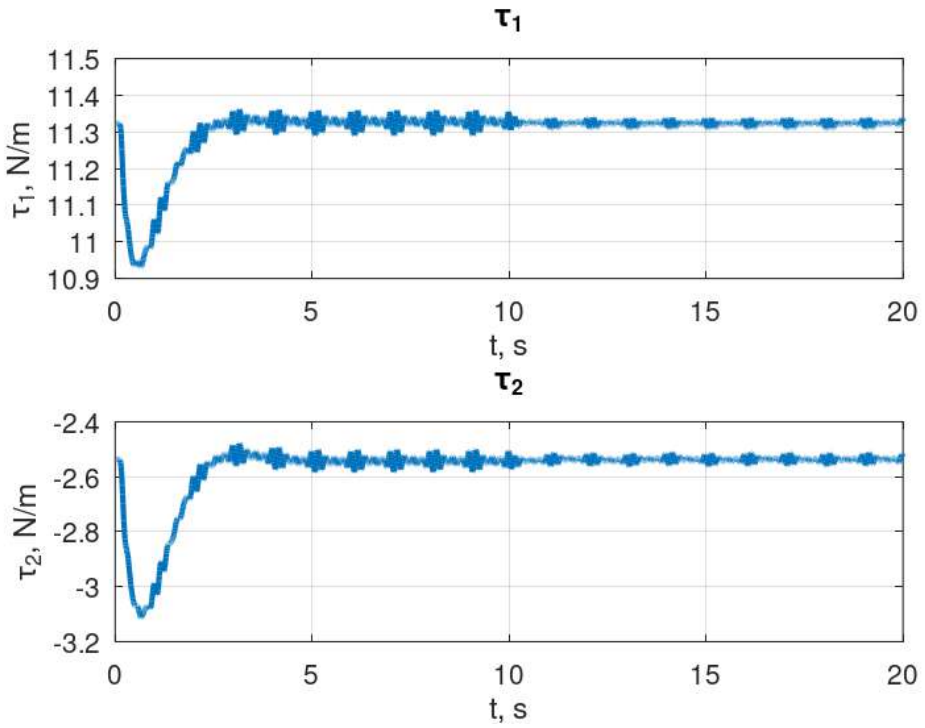

Fig. 3.16. Dynamics of the control signal $\boldsymbol{\tau}$ under periodic external disturbance with reduced delay.

3.5.3. Constant delay compensation

Now we will demonstrate the effect of the compensating transformation (3.36) of a multipurpose regulator synthesized without taking into account the delay. Again we will use the delay value $h = 0.1\text{s}$ and the eigenvalue $\lambda = -3$ to synthesize the dynamic corrector matrices $\boldsymbol{\alpha}_k$. First, let us consider the proper motion mode without external disturbance and with the corrector turned off. The dynamics of the system for this case is presented in Fig. 3.17. It can be seen that the plots are almost identical to Fig. 3.2 for the case without delay.

Next, we will apply a constant external disturbance and turn on the dynamic corrector. Fig. 3.18 also demonstrates dynamics that is almost identical to the case without delay.

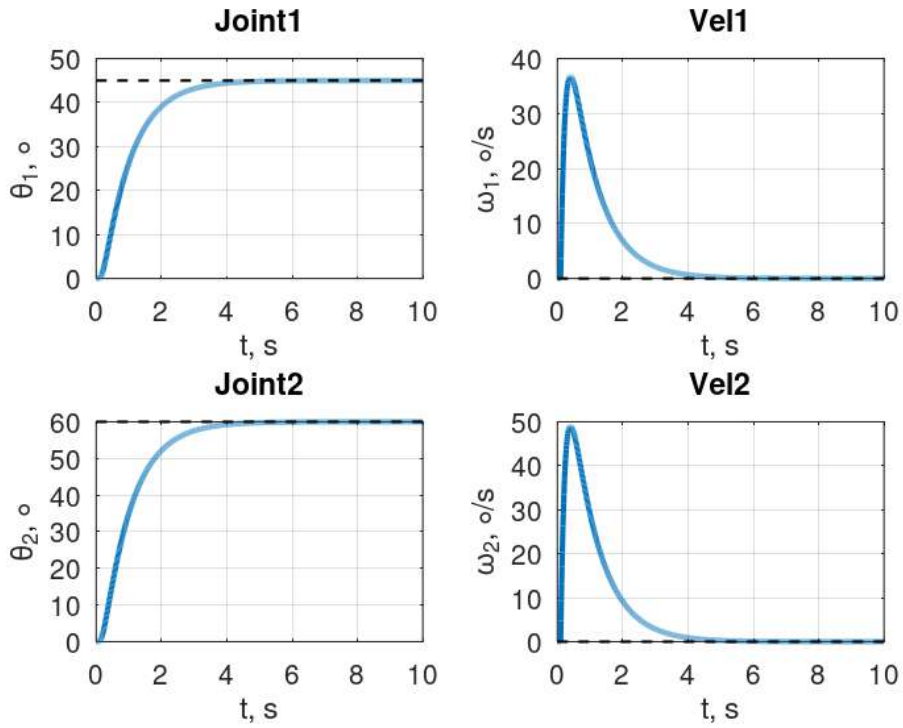

Fig. 3.17. System dynamics without external disturbance with constant delay compensation.

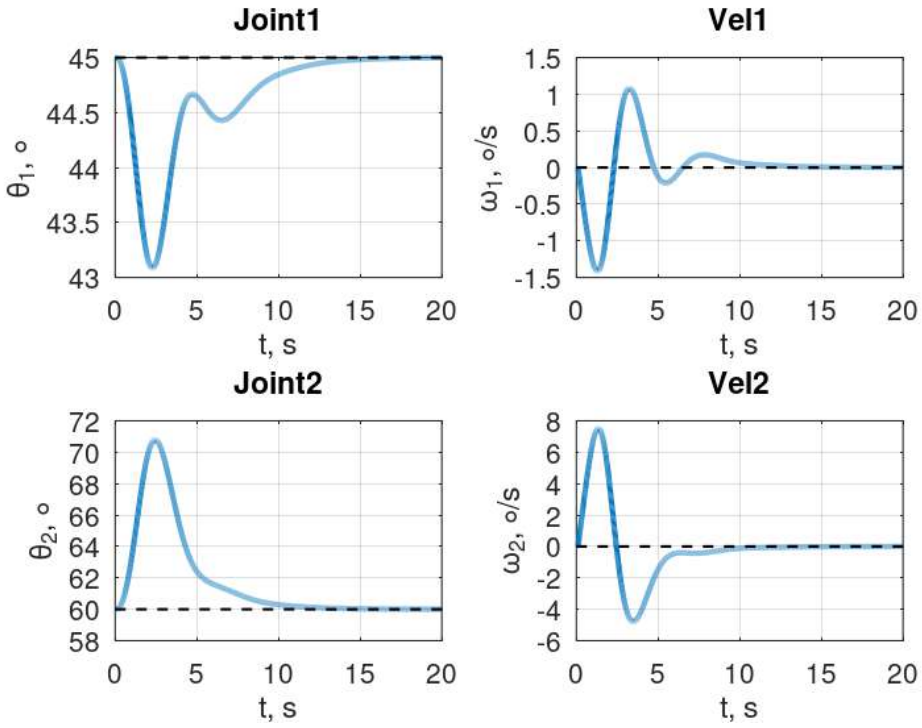

Fig. 3.18. System dynamics under constant external disturbance with constant delay compensation and corrector turned on.

Finally, let us turn to the operating mode under the influence of a periodic external disturbance and the presence of a constant delay in the channels of control and external disturbance. As before, we will turn on the dynamic corrector here only after 10 seconds of movement. The dynamics of the system motion for this case is presented in Fig. 3.19, while Fig. 3.20 shows the dynamics of the control signal $\boldsymbol{\tau}$ and Fig. 3.21 demonstrates the dynamics of the linear part $\mathbf{u}$ of the control signal $\boldsymbol{\tau}$. As it can be seen from the presented plots, the dynamics in this case is again almost identical to the dynamics in the case without delay.

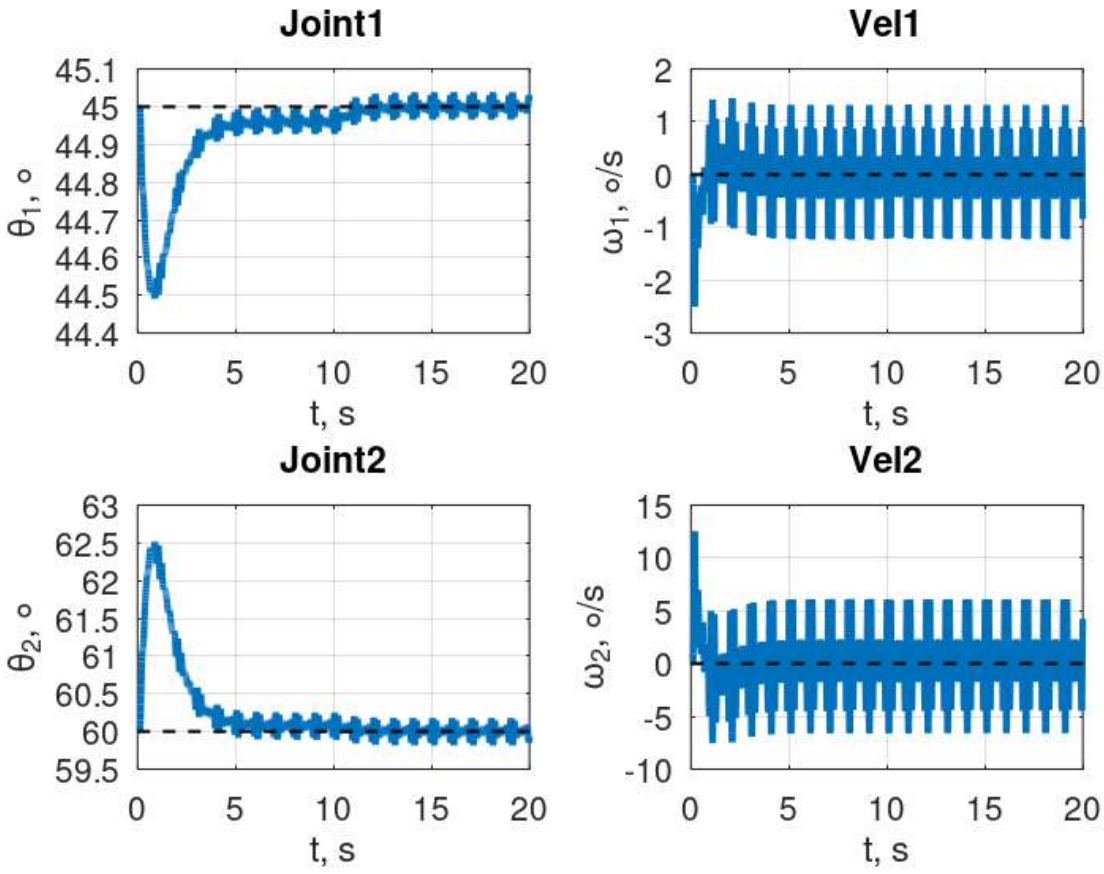

Fig. 3.19. Dynamics of a system under periodic external disturbance with constant delay compensation.

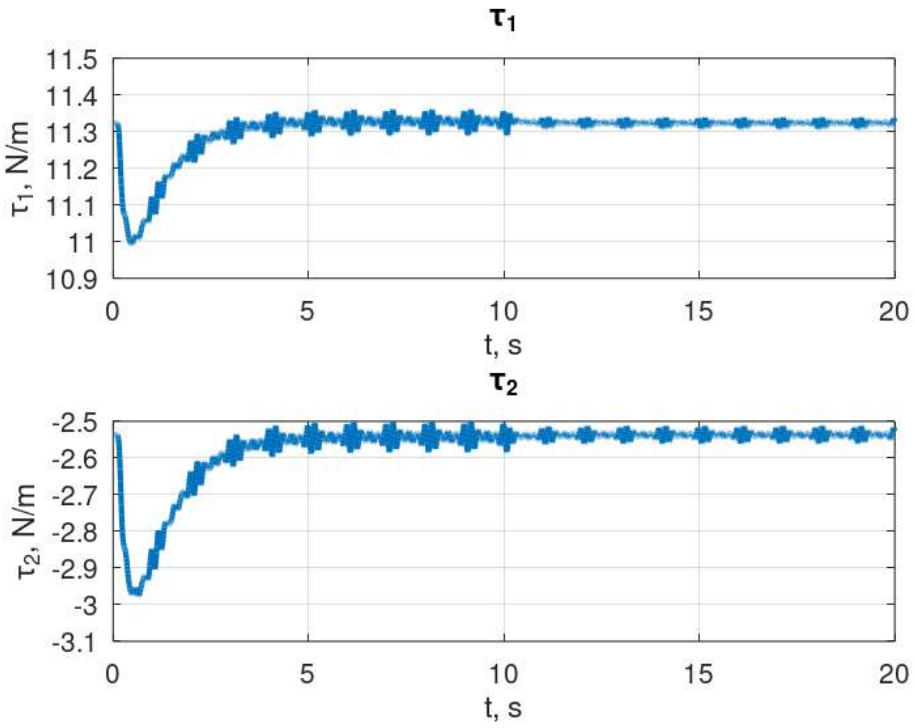

Fig. 3.20. Dynamics of the control signal $\boldsymbol{\tau}$ under periodic external disturbance with constant delay compensation.

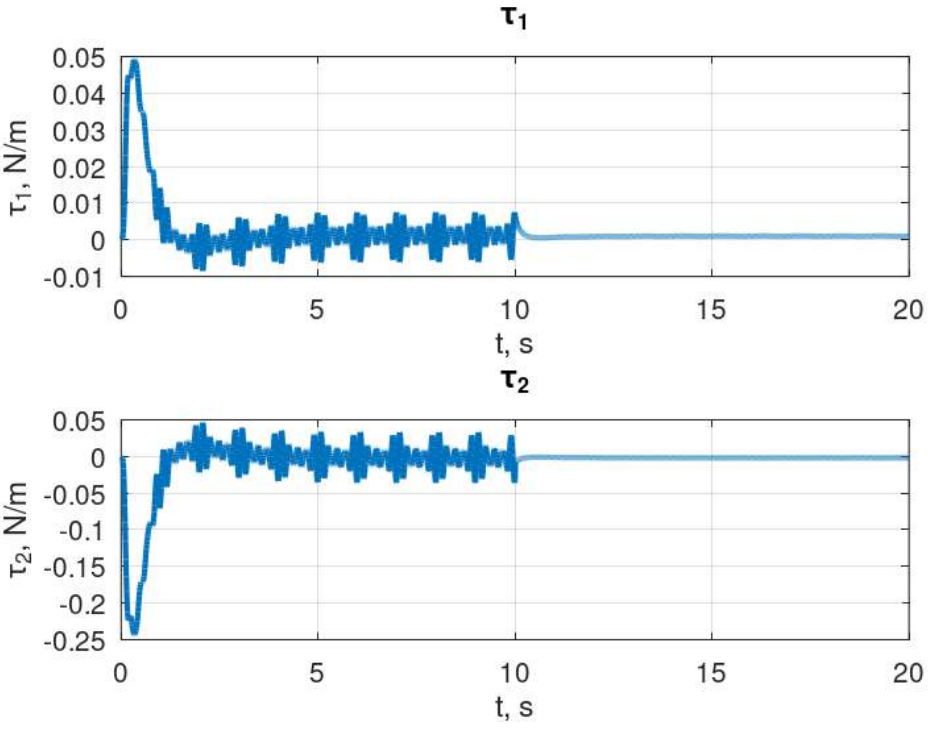

Fig. 3.21. Dynamics of the linear part $\mathbf{u}$ of the control signal $\boldsymbol{\tau}$ under periodic external disturbance with constant delay compensation.

Note that the use of asymptotic observers outputs $\mathbf{z}_\theta$ and $\mathbf{z}_\omega$ instead of the predicted values $\boldsymbol{\theta}_p$ and $\boldsymbol{\omega}_p$ in the calculation of matrices $\mathbf{M}$, $\mathbf{C}$ and $\mathbf{g}$ compensating for nonlinearity in the regulator with delay compensation also leads to a decrease in the intensity of the control signal $\boldsymbol{\tau}$ after turning on the dynamic corrector, as in the case without delay. The dynamics of the system motion for this case is presented in Fig. 3.22, the dynamics of the control signal $\boldsymbol{\tau}$ is shown in Fig. 3.23, and Fig. 3.24 demonstrates the dynamics of the linear part $\mathbf{u}$ of the control signal $\boldsymbol{\tau}$. It can be seen that the presented plots also practically coincide with similar plots for the case without delay.

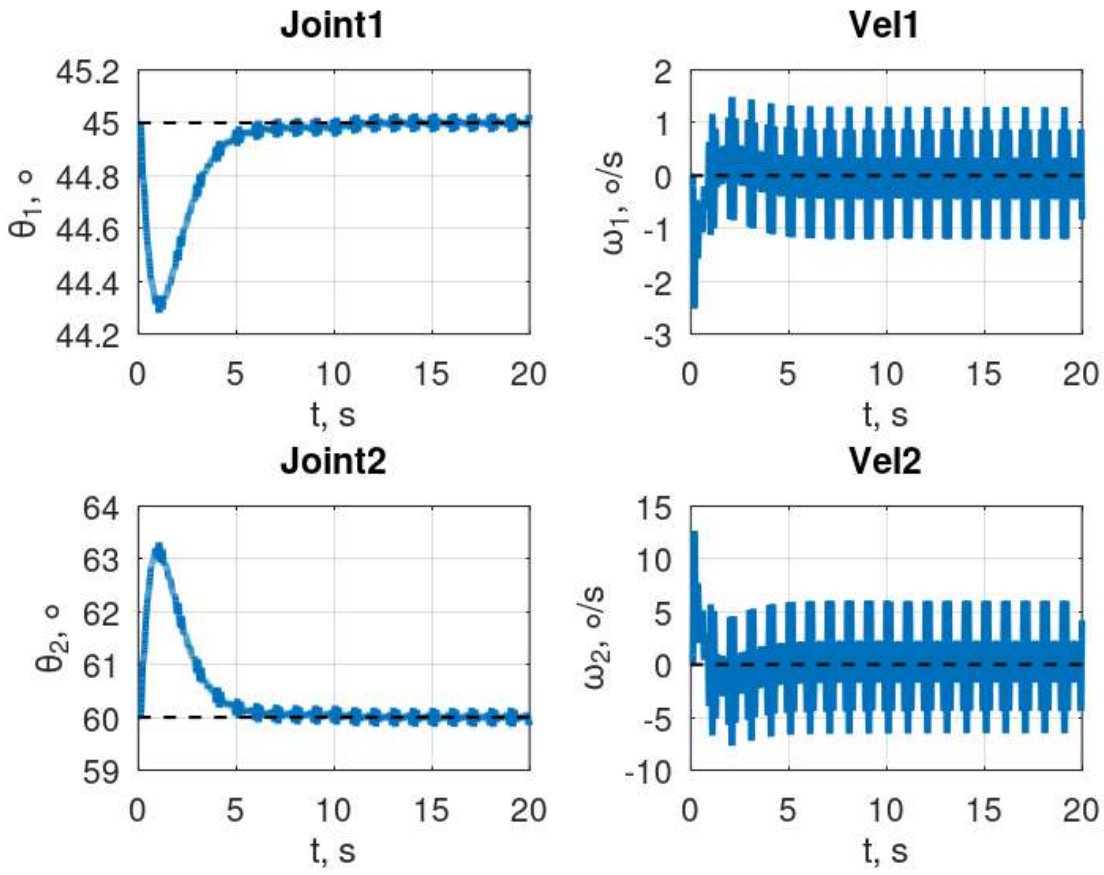

Fig. 3.22. System dynamics when using observer outputs to calculate matrices in the control signal.

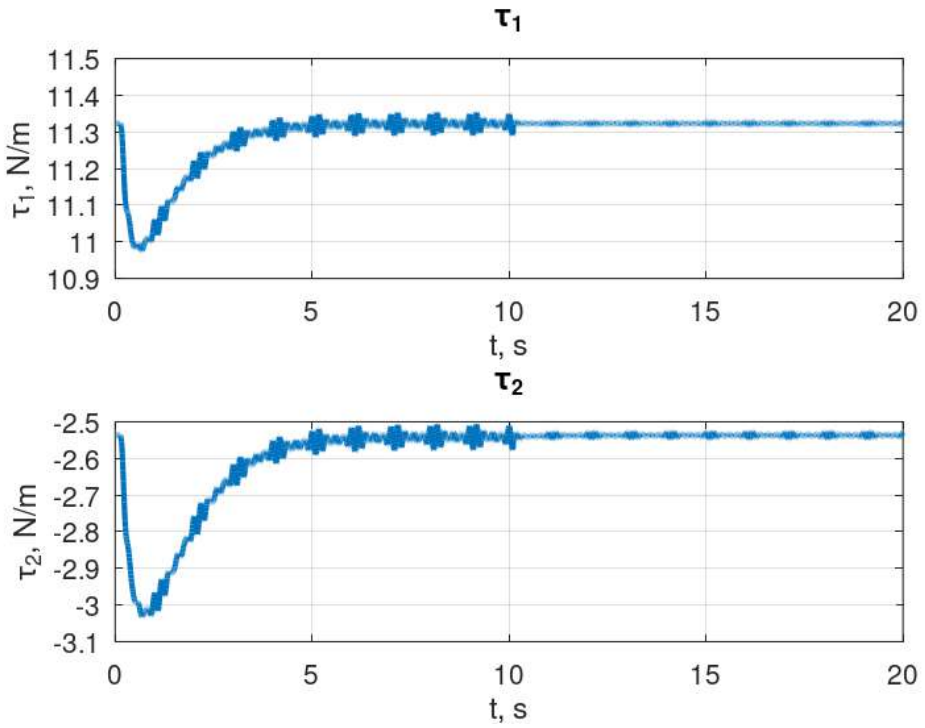

Fig. 3.23. Dynamics of the control signal $\boldsymbol{\tau}$ when using observer outputs to calculate matrices in the control signal.

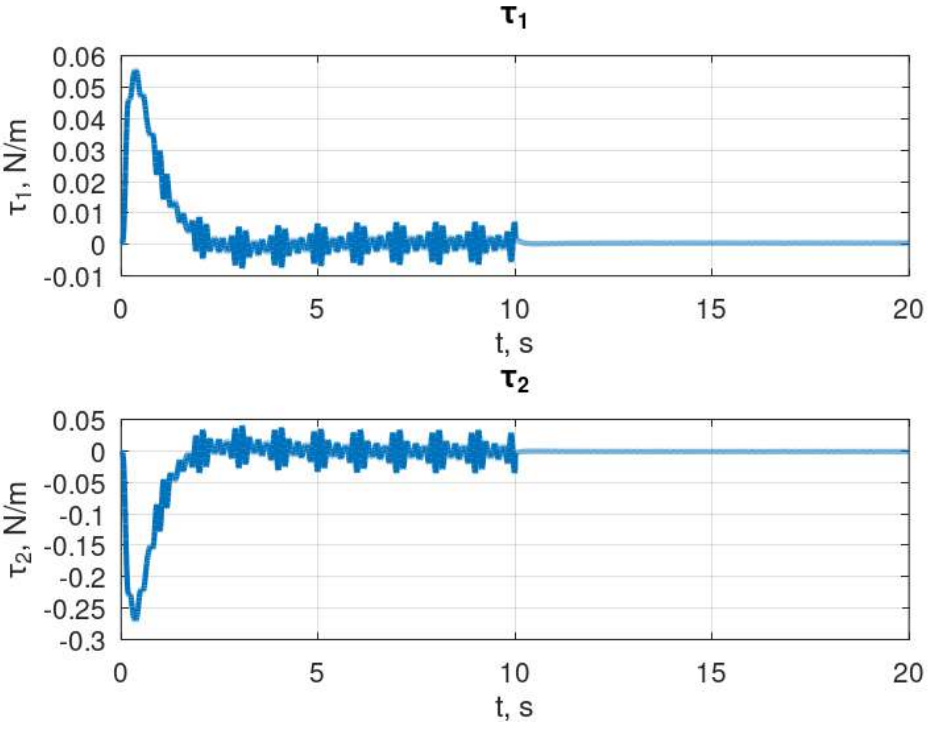

Fig. 3.24. Dynamics of the linear part $\mathbf{u}$ of the control signal $\boldsymbol{\tau}$ when using observer outputs to calculate matrices in the control signal.

Thus, the delay-compensating transformation (3.36) of a multipurpose regulator actually makes it possible to obtain the dynamics of a closed-loop system which practically coincides with the dynamics in the case without the presence of a constant delay.

3.6. Conclusions

Analysis of the plots obtained as a result of experiments with a computer model of a two-link manipulator allows to conclude that multipurpose regulators can effectively solve problems of stabilization of nonlinear systems when using the feedback linearization method, taking into account the requirements for dynamics in various modes, in particular in the presence of external disturbances. Let us recall that the main advantage of multipurpose regulators is the fact that the synthesis of separate adjustable elements can be done relatively independently of each other, and individual elements can be turned off depending on the current operating mode.

At the same time, the presence of a delay in the control channel significantly degrades the quality of the dynamics of the closed-loop system, up to the loss of stability. It is shown that for the delay compensation it is enough to synthesize a multipurpose regulator with the desired characteristics for a system without delay, and then carry out a special transformation of the resulting regulator. Such a transformation makes it possible to provide dynamic characteristics of a system with a delay that are almost identical to the case without a delay, i.e., in essence, to preserve the transfer matrix of the original regulator.

The disadvantages of the presented approach include the need to know the exact dynamic model to provide feedback linearization, difficult filtering of periodic external disturbances, and the need to measure external disturbances without delay.

Chapter 4. Multipurpose Control of the Air Cushion Vehicle

This chapter is devoted to the issues of the motion stabilization of a special class of marine objects – air cushion vehicles. A multipurpose approach is extremely important here, since the motion of such vessels is carried out under multi-mode conditions, in the presence of external disturbances of various kinds [90]. The implementation of control systems on the digital on-board equipment [43] also leads to the presence of delay in the control channel, which must be taken into account [46]. This chapter provides details of the synthesis process of a delay-compensating multipurpose regulator, described in the first chapter, for the motion stabilization, taking into account the described features.

Paragraph 4.1 provides a general description of the air cushion vehicle features and describes nonlinear equations for the dynamics of lateral motion, as well as a linearized model. Paragraph 4.2 is devoted to the formulation of the problem for a specific vessel with given numerical parameters. Paragraph 4.3 reveals the details of the synthesis of a multipurpose regulator without taking delay into account and presents the results of experiments with a computer model. Paragraph 4.4 is devoted to experiments in the presence of a constant delay with conventional and compensating controllers.

4.1. Air Cushion Vehicles

In order to demonstrate the efficiency of the proposed methods, let us consider a particular situation. Let us take an air cushion vehicle (ACV) as a plant. It is a special type of transport that reduces surface resistance due to the formation of an area of increased aerostatic pressure under the hull of the vessel. It is worth noting that, depending on the type of air cushion enclosure, there are two types of ACV – surface effect ships and amphibious vessels. The first type is characterized by a rigid side fence, partially submerged in water. The dynamics of such ships are more similar to classic ships. The fencing of the second type of hovercraft is

flexible and, as a rule, does not have direct contact with the underneath surface. The focus of this work is on amphibious vessels.

Let us consider the air cushion formation scheme in a simplified form (Fig. 4.1). The high-pressure zone (actually, the air cushion itself), which compensates for the weight of the vessel, receives an air flow from the lift fans. The air flow can optionally be directed through the rigid receiver 1 and flexible receiver 2 zones in order to distribute air pressure more evenly. The flexible air cushion fence is integrated with the ship's hull. Such a fence ensures that the hovercraft rises to a certain height, due to which, as a rule, the ship’s hull does not have direct contact with the underneath surface. Because of this, amphibious hovercrafts are capable of moving not only on water, but also on land, as well as through swamps, ice, etc.

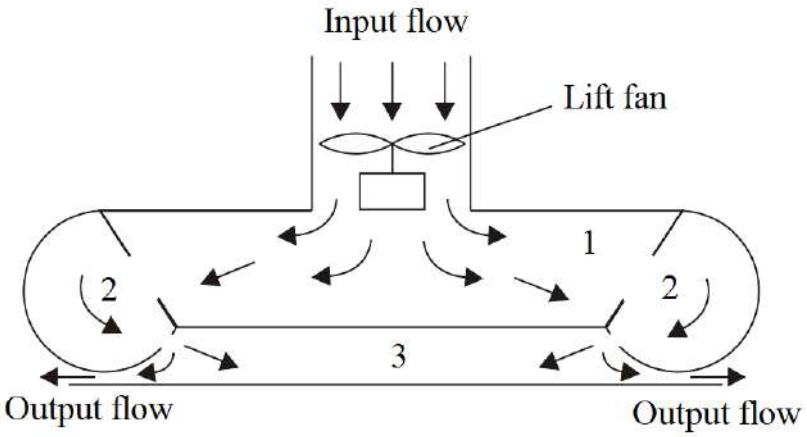

Fig. 4.1. Excess pressure generation under the bottom of the ACV.

The propulsors of the ACV are variable-pitch propellers installed on the deck. The motion direction can be changed either by controlling vertical aerodynamic rudders, or, in the case of multiple propulsors, by varying the thrust of the propellers. The first method is typical when moving at high speeds, and the second is more effective when accelerating the ship. It is worth noting that the presence of aerodynamic rudders is not necessary in cases where the propulsors themselves can be rotated, however, hovercraft models with such technologies are much less common. Next, we will consider an ACV model with a single propulsion device and vertical aerodynamic rudders in the mode of movement on the sea surface.

Let us note a few more features of the ACV dynamics. Unlike classical ship models, the motion of the hovercraft along the sea surface is not affected by the added masses of water, due to the absence of direct contact of the hull with the water. However, the air cushion still interacts with the surface of the water, so taking into account hydrodynamic drag forces is necessary. The following ACV-specific feature should also be noted here. Under the air cushion, a depression is formed in the water surface when moving at low speeds. However, the deepening disappears when overcoming a speed of about 30 knots (the so-called “hump speed”), while the hydrodynamic resistance decreases significantly [31].

Let us give a description of the nonlinear mathematical model of ACV. The necessary reference frames are shown in Fig. 4.2. Here $O_g\xi\eta\zeta$ is the base (terrestrial) coordinate system, which is stationary. $O\xi_1\eta_1\zeta_1$ – a semi-coupled (intermediate terrestrial) system, the origin of which is rigidly connected to the center of mass of the hovercraft, and the axes are parallel to the axes of the base coordinate system and, accordingly, have a fixed orientation. Finally, *Oxyz* is a coupled coordinate system, the axes of which, unlike the previous system, rotate together with the ship.

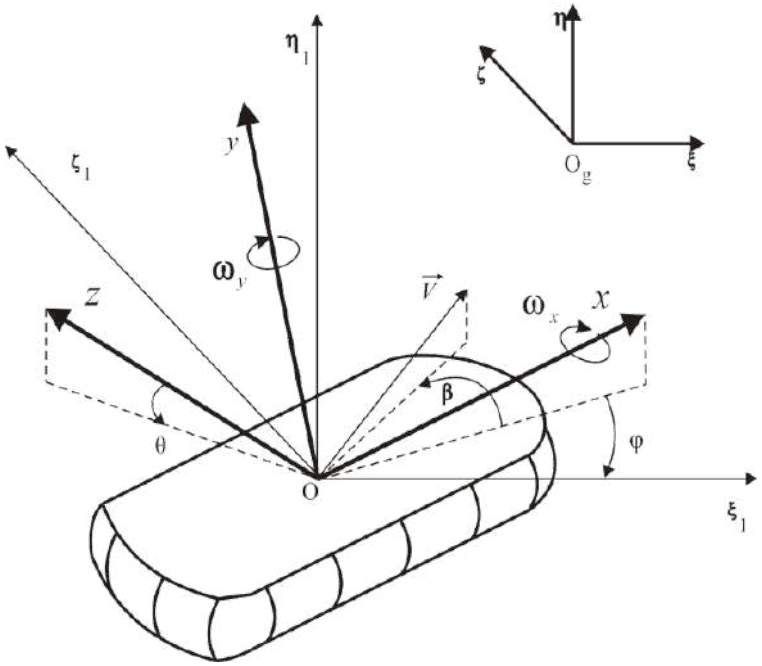

Fig. 4.2. Reference frames.

Taking into account the most significant forces influencing the dynamics of the ACV, the nonlinear differential equations of lateral motion can be written as a system [13, 103]

$$\begin{aligned} m(\dot{V}_x + V_z\omega_y) &= F_{xa} + F_{xh} + T, \\ m(\dot{V}_z - V_x\omega_y) &= F_{za} + F_{zh} + F_{zc} + F_{zr}, \\ I_x\dot{\omega}_x &= M_{xa} + M_{xh} + M_\theta + M_{xr}, \\ I_y\dot{\omega}_y &= M_{ya} + M_{yh} + M_{yr}, \end{aligned}$$

which can be transformed to a system of ordinary differential equations of the form

$$\begin{aligned} \dot{V}_x &= (F_{xa} + F_{xh} + T - V_z\omega_y)/m, \\ \dot{V}_z &= (F_{za} + F_{zh} + F_{zc} + F_{zr} + V_x\omega_y)/m, \\ \dot{\omega}_x &= (M_{xa} + M_{xh} + M_\theta + M_{xr})/I_x, \\ \dot{\omega}_y &= (M_{ya} + M_{yh} + M_{yr})/I_y, \end{aligned} \tag{4.1}$$

where V_x and V_z – linear velocities, ω_x and ω_y – angular velocities, m – ship's mass, I_x and I_y – moments of inertia. Forces and moments, marked with *a* index, are related to the aerodynamic drag, *h* – to the hydrodynamic drag. Index *r* denotes forces and moments, acting on the rudders. F_{zc} – reactive jet force, occurring in the case of a roll on the one side of the air cushion. M_θ – restoring moment during roll due to air pressure inside the air cushion. T – propulsor thrust force.

Aerodynamic drag forces and moments can be described by the formulas

$$\begin{aligned} F_{xa} &= 0.5C_{xa}(\beta_a)\rho_a V_0^2 S, \\ F_{za} &= 0.5C_{za}(\beta_a)\rho_a V_0^2 S, \\ M_{xa} &= 0.5F_{za}H, \\ M_{ya} &= 0.5(C_{mya}(\beta_a) + C_{mya}^{\omega_y}\frac{\omega_y L}{V_0})\rho_a V_0^2 SL, \end{aligned}$$

where β_a – aerodynamic drift angle with respect to the wind, ρ_a – air density, V_0 – ACV velocity with respect to the wind, S – ship's lateral surface area, L and H – vessel's length and height accordingly; $C_{xa}(\beta_a)$, $C_{za}(\beta_a)$, $C_{mya}(\beta_a)$, $C_{mya}^{\omega_y}$ – ship's hull aerodynamic coefficients.

Hydrodynamic drag is represented in the form

$$F_{xh} = 0.5C_{xh}(Fr,\beta)\rho_w V^2 W^{2/3},$$
$$F_{zh} = 0.5C_{zh}(Fr,\beta)\rho_w V^2 W^{2/3},$$
$$M_{xh} = 0.5F_{zh}H,$$
$$M_{yh} = 0.5(C_{myh}(Fr,\beta) + C_{myh}^{\omega_y}(Fr)\frac{\omega_y W^{1/3}}{V})\rho_w V^2 W,$$

where β – vehicle's drift angle, ρ_w – water density, V – ship's velocity, W – vessel displacement. $C_{xh}(Fr,\beta)$, $C_{zh}(Fr,\beta)$, $C_{mxh}(Fr,\beta)$, $C_{myh}(Fr,\beta)$, $C_{myh}^{\omega_y}$ – hydrodynamic coefficients. Fr – Froude number (dimensionless quantity used in shipbuilding to compare the hydrodynamic properties of hulls of different sizes). Froude number can be calculated as

$$Fr = \frac{V}{\sqrt{Lg}},$$

where g – gravitational acceleration.

Note the fact that, in general, the aerodynamic and hydrodynamic coefficients of real ship models are calculated during experiments in a wind tunnel and a specialized pool. Due to the complexity of the corresponding aerodynamic processes, an accurate description of the forces and moments acting on the rudders is quite complicated. In this regard, we will use the experimental approximation given in [13]:

$$F_{zr} = C_r \delta \frac{\rho_a}{2} V_0^2 S,$$
$$M_{yr} = F_{zr} x_r,$$
$$M_{xr} = -F_{zr} y_r,$$
$$C_r = C_{r1}[(1-k_r)(1+s)\frac{S_r^{''}}{S_r} + \frac{S_r^{'}}{S_r}],$$
$$k_r = \frac{1.9\pi\lambda_{1r}s}{\lambda_r(1.9\pi+\lambda_{1r})(s+1)},$$
$$s = \sqrt{\frac{1+2.53T}{(\rho_a D^2 V_0^2)}} - 1,$$

where C_r – force coefficient, δ – rudder deflection, x_r and y_r – rudder center geometric coordinates, C_{r1} – coefficient of the model without the propulsors. S_r – rudder surface area, $S_r^{'}$ and $S_r^{''}$ – rudder surface areas in and out of the air flow, λ_r and λ_{r1} – corresponding parts of the rudder lengths, D – air propeller diameter. k_r and s – auxiliary coefficients.

The theoretical description of the reactive force F_{zc} of the air flow and the restoring moment M_θ is also quite difficult. Generally, for modeling purposes it is sufficient to provide simplified formulas, which are experimental approximations:

$$\mathrm{F}_{zc} = mgk_\theta\theta,$$
$$M_\theta = -mgh\theta - N_\theta\omega_x,$$

where θ – roll angle, h – metacentric height, k_θ – air flow coefficients, N_θ – air cushion restoring moment coefficient. Coefficients k_θ and N_θ are calculated experimentally.

Assuming that there are no external disturbances, let us linearize the nonlinear system (4.1) in the vicinity of the equilibrium position $V_x = const$, $V_z = \omega_y = \theta = \delta_r = 0$. The dynamics of roll and longitudinal velocity in this mode can be neglected. Let us also note that for linear models of marine moving objects it is accepted to consider drift angle, which can be represented as $\beta = \frac{V_z}{V_x}$, instead of the lateral vessel velocity V_z.

Taking into account the above considerations, the linear model of the lateral dynamics of the ACV used for a stabilizing regulator synthesis can be described by the system of the equations

$$\begin{aligned} \dot{\beta} &= a_{11}\beta + a_{12}\omega_y + b_1\delta_r + h_1 d, \\ \dot{\omega}_y &= a_{21}\beta + a_{22}\omega_y + b_2\delta_r + h_2 d, \\ \dot{\varphi} &= \omega_y, \end{aligned} \qquad (4.2)$$

where φ – heading angle, d – scalar external disturbance (wind or waves); a_{ij}, b_i, h_i – constant model coefficients.

4.2. Problem Formulation

For specific parameter values of the ACV nonlinear model let use averaged data of various vessels from the works [13, 23, 31, 103]. The main characteristics are given in Table 4.1.

Table 4.1. Main characteristics of the considered ACV model.

Characteristic	**Units**	**Value**	**Notation**
Volumetric displacement	m^3	3 628.8	W
Length	m	27	L
Width	m	14	B
Height	m	9.6	H
Mass	kg	70 000	m
Longitudal moment of inertia	kg m^2	1 680 933.3	J_{xx}
Vertical moment of inertia	kg m^2	5 395 833.3	J_{yy}
Transvers moment of inertia	kg m^2	4 790 100	J_{zz}
Maximum rudder angle	deg	40	$\delta_{\max}$
Maximum rudder change rate	deg/s	15	$\dot{\delta}_{\max}$
Maximal velocity	m/s	28	$V_{\max}$
Rudder surface area	m^2	5.4	S_r
Longitudinal rudder arm	m	13.5	x_r
Vertical rudder arm	m	2.4	y_r
Water density	kg/m^3	1000	ρ_w
Air density	kg/m^3	1.292	ρ_a

We will assume that there is a constant delay τ in the control and external disturbance channels. Taking into account the dynamics of the rudder drive and considering that the measured output is the value of the heading angle φ, the linear model of the lateral motion of the ACV in the vicinity of the described equilibrium position is represented as a system

$$\begin{aligned}
\dot{\beta} &= a_{11}\beta + a_{12}\omega_{\text{y}} + b_1\delta_r(t-\tau) + h_1 d(t-\tau),\\
\dot{\omega}_{\text{y}} &= a_{21}\beta + a_{22}\omega_{\text{y}} + b_2\delta_r(t-\tau) + h_2 d(t-\tau),\\
\dot{\varphi} &= \omega_{\text{y}},\\
y &= \varphi,\\
\dot{\delta}_r &= u.
\end{aligned} \tag{4.3}$$

Let us consider the straightforward motion of the hovercraft with a constant longitudinal velocity $V_x = 12$ m/s. It is necessary to synthesize a delay-compensating multipurpose regulator to ensure the following characteristics of a closed-loop system in various driving modes:

1) In any mode, the asymptotic stability of the hovercraft motion must be ensured.

2) In the *proper motion mode*, it is necessary to ensure that the hovercraft is capable of rotating along the heading angle by $10°$ in 10 s with a maximum overshoot value of 3% of the specified angle.

3) In the *operating mode under the influence of a constant external disturbance* in the form of a side wind at a speed of 10 m/s (i.e. $d(t) = 10$), the deviation of the heading angle from the current value should not exceed $0.4°$.

4) For a *periodic external disturbance* consider the sea surface waves, approximately corresponding to 4 points on the Beaufort scale. In this mode, it is necessary to minimize the intensity of rudder deflections. As an approximate wave model, we will take a polyharmonic disturbance of the form

$$d(t) = 0.2\sin(0.65t) + 0.1\sin(0.55t) + 0.1\sin(0.75t). \qquad (4.4)$$

4.3. Practical Implementation of the Multipurpose Regulator Without the Delay

In order to test the above methods, a computer model of the nonlinear lateral ACV dynamics was implemented in the Matlab-Simulink environment. While performing straightforward motion at a speed of 12 m/s, the coefficients of the linear model (4.3) have the following values:

$$a_{11} = -0.3176,\ a_{12} = 0.852,$$
$$a_{12} = -0.0102,\ a_{22} = -0.1383,$$
$$b_1 = -0.005,\ b_2 = -0.0217,$$
$$h_1 = -0.0006, h_2 = 0.00025.$$

Let us compare nonlinear dynamics with the linear approximation. Fig. 4.3 demonstrates the transient process corresponding to the response to a step rudder deflection of magnitude $1°$. It can be noted that the models match almost perfectly. The dynamics of the models under the influence of an external step disturbance in the form of a side wind with a speed of 10 m/s is presented in Fig. 4.4. It can be seen that during the first few seconds there is a noticeable discrepancy in the drift angle, but in general the dynamics is also almost identical. Thus, we can conclude that the dynamics of the calculated linear model is a sufficient approximation of the original nonlinear system in the considered mode and is suitable for further synthesis of multipurpose and compensating controllers.

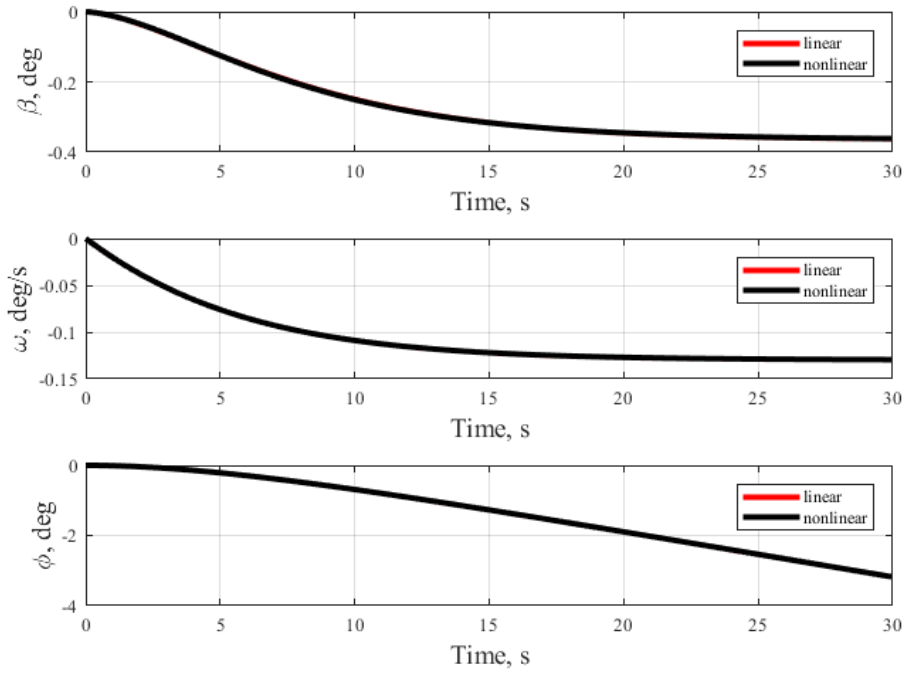

Fig. 4.3. Comparison of linear and nonlinear models with unit rudder deflection.

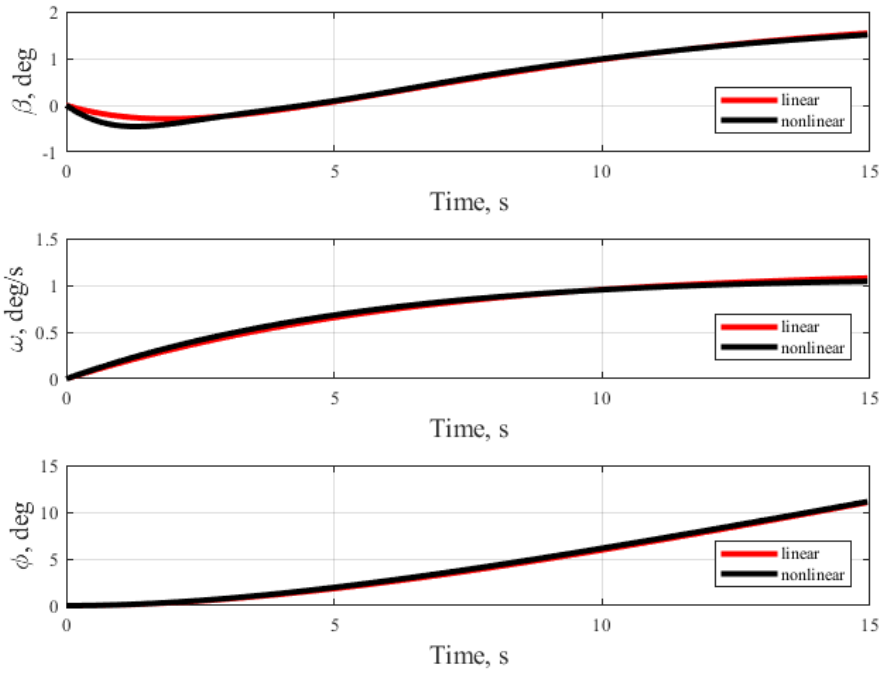

Fig. 4.4. Comparison of linear and nonlinear models when exposed to side wind.

The adjustable elements of the positional control law (1.17) corresponding to the requirements given in the problem formulation have the following values obtained as a result of LQR-optimal synthesis:

$$\mathbf{K}_x = \begin{pmatrix} 0.3365 & -23.1742 & -7.0711 \end{pmatrix}, \quad k_\delta = 1.006,$$

with the following quadratic functional weight matrices:

$$\mathbf{Q} = \operatorname{diag}\left(\begin{bmatrix} 0 & 1.5 & 0.5 & 0 \end{bmatrix}\right), \quad R = 0.01.$$

Now we will derive expressions for calculating the coefficients of the basic speed control law (1.13). In accordance with the remark given in paragraph 1.2, the search procedure in specific situations can be significantly simplified. Let us consider the linear system (4.2) without taking into account the external disturbance:

$$\begin{aligned} \dot{\beta} &= a_{11}\beta + a_{12}\omega_y + b_1\delta_r, \\ \dot{\omega}_y &= a_{21}\beta + a_{22}\omega_y + b_2\delta_r, \\ \dot{\varphi} &= \omega_y. \end{aligned}$$

The specified system must be resolved with respect to state variables ω_y, β and δ, obtaining the relations

$$\begin{aligned}
\beta &= [(a_{12}b_2 - a_{22})\dot{\varphi} - b_2\dot{\beta} + b_1\dot{\omega}_y]/q, \\
\omega_y &= \dot{\varphi}, \\
\delta &= [(a_{11}a_{22} - a_{21}a_{12})\dot{\varphi} - a_{11}\dot{\omega}_y + a_{21}\dot{\beta}]/q, \\
q &= a_{21}b_1 - a_{11}b_2.
\end{aligned} \tag{4.5}$$

Substituting the resulting equations (4.5) into the positional control law (1.17), we obtain the coefficients of the speed control law

$$\begin{aligned}
\nu &= k_3, \\
\mu_1 &= (a_{21}k_\delta - b_2k_1)/q, \\
\mu_2 &= (b_1k_1 - a_{11}k_\delta)/q, \\
\mu_3 &= ((a_{12}b_2 - b_1a_{22})k_1 + (a_{11}a_{22} - a_{12}a_{21})k_\delta)/q + k_2,
\end{aligned}$$

where $\begin{pmatrix} k_1 & k_2 & k_3 \end{pmatrix} = \mathbf{K}_x$, $\begin{pmatrix} \mu_1 & \mu_2 & \mu_3 \end{pmatrix} = \boldsymbol{\mu}$.

Let us substitute the calculated values $\mathbf{K}_x$ and k_δ into the given equations, as a result of which we obtain particular values of the speed control law parameters:

$$\begin{aligned}
\boldsymbol{\mu} &= \begin{pmatrix} -0.2757 & 46.2269 & 29.8032 \end{pmatrix}, \\
\nu &= 7.0711
\end{aligned}.$$

Now we present the results of experiments with a computer model without delay. The dynamics of the controlled motion of the hovercraft in the proper motion mode with reference signal when turning along the heading angle for 10° with a synthesized speed control law is shown in Fig. 4.5. It can be seen that in just 10 s there is a transition to the zone of 3% of the reference signal, i.e. requirements for overshoot and settling time are satisfied.

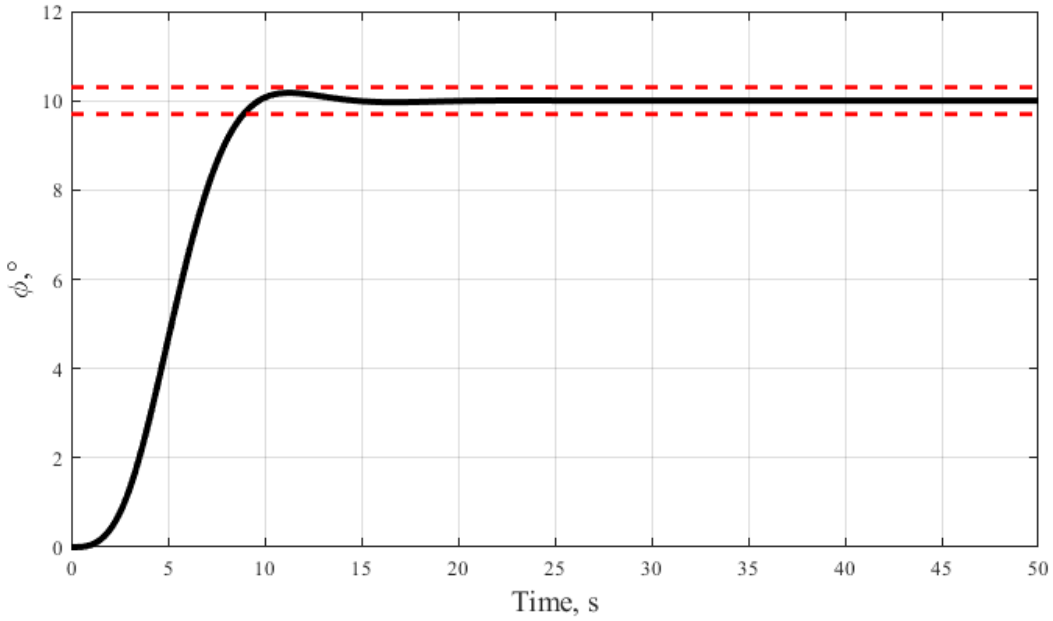

Fig. 4.5. Dynamics of heading angle when turning by 10º.

Next we move on to the synthesis of an asymptotic observer. In accordance with the requirement for dynamics in the motion mode under the influence of a constant external disturbance specified in the problem statement, as a result of synthesizing the observer as a Kalman filter, we obtain a matrix $\mathbf{G}$ for estimation errors in the form

$$\mathbf{G} = \begin{pmatrix} 1.4272 & 1.9543 & 1.977 \end{pmatrix}^{\mathrm{T}}.$$

In accordance with the methodology presented in the first chapter, we now proceed to the positional control law (1.14) based on the output of the asymptotic observer:

$$\mathbf{k} = \begin{pmatrix} -0.3843 & 23.1742 & -148.8717 \end{pmatrix}, \quad k_0 = -1.0006, \quad \nu_0 = 155.9427.$$

The dynamics of a system with a synthesized observer under the influence of a side wind is shown in Fig. 4.6. It can be noted that the stated requirement is met, the deviation does not exceed $0.4°$, while the convergence of the heading angle to a zero value is ensured, that is, the property of astatism is provided.

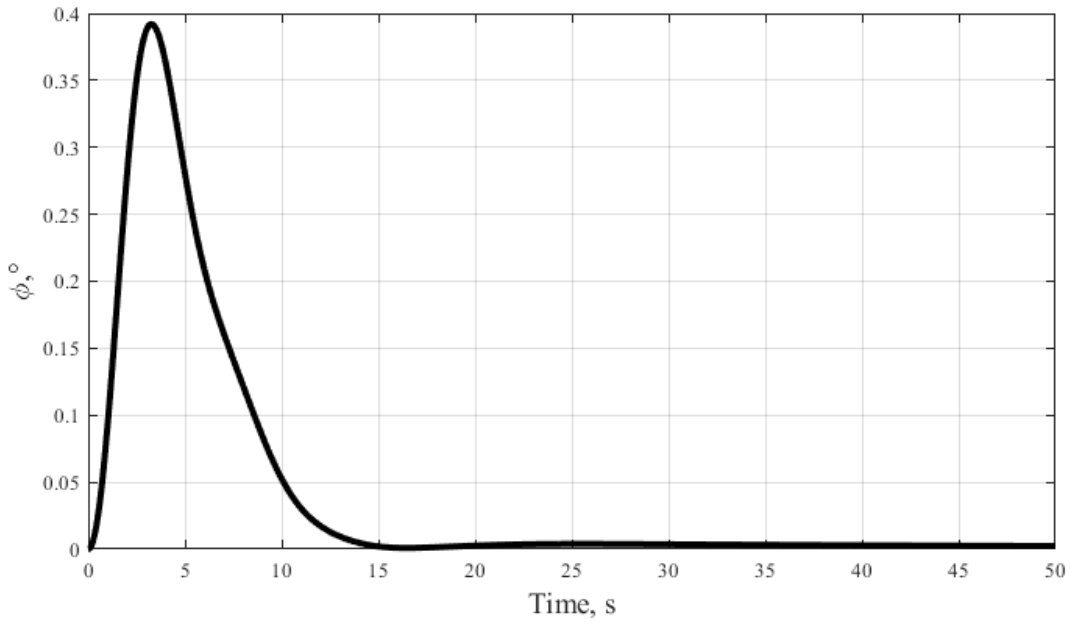

Fig. 4.6. Dynamics of the heading angle when exposed to a side wind at a speed of 10 m/s.

In conclusion let us proceed to the problem of synthesizing the dynamic corrector (1.12). In the framework of this work, as stated above, the goal of the corrector is to minimize the intensity of the rudder deflections in case of the influence of external periodic disturbances, such as sea waves.

For simplicity, let us take a harmonic oscillation with a constant frequency ω_0 as an approximate model of a periodic disturbance. Let us note the fact [9] that in this situation, in order to solve the problem, it is necessary to ensure that the transfer function from the current output to the position of the rudders is equal to zero at a given frequency ω_0, i.e. $F_{y\delta}(j\omega_0, F) = 0$. In turn, to satisfy this condition, the transfer function $F(s)$ of the dynamic corrector must satisfy the equality

$$F(j\omega_0) = [T_{12}(j\omega_0) - \tilde{T}T_{22}(j\omega_0)]^{-1}\tilde{T}, \tag{4.6}$$

where $\tilde{T} = T_{11}(j\omega_0)T_{21}^{-1}(j\omega_0)$; T_{11}, T_{12}, T_{21} and T_{22} – elements from (1.20).

For the value calculated using formula (4.6), we introduce a special notation $f_0 = F(j\omega_0)$. We take the matrix $\boldsymbol{\alpha}$ of the system (1.15) (i.e., the representation of the dynamic corrector in the state space) in the form

$$\boldsymbol{\alpha} = \begin{pmatrix} 0 & 1 \\ -\alpha_0 & -\alpha_1 \end{pmatrix}.$$

Let us note the fact that the transfer function $F(s)$ of the corrector is a rational function of the form

$$F(s) = \frac{\varepsilon(s)}{\alpha_p(s)},$$

where

$$\alpha_p(s) = \det(\mathbf{E}_2 s - \boldsymbol{\alpha}),$$

$$\varepsilon(s) = \alpha_p(s)\boldsymbol{\gamma}(\mathbf{E}_2 s - \boldsymbol{\alpha})^{-1}\boldsymbol{\beta} = \varepsilon_1 s + \varepsilon_0.$$

To provide the condition $F(j\omega_0) = f_0$ the following equalities must be satisfied:

$$\varepsilon_0 = \mathrm{Re}[f_0 \alpha_p(j\omega_0)],$$
$$\varepsilon_1 = \frac{\mathrm{Im}[f_0 \alpha_p(j\omega_0)]}{\omega_0}.$$

Let us take $\boldsymbol{\gamma} = \begin{pmatrix} 0 & 1 \end{pmatrix}$, the column we can get $\boldsymbol{\beta} = \begin{pmatrix} \beta_0 \\ \beta_1 \end{pmatrix}$, as a solution to linear system

$$\begin{pmatrix} 0 & 1 \\ -\alpha_0 & 0 \end{pmatrix}\begin{pmatrix} \beta_0 \\ \beta_1 \end{pmatrix} = \begin{pmatrix} \varepsilon_0 \\ \varepsilon_1 \end{pmatrix}.$$

From this we obtain

$$\begin{pmatrix} \beta_0 \\ \beta_1 \end{pmatrix} = \begin{pmatrix} \varepsilon_0 \\ -\varepsilon_1/\alpha_0 \end{pmatrix}.$$

Let us take the particular frequency value $\omega_0 = 0.65$ as average frequency of the disturbance (4.4). Set the roots of the denominator of the corrector transfer function as $\lambda_0 = \lambda_1 = -0.2$. Then, in accordance with the described approach, the matrices of the corrector model in the state space have the following values:

$$\boldsymbol{\alpha} = \begin{pmatrix} 0 & 1 \\ -0.04 & -0.4 \end{pmatrix}, \quad \boldsymbol{\beta} = \begin{pmatrix} -69.2093 \\ -83.98 \end{pmatrix}, \quad \boldsymbol{\gamma} = \begin{pmatrix} 0 & 1 \end{pmatrix}.$$

Fig. 4.7 shows a plot of the frequency response of a closed-loop system from external disturbance to rudder deflection in two modes: with the corrector turned on and without it. It can be noted that at a given frequency the amplitude with the filter turned on is zero, which was the goal of the synthesis.

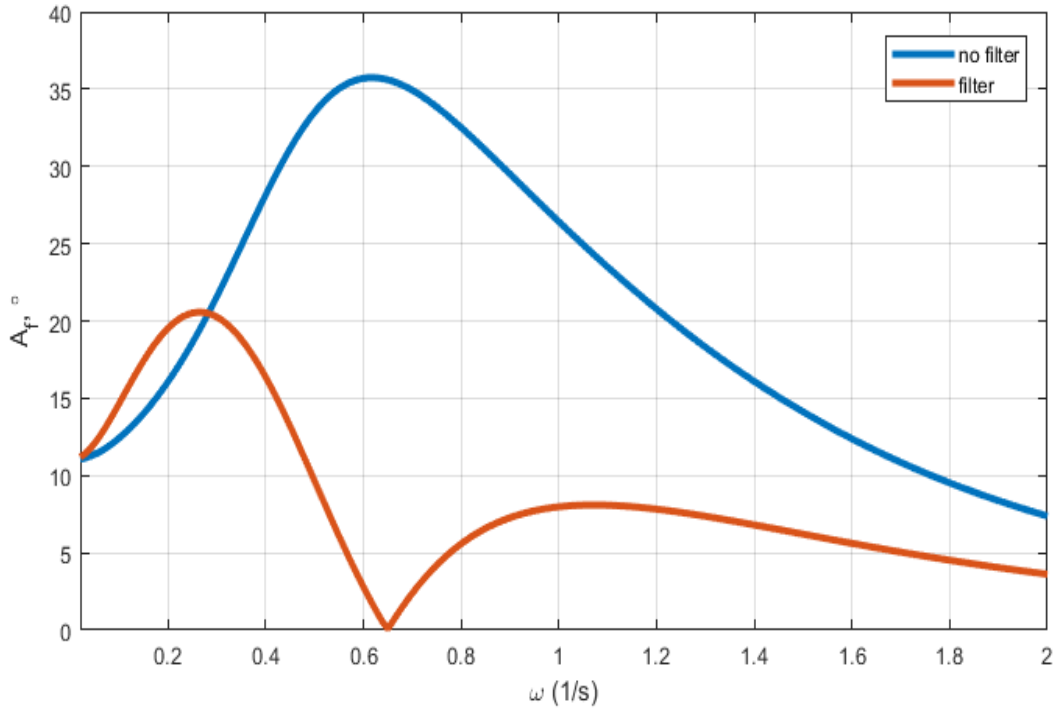

Fig. 4.7. Frequency response of a closed-loop system (4.6), (1.16) from disturbance to rudder deflection.

Let us consider the dynamics of the vessel in this mode, shown in Fig. 4.8 and Fig. 4.9. The ACV is affected by a polyharmonic external disturbance (4.4). The dynamic corrector was turned off during the first 300 s, and during this time period significant oscillations in the rudder deflections can be noted. Further activation of the corrector, as can be seen, leads to a significant decrease in the intensity of oscillations of the rudders, and the amplitude of oscillations of the heading angle also decreases. As a result, it can be noted that the dynamic corrector in the above situation really makes it possible to achieve the control goal, effectively reducing the control intensity without losing the quality of the heading angle stabilization. Note also that the presence of additional harmonics in the adopted disturbance model (4.4) has almost no effect on the quality of the

corrector’s work, since the values of the frequency response at these frequencies are also significantly lower than in the case of the corrector being turned off.

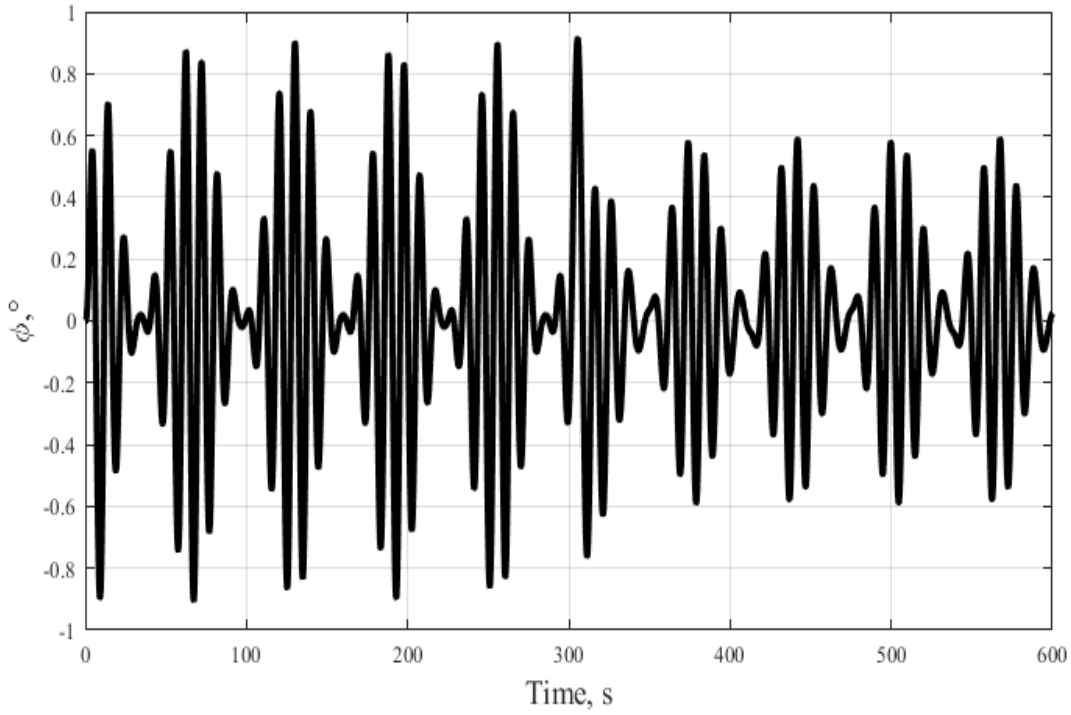

Fig. 4.8. Dynamics of heading angle under the influence of sea waves.

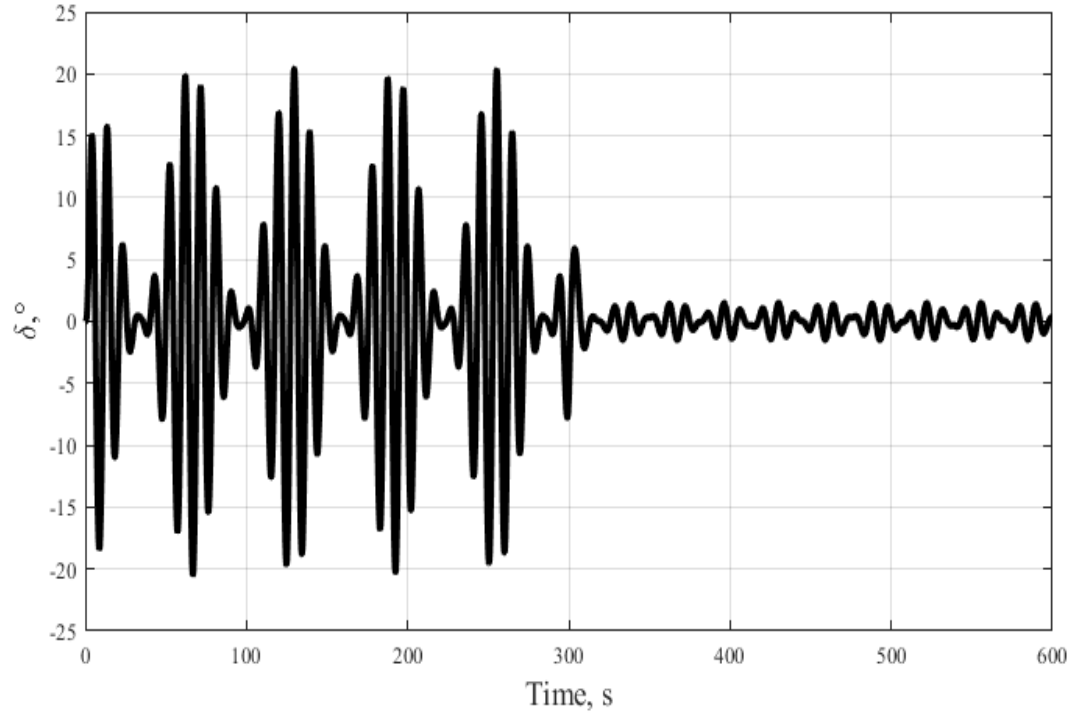

Fig. 4.9. Dynamics of rudder deflections under the influence of sea waves.

4.4. Practical Implementation of the Delay-Compensating Multipurpose Regulator

Let us now face the issue of the delay influence on the dynamics of a closed-loop system with a multipurpose regulator synthesized earlier. First, consider the proper motion mode in a situation where there are no external disturbances. Fig. 4.10 shows the ACV turning by 10º in the presence of a constant delay $\tau = 0.8\,\text{s}$. One can note a significant deterioration in the quality of control due to the appearance of noticeable oscillations in the transient process. As the delay increases to $\tau = 1.2\,\text{s}$, the oscillations cease to be damped and the amplitude becomes constant and significant (Fig. 4.11).

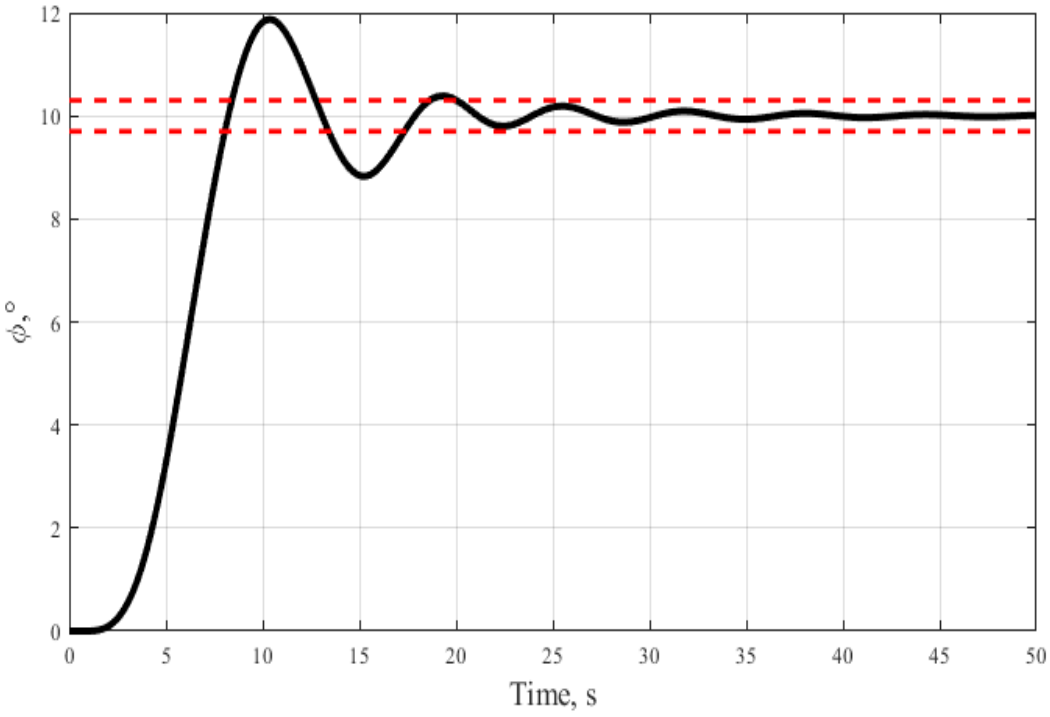

Fig. 4.10. Dynamics of heading angle while turning by 10º with delay $\tau = 0.8\,\text{s}$.

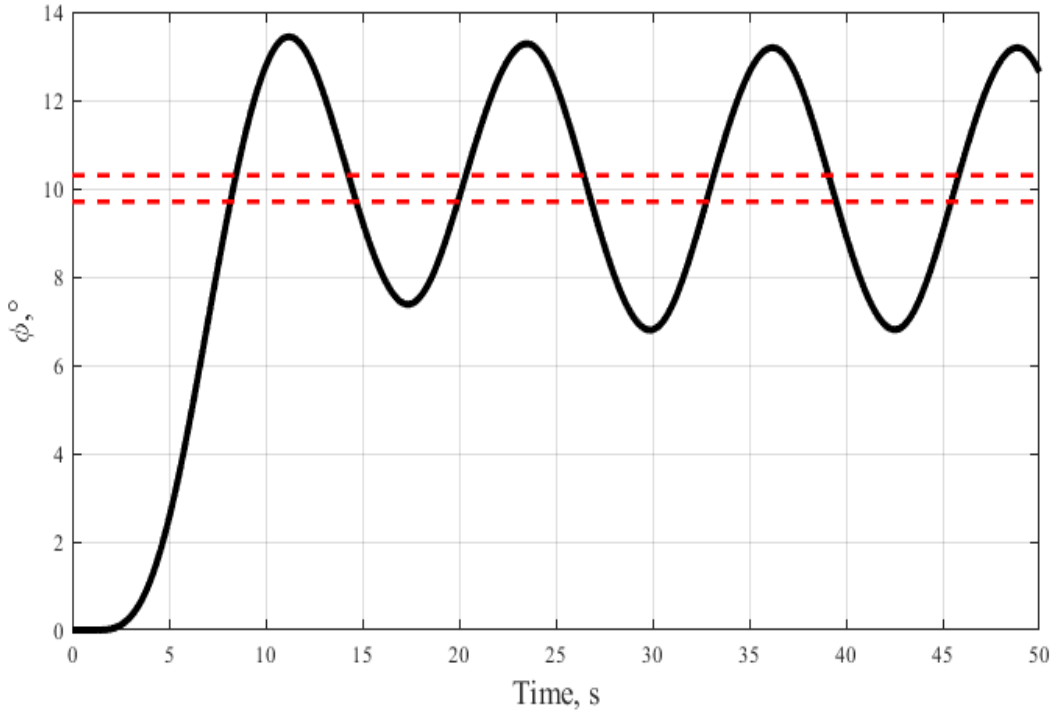

Fig. 4.11. Dynamics of heading angle while turning by 10° with delay $\tau = 1.2$ s.

The presented plots convincingly demonstrate that delay must be taken into account when designing plant control systems. In accordance with the compensation approach described in paragraph 1.3, we transform the original multipurpose regulator for the delay compensation. Taking into account the notation adopted in the first chapter, the control signal will be supplied to the rudder drives in the form

$$u = k_u(\delta_z - \delta), \quad k_u = 100.$$

Fig. 4.12 shows the dynamics of a closed-loop system with a multipurpose compensating regulator when turning by 10° with a delay $\tau = 0.8$s. In this case, the quality of control in general is identical to the dynamics of a closed-loop system without delay, which is the goal of the compensation approach.

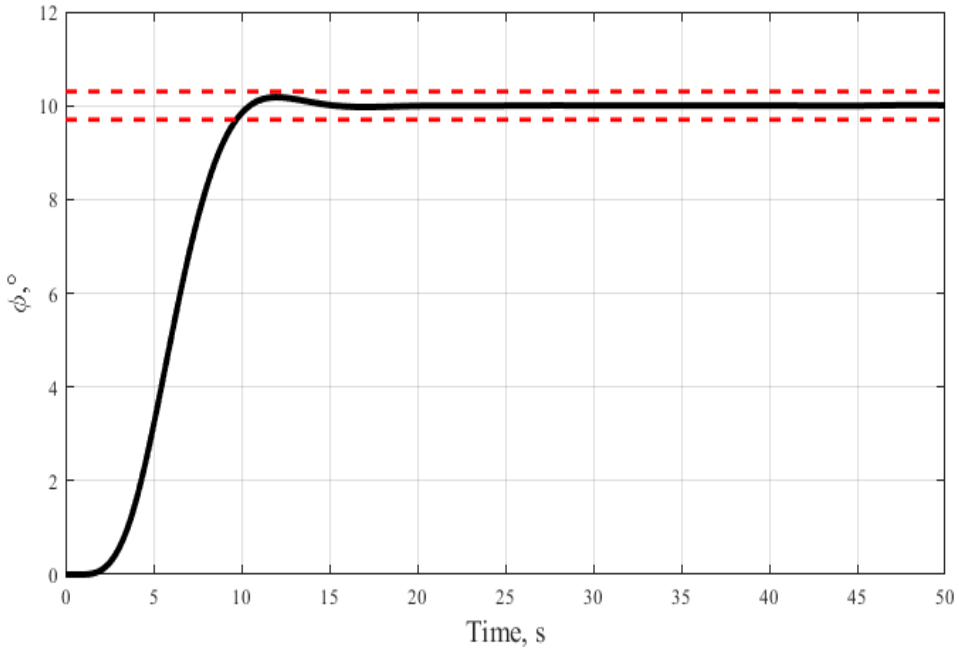

Fig. 4.12. Dynamics of a system closed by compensating feedback when rotated by 10º with delay $\tau = 0.8\,\text{s}$.

Now we introduce a constant external disturbance in the form of a side wind with a speed of 10 m/s. In this situation, the quality of the dynamics deteriorates significantly even with a delay $\tau = 0.5\,\text{s}$, as can be seen from Fig. 4.13. As the delay increases to 0.8s, the amplitude of the oscillations becomes constant (Fig. 4.14). Thus, in this mode, it is also necessary to take the delay into account.

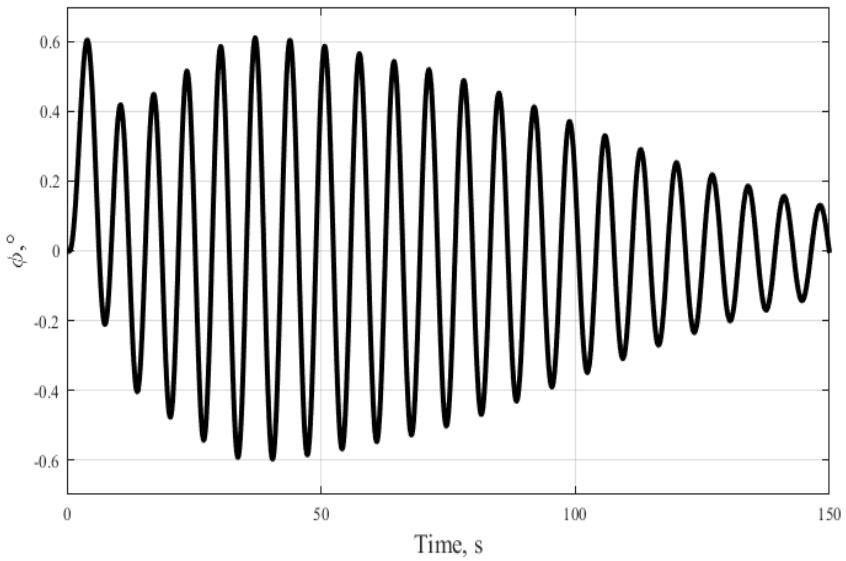

Fig. 4.13. Dynamics of the system under the influence of a side wind with a speed of 10 m/s with delay $\tau = 0.5\,\text{s}$.

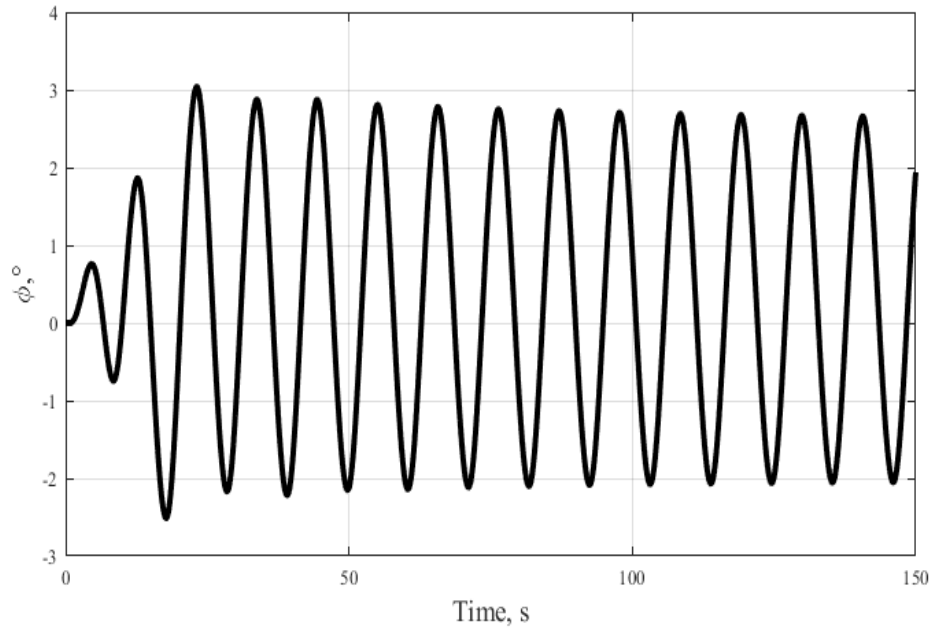

Fig. 4.14. Dynamics of the system under the influence of a side wind with a speed of 10 m/s with delay $\tau = 0.8$ s.

Let us now consider the behavior of a system closed by a compensating regulator in this situation. From Fig. 4.15 it is clear that in this case, the compensation approach makes it possible to preserve the dynamic characteristics of the original system without delay, eliminating the negative impact of delay.

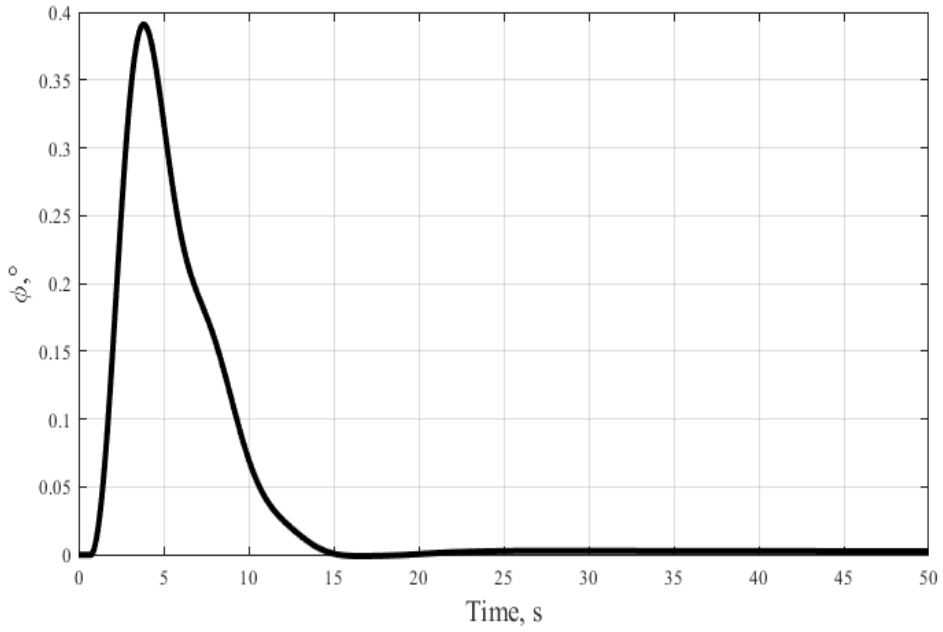

Fig. 4.15. Dynamics of a system closed by compensating feedback under the influence of a side wind with a speed of 10 m/s with delay $\tau = 0.5$ s.

Finally, let us face the issue of the influence of delay on the dynamics of the system in the presence of a periodic disturbance. As it can be seen from Fig. 4.16 and Fig. 4.17, the amplitude of oscillations in a closed-loop system without delay compensation with the corrector turned off increases noticeably with the delay value $\tau = 0.8\,\text{s}$. However, turning on the dynamic corrector leads to a significant reduction in the oscillation amplitude.

Now we apply a compensating regulator; the corresponding dynamics is shown in Fig. 4.18 and Fig. 4.19. And again, it can be noted that the dynamics of controlled motion in this case corresponds to the dynamics of the system without delay, i.e. the applied regulator actually compensates the delay. Thus, we can conclude that the multipurpose compensating regulator can be effectively used in sea waves, even if provided there is a delay.

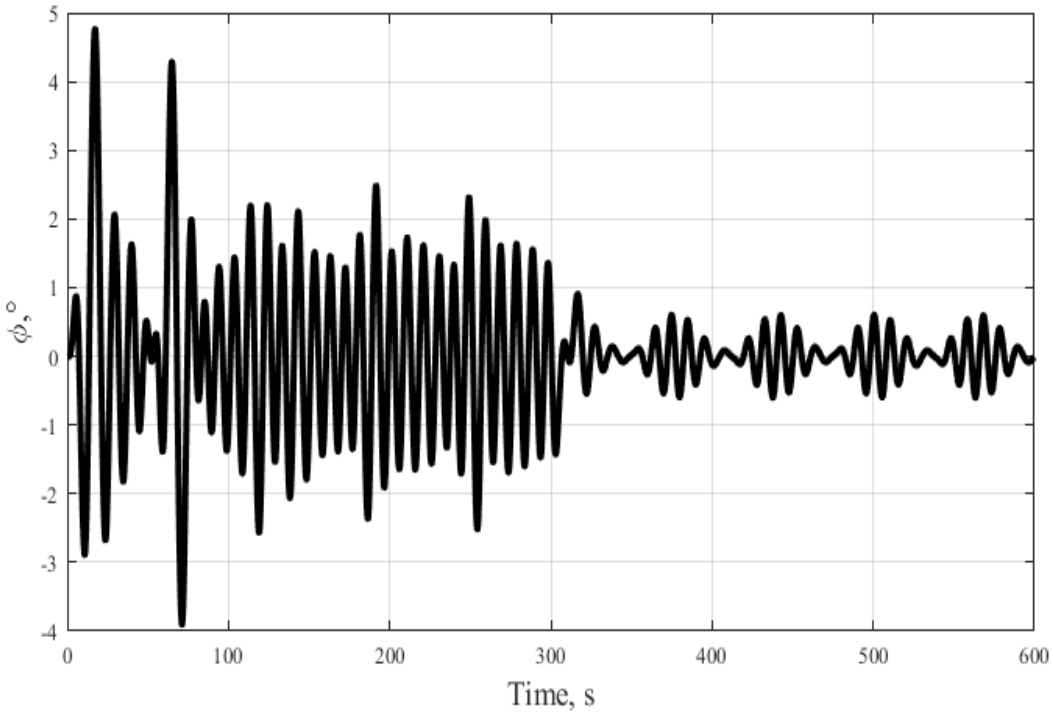

Fig. 4.16. Dynamics of the heading angle under the influence of waves and delay $\tau = 0.8\,\text{s}$.

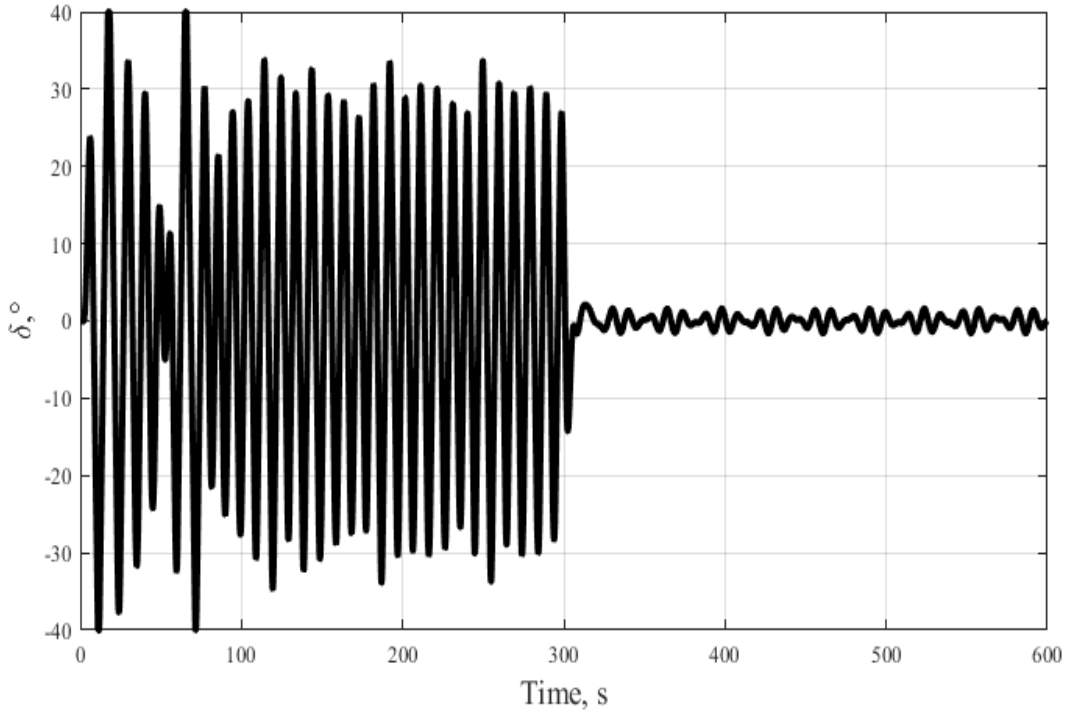

Fig. 4.17. Dynamics of rudder deflections under the influence of waves and delay $\tau = 0.8$ s.

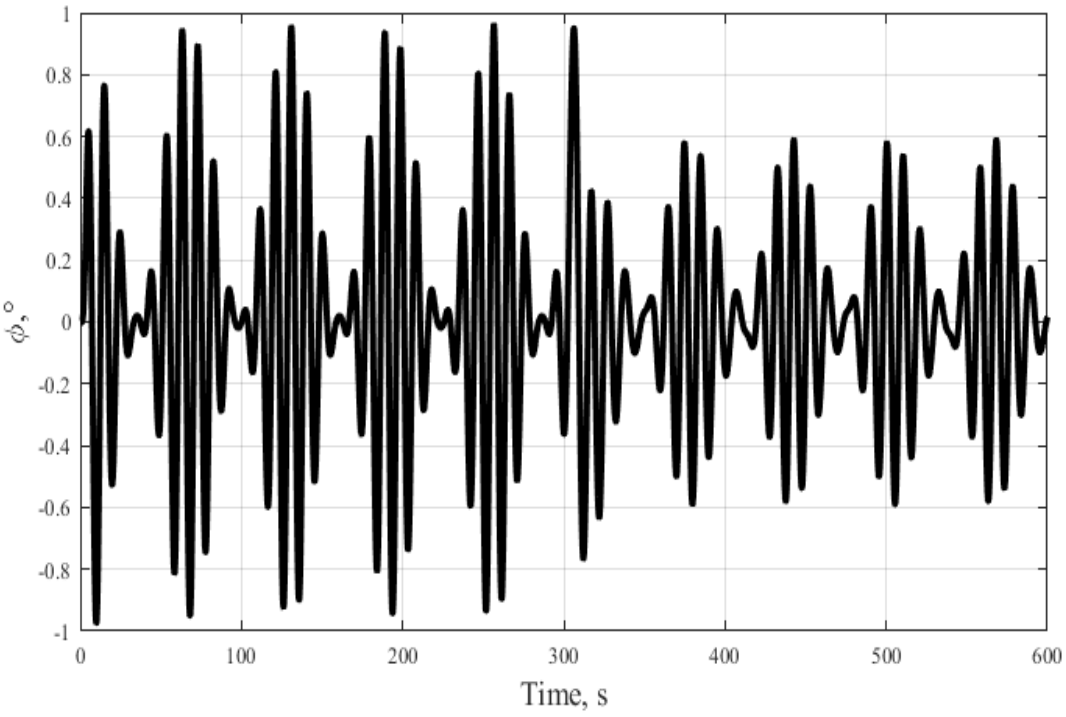

Fig. 4.18. Dynamics of the heading angle when using a compensating regulator under the influence of waves and delay $\tau = 0.8$ s.

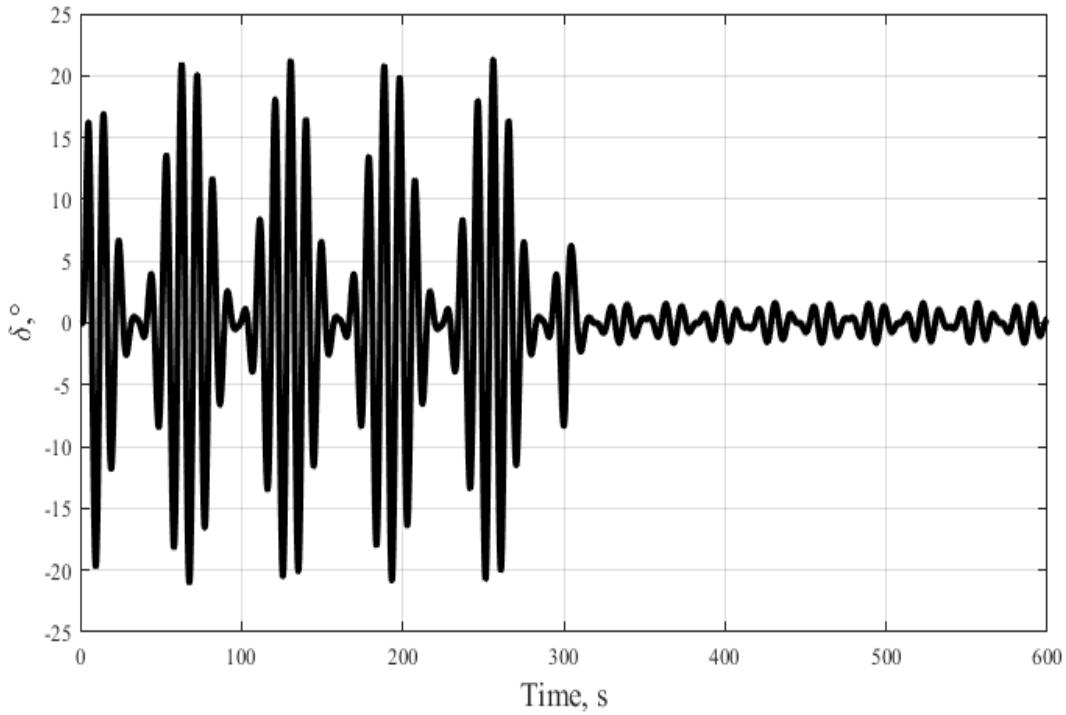

Fig. 4.19. Dynamics of the rudder deflections when using a compensating regulator under the influence of waves and delay $\tau = 0.8$ s.

4.5. Conclusions

The results obtained demonstrate the effectiveness of the multipurpose regulator applications for plant motion stabilization in various modes, while taking into account a whole range of requirements for the dynamics of controlled motion. The process of the multipurpose structure elements synthesis is greatly simplified due to the relative independence of the pieces that make up the regulator. The ability to turn off individual elements of the controller depending on the current mode is also a significant advantage.

It should be noted that the quality of control of a system closed by a multipurpose regulator is significantly deteriorated in the presence of a delay in the control channel. The degree of degradation may vary depending on the selected values of the adjustable elements of the multipurpose structure and the magnitude of the delay, up to loss of stability. Thus, when designing a control system, it is necessary to take the delay into account.

Using the compensation approach allows to preserve the dynamic characteristics of the original system without delay, i.e. to keep its transfer matrix. The results of numerical experiments show that the transient processes in both cases are almost identical. It is important to note the fact that with the compensation approach there is no need to solve a separate synthesis problem for a system with a delay. If the controller of the original system has been synthesized, then it is enough to add the dynamics equation of the auxiliary vector function and transform the controller input taking into account the prediction.

The disadvantages of the described approach include the need to measure the magnitude of the external disturbance. In some cases, accurate measurement is not possible. In addition, the issue of robust properties of the used controller is also subject to further research.

Nevertheless, we can conclude that the application of the approach described in this chapter in general makes it possible to ensure optimal control of moving plants, taking into account external disturbances of various nature and delay of the control signal.

C O N C L U S I O N

The dissertation is devoted to the issues of modeling, analysis and synthesis of multipurpose laws for moving plants motion control taking delay into account.

As a result of the research, the following main results were obtained:

- The issues of the prediction usage for the delay compensation in the problem of multipurpose control of moving plants with linear dynamic models have been studied. A method has been developed for transforming a multipurpose regulator synthesized for an object without delay, providing delay compensation and preserving the transfer matrix of the original closed-loop system.
- Multipurpose control methods have been developed for the problem of visual positioning of moving objects. An algorithm for the multipurpose regulator synthesis with visual feedback has been developed, taking into account the dynamics of the control object.
- A delay-compensating transformation of a multipurpose regulator with visual information in the feedback loop has been described. Examples of the synthesis of such regulators for two types of mobile robots, fully-actuated and underactuated, taking into account the delay are considered.
- Methods for multipurpose control of moving objects with non-linear dynamic models have been developed. An algorithm for the synthesis of a multipurpose regulator with feedback linearization is proposed.
- A method has been developed for the transformation of the described multipurpose regulator for the delay compensation. An example of the synthesis of such a regulator for a two-link robot manipulator with a delay is considered.
- An example of the delay-compensating multipurpose regulator synthesis for the stabilization of a hovercraft motion is presented.

References

1. Aleksandrov A. Y., Zhabko A. P., Platonov A. V. Ustojchivost’ dvizhenij diskretnyh dinamicheskih. SPb. : Izdatel’skij Dom Fedorovoj G.V., 2015. 154 p. (In Russian)
2. Optimizaciya linejnyh invariantnyh vo vremeni sistem upravleniya / Aliev F. A., Larin V. B., Naumenko K. I., Suncev V. N. Kiev : Naukova dumka, 1978. 327 p. (In Russian)
3. Barabanov A. E., Pervozvanskij A. A. Optimizaciya po ravnomerno-chastotnym pokazatelyam (H-teoriya) // Avtomatika i telemekhanika. 1992. № 9. P. 3–32. (In Russian)
4. Borodaj I. K., Necvetaev Y. A. Kachka sudov na morskom volnenii. L. : Sudostroenie, 1969. 432 p. (In Russian)
5. Veremey E. I., Korchanov V. M. Mnogocelevaya stabilizaciya dinamicheskih sistem odnogo klassa // Avtomatika i telemekhanika. 1988. № 9. P. 126–137. (In Russian)
6. Veremey E. I., Eremeev V. V., Korchanov V. M. Sintez algoritmov robastnogo upravleniya dvizheniem podvodnyh lodok vblizi vzvolnovannoj poverhnosti morya // Giroskopiya i navigaciya. 2000. № 2. P. 34–43. (In Russian)
7. Komp’yuternoe modelirovanie sistem upravleniya dvizheniem morskih podvizhnyh ob"ektov / Veremey E. I., Korchanov V. M., Korovkin M. V., Pogozhev S. V. SPb. : NII Himii SPbGU, 2002. 370 p. (In Russian)
8. Veremey E. I., Sotnikova M. V. Mnogocelevaya struktura zakonov upravleniya morskimi podvizhnymi ob"ektami // Trudy: XII Vserossijskoe soveshchanie po problemam upravleniya (VSPU-2014). 2014. P. 3289–3300. (In Russian)
9. Veremey E. I. Srednekvadratichnaya mnogocelevaya optimizaciya: ucheb. posobie. SPb. : Izd-vo S.-Peterb. un-ta, 2016. 408 p. (In Russian)

10. Veremey E. I. Kompensiruyushchie regulyatory po vyhodu dlya LTI sistem s zapazdyvaniem po upravleniyu // Sovremennye metody prikladnoj matematiki, teorii upravleniya i informacionnyh tekhnologij (PMTUKT-2017). Sbornik trudov X mezhdunarodnoj konferencii. 2017. P. 106–110. (In Russian)
11. Veremey E. I., Pogozhev S. V., Sevostyanov R. A. Stabilizaciya kursa morskih sudov v ekonomichnom rezhime dvizheniya // Sovremennye metody prikladnoj matematiki, teorii upravleniya i informacionnyh tekhnologij (PMTUKT-2015). Sbornik trudov VIII mezhdunarodnoj konferencii. 2015. P. 92–95. (In Russian)
12. Veremey E. I., Pogozhev S. V., Sevostyanov R. A. Fil’truyushchaya korrekciya mnogocelevyh zakonov upravleniya dvizheniem morskih sudov // Sistemy upravleniya i informacionnye tekhnologii. 2015. № 4 (62). P. 4–7. (In Russian)
13. Vojtkunskij Y. I. Spravochnik po teorii korablya: v trekh tomah. Tom 3. Upravlyaemost’ vodoizmeshchayushchih sudov. Gidrodinamika sudov s dinamicheskimi principami podderzhaniya. L. : Sudostroenie, 1985. 544 p. (In Russian)
14. Dezoer C., Vid’yasagar M. Sistemy s obratnoj svyaz’yu: Vhod-vyhodnye sootnosheniya. M. : Nauka, 1972. 278 p. (In Russian)
15. Dmitriev S. P., Pelevin A. E. Zadachi navigacii i upravleniya pri stabilizacii sudna na traektorii. SPb. : GNC RF-CNII «Elektro-pribor», 2002. 160 p. (In Russian)
16. Zhabko A. P., Haritonov V. L. Metody linejnoj algebry v zadachah upravleniya. SPb. : Izd-vo S.–Peterb. un-ta, 1993. 320 p. (In Russian)
17. Zubov V. I. Lekcii po teorii upravleniya. M. : Nauka, 1975. 496 p. (In Russian)
18. Zubov V. I. Teoriya optimal’nogo upravleniya sudnom i drugimi podvizhnymi ob"ektami. L. : Sudostroenie, 1966. 352 p. (In Russian)

19. Zubov V. I. Matematicheskie metody issledovaniya sistem avtomaticheskogo regulirovaniya. L. : Mashinostroenie, 1974. 336 p. (In Russian)
20. Kalman R., B'yusi R. Novye rezul'taty v linejnoj fil'tracii i teorii predskazanij // Trudy amerikanskogo obshchestva inzhenerov-mekhanikov. Ser. D. Tekhnicheskaya mekhanika. 1961. T. 83, № 1. P. 123–141. (In Russian)
21. Katkovnik V. Y., Poluektov R. A. Mnogomernye diskretnye sistemy upravleniya. M. : Nauka, 1966. 420 p. (In Russian)
22. Kvakernaak H., Sivan R. Linejnye optimal'nye sistemy upravleniya. M. : Mir, 1977. 650 p. (In Russian)
23. Kolyzaev B. A., Kosorukov A. I., Litvinenko V. A. Spravochnik po proektirovaniyu sudov s dinamicheskimi principami podderzhaniya. L. : Sudostroenie, 1980. 472 p. (In Russian)
24. Krasovskij N. N. Nekotorye zadachi teorii ustojchivosti dvizheniya. M. : Fizmatgiz, 1959. 211 p. (In Russian)
25. Krasovskij A. A. Sistemy avtomaticheskogo upravleniya poletom i ih analiticheskoe konstruirovanie. M. : Nauka, 1973. 558 p. (In Russian)
26. Kuzovkov N. T. Modal'noe upravlenie i nablyudayushchie ustrojstva. M. : Mashinostroenie, 1976. 184 p. (In Russian)
27. Larin V. B., Suncev V. N. O zadache analiticheskogo konstruirovaniya regulyatorov // AN SSSR. Avtomatika i telemekhanika. 1968. № 12. P. 142–144. (In Russian)
28. Letov A. M. Analiticheskoe konstruirovanie regulyatorov // AN SSSR. Avtomatika i telemekhanika. 1960. № 4–6; 1961. № 4, 11. (In Russian)
29. Letov A. M. Dinamika poleta i upravlenie. M. : Nauka, 1969. 359 p. (In Russian)
30. Letov A. M. Matematicheskaya teoriya processov upravleniya. M. : Nauka, 1981. 256 p. (In Russian)
31. Lukomskij Y. A., Chugunov V. S. Sistemy upravleniya morskimi podvizhnymi ob"ektami. L. : Sudostroenie, 1988. 272 p. (In Russian)

32. Lukomskij Y. A., Korchanov V. M. Upravlenie morskimi podvizhnymi ob"ektami. SPb. : Elmor, 1996. 320 p. (In Russian)
33. Miroshnik I. V. Teoriya avtomaticheskogo upravleniya. Nelinejnye i optimal’nye sistemy. SPb. : Piter, 2005. 271 p. (In Russian)
34. Olsson G., Piani D. Cifrovye sistemy avtomatizacii i upravleniya. SPb. : Nevskij Dialekt, 2001. 557 p. (In Russian)
35. Pelevin A. E. Identifikaciya parametrov modeli ob"ekta v usloviyah vneshnih vozmushchenij // Giroskopiya i navigaciya. 2014. №4 (87). P. 111–120. (In Russian)
36. Petrov Y. P. Optimizaciya upravlyaemyh sistem, ispytyvayushchih vozdejstvie vetra i morskogo volneniya. L. : Sudostroenie, 1973. 216 p. (In Russian)
37. Petrov Y. P. Variacionnye metody teorii optimal’nogo upravleniya. L. : Energiya, 1977. 280 p. (In Russian)
38. Petrov Y. P. Sintez ustojchivyh sistem upravleniya, optimal’nyh po srednekvadratichnym kriteriyam kachestva // AN SSSR, Avtomatika i telemekhanika. 1983. № 7. P. 5–24. (In Russian)
39. Polyak B. T., Shcherbakov P. S. Robastnaya ustojchivost’ i upravlenie. M. : Nauka, 2002. 303 p. (In Russian)
40. Polyakov K. Y. Osnovy teorii cifrovyh sistem upravleniya: uchebnoe posobie. SPb. : SPbGMTU, 2006. 161 p. (In Russian)
41. Sevost’yanov R. A. Kompensaciya vneshnih vozmushchenij v zadache vizual’nogo pozicionirovaniya mobil’nogo robota // Sovremennye informacionnye tekhnologii i IT-obrazovanie. 2022. T. 18, № 4. P. 790–798. (In Russian)
42. Sevost’yanov R. A. Vizual’noe pozicionirovanie mobil’nogo robota s uchetom zapazdyvaniya // Matematicheskaya teoriya upravleniya i ee prilozheniya (MTUiP-2020), materialy konferencii. Gosudarstvennyj nauchnyj centr Rossijskoj Federacii AO «Koncern «CNII «Elektropribor». 2020. P. 77–79. (In Russian)

43. Sevost’yanov R. A., Shayahmetova L. V. Sistema avtomatizacii processa issledovaniya dinamiki modeli sudna na vozdushnoj podushke // Sovremennye informacionnye tekhnologii i IT-obrazovanie. 2016. T. 12, № 1. P. 127–134. (In Russian)
44. Sevost’yanov R. A. Programmnaya podderzhka processov upravleniya mobil’nym robotom s vizual’noj obratnoj svyaz’yu // Sistemy upravleniya i informacionnye tekhnologii. 2019. № 4 (78). P. 83–86. (In Russian)
45. Sevost’yanov R. A. Upravlenie nepolnoprivodnym robotom s vizual’noj obratnoj svyaz’yu // Sovremennye metody prikladnoj matematiki, teorii upravleniya i informacionnyh tekhnologij (PMTUKT-2018). Sbornik trudov XI mezhdunarodnoj konferencii. 2018. P. 244–247. (In Russian)
46. Sevost’yanov R. A. Stabilizaciya dvizheniya sudna na vozdushnoj podushke s uchetom zapazdyvaniya // Sovremennye metody prikladnoj matematiki, teorii upravleniya i informacionnyh tekhnologij (PMTUKT-2018). Sbornik trudov XI mezhdunarodnoj konferencii. 2018. P. 248–251. (In Russian)
47. Sevost’yanov R. A. Cifrovaya stabilizaciya dvizheniya kolesnogo robota // Sistemy upravleniya i informacionnye tekhnologii. 2018. № 1 (71). P. 43–36. (In Russian)
48. Sevost’yanov R. A. Stabilizaciya dvizheniya robota pri nalichii transportnogo zapazdyvaniya // Navigaciya i upravlenie dvizheniem: materialy XVI konferencii molodyh uchenyh. 2014. P. 258–264. (In Russian)
49. Sevost’yanov R. A. Upravlenie dvizheniem mobil’nogo robota s uchetom transportnogo zapazdyvaniya // Processy upravleniya i ustojchivost’: Trudy 45-j mezhdunarodnoj nauchnoj konferencii aspirantov i studentov. 2014. P. 385–390. (In Russian)
50. Fomin V. N. Metody upravleniya linejnymi diskretnymi ob"ektami. L. : Izd-vo Leningr. un-ta, 1985. 336 p. (In Russian)
51. Forsajt D, Pons Z. Komp’yuternoe zrenie. Sovremennyj podhod. M. : Vil’yams, 2004. 928 p. (In Russian)

52. Chang S. Sintez optimal’nyh sistem avtomaticheskogo upravleniya. M. : Mashinostroenie, 1964. 440 p. (In Russian)
53. Cherneckij V. I. Matematicheskoe modelirovanie dinamicheskih sistem. Petrozavodsk : Izd-vo Petrozavodsk. gos. un-ta, 1996. 432 p. (In Russian)
54. Yanushevskij R. T. Upravlenie ob’ektami s zapazdyvaniem. M. : Nauka, 1978. 416 p. (In Russian)
55. Billard A., Kragic D. Trends and challenges in robot manipulation // Science. 2019. Vol. 364, № 6446. P. eaat8414.
56. Speeded up robust features (SURF) / Bay H. [et al.] // Computer Vision and Image Understanding. 2008. Vol. 110, № 3. P. 346–359.
57. Bogsra O. H., Kwakernaak H., Meinsma G. Design methods for control systems. Notes for a course of the Dutch Institute of Systems and Control. 2006. 325 p.
58. Braunl Th. Embedded Robotics: Mobile Robot Design and Applications with Embedded Systems. 2nd ed. Berlin : Springer-Verlag, 2006. 458 p.
59. Carona R., Aguiar A. P., Gaspar J. Control of unicycle type robots: tracking, path following and point stabilization // Proceedings of IV Jornadas de Engenharia de Electronica e Telecomunicacoes e de Computadores. 2008. P. 180–185.
60. Caspi P., Maler O. From Control Loops to Real-Time Programs // Handbook of Networked and Embedded Control Systems / ed. by D. Hristu, W.S. Levine. Boston : Birkhauser, 2005. P. 395–418.
61. Chaumette F., Hutchinson S. Visual Servo Control: Basic Approaches // IEEE Robotics & Automation Magazine. 2006. Vol. 13, № 4. P. 82–90.
62. Chaumette F., Hutchinson S. Visual Servo Control: Advanced Approaches // IEEE Robotics & Automation Magazine. 2007. Vol. 14, № 1. P. 109–118.
63. Doyle J., Francis B., Tannenbaum A. Feedback control theory. New York : Macmillan Publ. Co., 1992. 227 p.
64. Fossen T. I. Guidance and Control of Ocean Vehicles. John Wiley & Sons, 1994. 494 p.

65. Fossen T. I. Handbook of Marine Craft Hydrodynamics and Motion Control. John Wiley & Sons, 2011. 596 p.
66. Francis B. A. A course in Hinf control theory // Lecture Notes in Control and Information Sciences. Berlin : Springer-Verlag, 1987. Vol. 88. 156 p.
67. Automatic generation and detection of highly reliable fiducial markers under occlusion / Garrido-Jurado S., Muñoz-Salinas R., Madrid-Cuevas F. J., Marín-Jiménez M. J. // Pattern Recogn. 2014. Vol. 47, № 6. P. 2280–2292.
68. Hartley R., Zisserman A. Multiple view geometry in computer vision. 2nd ed. Cambridge University Press, 2004. 672 p.
69. Isidori A. Nonlinear Control Systems. London : Springer, 1995. 549 p.
70. Kalman R. E. Contributions to the theory of optimal control // Boletin de la Sociedad Matematica Mexicana. 1960. Vol. 5. P. 102–119.
71. Khalil H. K. Nonlinear systems. 3rd ed. NJ : Prentice Hall, 2002. 750 p.
72. Kharitonov V. L. Time-Delay Systems. Lyapunov Functionals and Martices. Birkhäuser, 2013. 312 p.
73. Krstic M. Delay Compensation for Nonlinear, Adaptive, and PDE Systems. Birkhäuser, 2009. 466 p.
74. Landau I. D., Zito G. Digital Control Systems: Design, Identification and Implementation. London : Springer-Verlag, 2006. 484 p.
75. Loria A., Fossen T. I., Panteley E. A Separation Principle for Dynamic Positioning of Ships: Theoretical and Experimental Results // IEEE Transactions of Control Systems Technology. 2000. Vol. 8, № 2. P. 332–343.
76. Lowe D. G. Distinctive image features from scale-invariant keypoints // International Journal of Computer Vision. 2004. Vol. 2, № 60. P. 91–110.
77. Lynch K. M., Park F. C. Modern Robotics: Mechanics, Planning, and Control. Cambridge University Press, 2017. 624 p.
78. Malis E., Chaumette F., Boudet S. 2 1/2 D Visual Servoing // IEEE Transactions on Robotics and Automation. 1999. Vol. 15, № 2. P. 238–250.

79. Time-Delay Systems. Stability and Performance Criteria with Applications / Marshall J. E., Gorecki H., Korytowski A., Walton K. Ellis Horwood, 1992. 244 p.
80. Michiels W., Niculescu S.-I. Stability and Stabilization of Time-Delay Systems. An Eigenvalue-Based Approach. Philadelphia : SIAM, 2007. 378 p.
81. Mondie S., Michiels W. Finite spectrum assignment of unstable time-delay systems with a safe implementation // IEEE Trans. Automat. Control. 2003. Vol. 48, № 12. P. 2207–2212.
82. Dynamical Models for Omni-directional Robots with 3 and 4 Wheels / Oliviera H. P., Sousa A. J., Moreira A. P, Costa P. J. // Proceedings of the 5th International Conference on Informatics in Control, Automation and Robotics. 2008. P. 189–196.
83. Perez T. Ship Motion Control: Course Keeping and Roll Stabilization Using Rudder and Fins. London : Springer-Verlag, 2005. 300 p.
84. The mathematical theory of optimal processes / L. S. Pontryagin, V. G. Boltyanskii, R. V. Gamkerelidze, E. F. Mischenko. New York : John Wiley, 1962. 360 p.
85. Sami Fadali M., Visoli A, Digital Control Engineering: Analysis and Design. Burlington : Academic Press, 2009. 552 p.
86. Sevostyanov R. A. Delay-compensating Visual Positioning Of The Mobile Robot // Journal of Physics: Conference Series. 13. "13th Multiconference on Control Problems, MCCP 2020". 2021. P. 012038.
87. Sevostyanov R. Multipurpose Visual Positioning of the Underactuated Mobile Robot // Stability and Control Processes: Proceedings of the 4th International Conference Dedicated to the Memory of Professor Vladimir Zubov, Saint Petersburg, 05–09 october 2020. Cham : Springer, 2022. P. 329–334.
88. Sevostyanov R., Shayakhmetova L. Application of the Asymptotic Observers for the Stabilization of the Time-Delay Linear Equations // Convergent Cognitive Information Technologies. Convergent 2018. Communications in Computer and Information Science. 2020. Vol. 1140. P. 223–230.

89. Sevostyanov R., Shayakhmetova L. Stabilization of the inverted pendulum considering delay // Selected Papers of the II International Scientific Conference "Convergent Cognitive Information Technologies" (Convergent 2017). 2018. P. 318–324.
90. Sevostyanov Ruslan A., Veremey Evgeny I. Multipurpose stabilization of the advanced marine surface crafts // 6th Seminar on Industrial Control Systems - Analysis, Modeling and Computation, ITM Web of Conferences. 2016. Vol. 6. P. 01004.
91. Handbook of Robotics / ed. by B. Siciliano, O. Khatib. Berlin : Springer-Verlag, 2008. 1628 p.
92. Robotics: modelling, planning and control / B. Siciliano, L. Sciavicco, L. Villani, G. Oriolo. London : Springer-Verlag, 2009. 644 p.
93. Slotine J. J. E., Li W. Applied Nonlinear Control. NJ : Prentice-Hall, 1991. 461 p.
94. Smith O. J. M. A Controller to overcome dead time // ISAJ. 1959. Vol. 6, № 2. P. 28–33.
95. Sotnikova M, Sevostyanov R. Visual Positioning of a Moving Object Using Multi-objective Control Algorithm // Lecture Notes in Computer Science 2023. Vol. 13930 LNCS. P. 425–438.
96. Spong M. W., Hutchinson S., Vidyasagar M. Robot Modeling and Control. John Wiley & Sons, 2005. 496 p.
97. Szeliski R. Computer Vision: Algorithms and Application. London : Springer-Verlag, 2011. 812 p.
98. Van der Schaft A. J. L2-Gain and passivity techniques in nonlinear control. 2nd ed. London : Springer-Verlag, 2000. 248 p.
99. Veremey E. I. Dynamical Correction of Control Laws for Marine Ships' Accurate Steering // Journal of Marine Science and Application. 2014. Vol. 13, № 2. P. 127–133.

100. Veremey E. I. Optimization of filtering correctors for autopilot control laws with special structures // Optimal Control Applications and Methods. 2016. Vol. 37, № 2. P. 323–339.
101. Vidyasagar M. Control system synthesis: A factorization approach. Cambridge (Mass.) : MIT Press, 1985. 436 p.
102. Xianzhou W., Hanzhen X. Robust autopilot with wave filter for ship steering // Journal of Marine Science and Application. 2006. Vol. 5. P. 24–29.
103. Yun L., Bliault A. Theory and Design of Air Cushion Craft. London : Arnolds, 2000. 632 p.